

©Copyright 2019
Ahmad H. Milyani

The Design of Carbon Taxes in Electric Power Systems and the Effects on Market Participation

Ahmad H. Milyani

A dissertation
submitted in partial fulfillment of the
requirements for the degree of

Doctor of Philosophy

University of Washington

2019

Reading Committee:

Daniel Kirschen, Chair

Nicholas Nagel

Baosen Zhang

Program Authorized to Offer Degree:
Electrical & Computer Engineering

University of Washington

Abstract

The Design of Carbon Taxes in Electric Power Systems and the Effects on Market Participation

Ahmad H. Milyani

Chair of the Supervisory Committee:
Professor Daniel Kirschen
Electrical Engineering

The escalating evidence of climate change caused by the release of anthropogenic greenhouse gases (GHGs) in the atmosphere is prompting many nations to act swiftly. Imposing carbon taxes to mitigate carbon dioxide (CO₂) emissions from the electricity sector is amongst the commonly used methods to counteract the detrimental effects of GHGs on the environment. Regardless of how successful they are in reducing CO₂ emissions, widespread adoption of carbon taxes as a policy to combat climate change has been hindered due to concerns about their competency. More specifically, environmental advocates have raised the issue that, unlike a cap-and-trade policy, levying carbon taxes does not set a ceiling on the level of emissions in the targeted sector but rather incorporates the cost of damaging the environment into the overall cost of production leading to circumstances where the level of emissions is higher than desired. Moreover, fiscal conservatives often avoid additional taxes fearing not only political ramifications but cost increases and efficiency reductions as well. Addressing these concerns would arguably advance the debate of policy selection and facilitate its implementation. Therefore, the main purpose of this dissertation is to develop frameworks that assess the viability of using a carbon tax as a driving force for reducing CO₂ emissions in electric power systems and the ensuing consequences of its implementation.

In this dissertation, we investigate the impacts of carbon taxes considering three different

perspectives. The first being a regulating authority or a policy maker who is looking to meet a desired reduction target in CO₂ emissions via a carbon tax. In this regard, we present a model that utilizes the revenue generated from the imposition of a carbon tax to incentivize low-polluting producers in the form of monetary subsidies. The developed algorithm is attractive to regulators and policy makers because it finds the optimal combined tax/subsidy policy that achieves the intended reduction in CO₂ emissions.

The second and third frameworks look at the effects of carbon taxes on the participation of power producers and electric vehicle (EV) aggregators, respectively, in electricity markets. Each framework is intended to take the perspective of either the supply side or the demand side in carbon regulated electricity markets. In the case of power producers, we look at the market power of those producers when levying a carbon tax and the resulting consequences of exercising that market power through strategic offering. Finally, in the case of EV aggregators, we develop a model to find the optimal charging and discharging schedules at minimum cost. We then look at how the optimal charging and discharging profiles change with the imposition of a carbon tax, and the change in carbon emissions resulting from those profiles.

TABLE OF CONTENTS

	Page
Acknowledgements	v
Dedication	vii
Glossary	viii
List of Figures	xi
List of Tables	xiv
Chapter 1: Introduction	1
1.1 Background	1
1.2 Targeting CO ₂ Emissions in the Electricity Sector	3
1.3 Market-Based Approaches to Reduce CO ₂ Emissions	4
1.4 Outline of the Dissertation	5
Chapter 2: Optimally Designed Subsidies for Achieving Carbon Emissions Targets in Electric Power Systems	8
2.1 Introduction	8
2.1.1 Motivation	8
2.1.2 Proposed Solution	8
2.2 Literature Survey	9
2.2.1 The Effectiveness and Associated Socio-Economic Costs of Carbon Taxes	9
2.2.2 The Case for Revenue Recycling and Financial Incentives	10
2.2.3 Multilevel Optimization	12
2.3 Contributions	12
2.4 Chapter Organization	13
2.5 Model Formulation	13

2.5.1	Upper-Level Problem	13
2.5.2	Middle-Level Problem	15
2.5.3	Lower-Level Problem	15
2.5.3.1	Nodal Power Balance	16
2.5.3.2	Network Constraints	16
2.5.3.3	Dispatch Constraints	16
2.5.3.4	Angle Stability Constraints	17
2.6	Solution Methodology	17
2.6.1	Transformation to a Bilevel Problem	17
2.6.1.1	MPEC	17
2.6.1.2	Linearizing the MPEC	19
2.6.1.3	Complete Bilevel Model	19
2.6.2	Solving the Bilevel Problem	22
2.7	Simulation Results	24
2.7.1	Illustrative Example: 14-Bus Test System	24
2.7.1.1	System Characteristics	24
2.7.1.2	Discussion	25
2.7.2	Case Study: IEEE 24-Bus Reliability Test System	28
2.7.2.1	Test Cases	28
2.7.2.2	Results	29
2.7.2.3	The Flexibility of Subsidies	40
2.8	Summary	44
Chapter 3:	Market Power in the Presence of Carbon Taxes in Electricity Markets .	46
3.1	Introduction	46
3.2	Literature Survey	50
3.2.1	Market Power in Electricity Markets	50
3.2.1.1	Empirical Evidence	50
3.2.1.2	Academic Works	51
3.2.2	Environmental Regulation and Market Power	52
3.2.3	Stackelberg Games in Electric Power Systems	53
3.3	Contribution	54
3.4	Chapter Organization	54

3.5	The Stackelberg Game	54
3.6	Mathematical Model	56
3.7	Solution Technique	58
3.8	Case Study: IEEE 24-Bus Reliability Test System	60
3.8.1	Test System Data and Setup	60
3.8.2	Effect on Consumption Cost	61
3.8.3	Effect on Emissions	63
3.9	Summary	71
Chapter 4:	The Impact of Carbon Pricing on the Optimal Participation of Electric Vehicle Aggregators in the Day-ahead Energy Market	72
4.1	Introduction	72
4.2	Literature Survey	74
4.2.1	Electric Vehicles in Electric Power Systems	74
4.2.2	Electric Vehicles and GHG Emissions	76
4.3	Contribution	78
4.4	Chapter Organization	79
4.5	Market Framework	79
4.5.1	Electric Vehicle Aggregator	79
4.5.2	Day-ahead Market	81
4.6	Mathematical Model Formulation	82
4.6.1	Competitive EV Aggregator	83
4.6.2	Strategic EV Aggregator	85
4.7	Solution Methodology	87
4.7.1	MPEC for the competitive model	87
4.7.2	MPEC for the strategic model	88
4.7.3	MPEC Linearization	89
4.8	Case Study: IEEE 24-bus Reliability Test System	89
4.8.1	Data Setup	89
4.8.1.1	EV Data	89
4.8.1.2	Power System Data	90
4.8.2	Competitive vs. Strategic Participation	90
4.8.3	The Effects on Arbitrage	92

4.8.4	The Effects on Carbon Emissions	93
4.8.4.1	Unidirectional Mode	93
4.8.4.2	Bidirectional Mode	96
4.9	Summary	103
Chapter 5:	Conclusion and Future Work	104
5.1	Conclusions	104
5.2	Suggestions for Future Work	105
Bibliography	109
Appendix A:	Nomenclature	125
A.0.1	Sets and Indices	125
A.0.2	Parameters	125
A.0.3	Variables	127
A.0.4	Dual Variables	128
Appendix B:	14-Bus Test System Data	129
Appendix C:	Linear Equivalent of the Upper-level Objective Function	134
C.1	Competitive Model	134
C.2	Strategic Model	135

ACKNOWLEDGEMENTS

First and foremost, my utmost gratitude goes to my parents, Dr. Hisham Milyani and Eman Fakahani. Without their unconditional love, support, and guidance from the moment I was born, I would not have become the person I am today.

I would like to thank my brothers, Wael and Hossam, for always being there whenever I needed them, and my aunt, Jaleelah, for being thoughtful and caring. My thanks also go to my parents-in-law, Majed and Rowaidah, for always keeping me in their thoughts and prayers, and my brothers- and sister-in-law, Youssef, Abdulrahman, Rayyan, and Nuha, for their continuous love and encouragement throughout this journey.

I would like to express my deepest and sincerest thanks to my wife, Roaa, for constantly offering me her endless love and support throughout the years, for her unrelenting belief in my abilities which kept me going through the tough times, for always trying to cheer me up whenever I'm down, and above all, for giving me the greatest gift in my life, my son Hisham. This thesis would not have been possible without her by my side, and for that, I will always be indebted to her.

* * *

I'm incredibly grateful to my advisor, Dr. Daniel Kirschen, for welcoming me into his lab, and for his invaluable mentoring and guidance throughout my research. Under his tutelage, I have developed academically, professionally, and personally; and for that, I will always feel privileged to have worked with him. In addition, I would like to thank my committee members, Dr. Nicholas Nagel, Dr. Baosen Zhang and Dr. John Kramlich for their valuable comments that helped in improving this dissertation. My gratitude also goes to Dr. Mohamed El-Sharkawi for his support and advice early in my career.

My thanks go to all of my colleagues and friends from the REAL research group at the University of Washington, specially, Dr. Daniel Olsen for inspiring me to choose this topic, for our long insightful discussions, and for helping me in crafting the title of this dissertation. I would also like to thank Dr. Abeer Al-Maimouni for our venting sessions (as she describes them), Dr. Jesus Contreras-Ocaña for his infectious positive attitude, and Dr. Yushi Tan for our fun, long walks together.

* * *

I must also acknowledge all of my friends who helped me during this journey: Motasem, Saud, Abdulrahman, Ziad, Ghassan (Al-Ghamdi), Ahmed, Mohammed (Al-Shammari), Ghassan (Bukhari), Faleh, Sedrick, Hareth, Sultan, Majed, Khalifa, Jamal, Abdullah (Al-Khamis), Mahdi, Hani, Mohammed (Al-Malik), Ali, Mohammed (Al-Mathami), Nabil, Hamad, Omar, Abdullah (Al-Ameri), Abdulaziz, Juma, Badr, Salim, James, and Munadir.

Finally, I would like to thank King Abdulaziz University and the University of Washington for financially supporting this thesis.

DEDICATION

To my loving parents, Hisham and Eman,
and to my wonderful wife and son, Roa'a and Hisham Jr.

GLOSSARY

BEV: Battery Electric Vehicle

CAISO: California Independent System Operator

CO₂: Carbon Dioxide

CPLEX: Optimization software package

DAM: Day-Ahead Market

DC: Direct Current

DER: Distributed Energy Resources

DOJ: Department of Justice

DR: Demand Response

ED: Economic Dispatch

EPA: Environmental Protection Agency

EPEC: Equilibrium problem with equilibrium constraints

ES: Energy Storage

ETS: Emissions Trading System

EU: European Union

EV: Electric Vehicle

FERC: Federal Energy Regulatory Commission

FTC: Federal Trade Commission

GAMS: General Algebraic Modeling System

GHG: Greenhouse Gas

GWP: Global Warming Potential

HHI: HerfindahlHirschman Index

HFC: Hydrofluorocarbon

HOV: High-occupancy vehicle

IEEE: Institute of Electrical and Electronics Engineers

IHR: Incremental Heat Rate

IPCC: Intergovernmental Panel on Climate Change

ISO: Independent System Operator

KKT: Karush-Kuhn-Tucker

LDV: Light-duty vehicle

LL: Lower Level

LMP: Locational Marginal Price

LP: Linear Program

CH₄: Methane

MG: Micro-grid

MILP: Mixed Integer Linear Program

MPEC: Mathematical Problem with Equilibrium Constraints

MO: Market Operator

N₂O: Nitrous oxide

NYISO: New York Independent System Operator

OPF: Optimal Power Flow

PHEV: Plug-in Hybrid Electric Vehicle

PJM: Pennsylvania-Jersey-Maryland Interconnection

PFC: Perfluorocarbon

RF: Radiating Forcing

RPS: Renewable Portfolio Standard

RSI: Residual Supply Index

RTS: Reliability Test System

SO: System Operator

SF₆: Sulphur hexafluoride

SW: Social Welfare

TO: Transmission Operator

UC: Unit Commitment

UL: Upper Level

US: United States

V2G: Vehicle-to-Grid

LIST OF FIGURES

Figure Number	Page
1.1 (a) Concentration of carbon dioxide, methane, and nitrous oxide in the atmosphere, and (b) land and ocean surface average combined temperature anomalies relative to the average over the period of 1986 to 2005	2
1.2 US Greenhouse Gas Emissions in 2016 by gas type.	3
1.3 US Greenhouse Gas Emissions in 2016 by sectoral output. The graph was generated using data obtained from the United States Environmental Protection Agency (EPA).	4
2.1 An illustration depicting how the different levels interact in the proposed trilevel model	14
2.2 An illustration of the interface between the different levels of the resultant bilevel model	21
2.3 Flowchart for finding the optimal tax rate using the False Position method .	23
2.4 Required tax rate as a function of CO ₂ emissions	25
2.5 Total cost of subsidies as a function of CO ₂ emissions	26
2.6 Total cost of consumption (with reimbursement) as a function of CO ₂ emissions	27
2.7 Share of total production for each generating unit as a function of CO ₂ emissions reduced (relative to the highest achievable reduction target)	28
2.8 The amount of CO ₂ emissions under no taxes (ZT), carbon taxes only (CT), and carbon taxes with subsidies (ODS) in addition to the necessary tax rate associated with the ODS method to achieve the reduction target for all test cases. Note that the same tax rate used in the ODS method was also used in the CT method.	31
2.9 Total cost of subsidies under the three schemes for all scenarios.	33
2.10 (a) Total cost of supplying the load after adjusting for the tax penalty and subsidies, (b) total cost of consumption after consumer reimbursement in the case of CT, and (c) average cost of electricity paid by consumers under the three schemes for all scenarios.	35
2.11 Average Hourly Locational Marginal Prices	36

2.12	Merchandizing surplus under the three schemes for all scenarios.	37
2.13	Cumulative profit of all generating units broken down by fuel type. Note that the profits of oil units are zero in all test cases except under ZT and CT in the coal retirement scenario where the profits are \$185.46 and \$202.05 respectively.	39
2.14	Base case results for each iteration of the False Position method.	40
2.15	Tax rate required for the ODS method for different percentages of κ_{TR}	41
2.16	(a) Total cost of subsidies, and (b) average cost of electricity paid by consumers for different percentages of κ_{TR}	42
3.1	The generation stack for the Pennsylvania-Jersey-Maryland (PJM) electric power market. Note that the supply curve depicted in this figure is from approximately 2008. Since then, the type of units may have changed, however, the general shape of the curve is still comparable.	48
3.2	The average hourly load for an entire week in the PJM Mid-Atlantic Region. The black, red, and blue traces represent Spring, Summer, and Winter, respectively.	49
3.3	Flowchart depicting the interaction between the two players in the Stackelberg game.	56
3.4	The percentage change, relative to a perfectly competitive market, in the cost incurred by consumers given that a single firm is offering strategically.	64
3.5	The generation capacity of the participating firms ordered by merit for different tax rates, and the system-wide hourly load.	65
3.6	The percentage change, relative to a perfectly competitive market, in the strategic firm's output, and the system-wide CO ₂ emissions given that a single firm is offering strategically.	68
3.7	The change in total production over the scheduling horizon, relative to a perfectly competitive market, for non-strategic firms given that a single firm is offering strategically. Note that firms that are not shown in a subplot exhibit a zero net change.	69
4.1	Flowchart depicting the interaction between the different levels of the bilevel optimization when the aggregator is participating (a) competitively, and (b) strategically.	82
4.2	The average hourly locational marginal prices for different penetration levels and a zero tax rate.	91
4.3	Illustrative supply curve.	92

4.4	The total energy discharged for the entire scheduling horizon by the EV fleet under different tax rates.	94
4.5	Monetary savings gained by the EV aggregator due to engaging in arbitrage.	95
4.6	Box plot displaying the distribution of the hourly charging profile under varying tax rates.	97
4.7	Box plot displaying the distribution of the hourly discharging profile under varying tax rates.	98
4.8	CO ₂ emissions due to charging EVs, relative to the zero-tax case, for different tax rates.	99
4.9	The increase in power output of gas and coal units under different tax rates for different penetration levels. Note that nuclear, hydro, and oil units exhibit zero change.	100
4.10	The change in CO ₂ emissions due to arbitrage for different tax rates.	101
4.11	The difference in power output, relative to the unidirectional case, of gas and coal units under different tax rates for different penetration levels. Note that nuclear, hydro, and oil units exhibit zero change.	102
B.1	14-Bus System Topology	130
B.2	Total System Load	131

LIST OF TABLES

Table Number	Page
2.1 Production (in MW) by fuel type for all scenarios. Note that the output of nuclear and hydro units is constant at 9,600MW and 7,200MW respectively in all test cases.	32
2.2 Abatement cost defined as the extra cost consumers pay per unit reduction of CO ₂ emissions when compared to the zero tax case.	34
2.3 False Position Method Computational Performance	38
2.4 Outcomes of the different subsidy design methods for the base case	44
3.1 Data for the participating firms	62
3.2 Tax revenue (in k\$) generated for different tax rates considering strategic and competitive behaviors of firms. Note that the difference in tax revenue between participating strategically and participating competitively is zero for firms that are not shown.	70
B.1 Load Distribution Among Buses	131
B.2 Transmission Line Data	132
B.3 Generating Units Data	133

Chapter 1

INTRODUCTION

1.1 Background

Climate change refers to long-lasting changes in weather patterns or changes in average weather conditions relative to long-term average conditions, and it is widely considered as the greatest challenge that faces our generation. The release of anthropogenic greenhouse gases (GHGs) in the atmosphere is regarded as one of the biggest culprits that is causing the change in climate we are experiencing. GHGs are gases that absorb the energy radiated from Earth towards space effectively trapping the heat in the lower atmosphere [1]. Many of which are naturally occurring in the atmosphere to maintain life sustaining temperatures. However, human activities have increased their concentration in the atmosphere, thereby raising the temperature of the planet beyond normal as can be seen in Fig. 1.1.

In recognition of the adverse effects associated with climate change (e.g., see [2]), The Kyoto Protocol was adopted on 11 December 1997 with the goal of reducing emissions from the following GHGs by at least 5% compared to 1990 levels [3]:

1. Carbon dioxide (CO_2)
2. Methane (CH_4)
3. Nitrous oxide (N_2O)
4. Hydrofluorocarbons (HFCs)
5. Perfluorocarbons (PFCs)
6. Sulphur hexafluoride (SF_6)

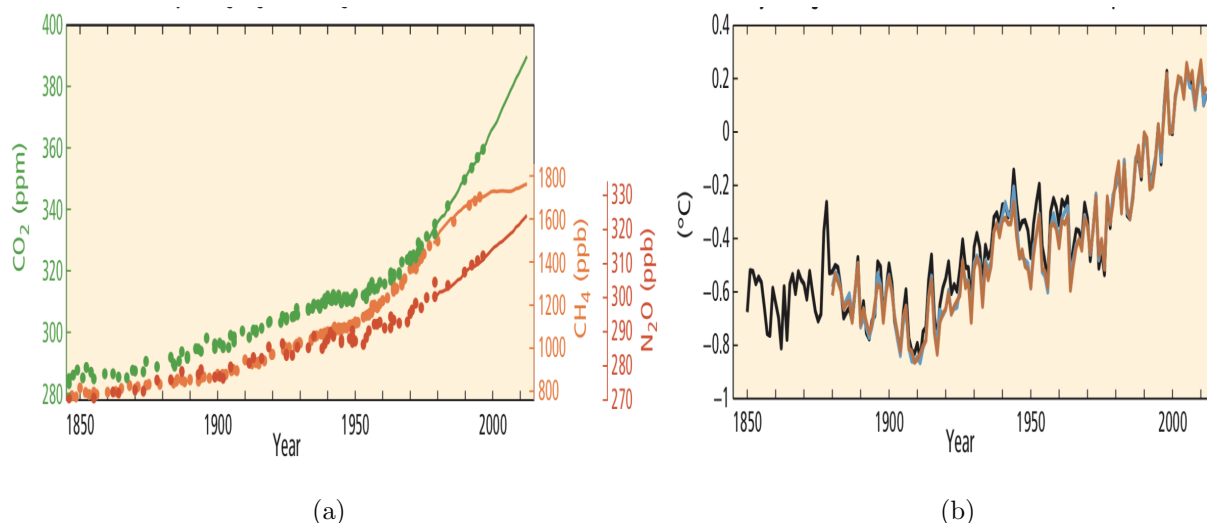


Figure 1.1: (a) Concentration of carbon dioxide, methane, and nitrous oxide in the atmosphere, and (b) land and ocean surface average combined temperature anomalies relative to the average over the period of 1986 to 2005 [7].

The legally binding protocol came into force in 16 February 2005 and had been ratified by 192 parties since its inception [4]. The protocol expired on 31 December 2012, however, it was extended to 2020 after the Doha amendment [5]. Currently, the extension is not enforced since it only has 112 ratifiers which is below the required threshold of 144.

Furthermore, the Paris Agreement, a separate instrument to combat climate change, was adopted on 12 December 2015. The main objective of the agreement is to hold the global average temperature to below 2°C above pre-industrial levels [6]. In contrast to the Kyoto Protocol, the Paris Agreement does not exempt developing countries from the responsibility of reducing emissions, and it gives individual countries the flexibility to choose the most suitable climate strategy. Nevertheless, the fact that the agreement is not legally binding has raised some concerns on whether it will achieve the desired outcome.

1.2 Targeting CO₂ Emissions in the Electricity Sector

Even though CO₂ has the smallest value of global warming potential (GWP), as presented in [8], relative to other GHGs (it absorbs less heat per molecule by comparison), it has been the primary focus when addressing the challenge of climate change. Due to its abundance in the atmosphere (see Fig. 1.2) and long decay time, CO₂ has the highest Radiative Forcing (RF), which is, according to the Intergovernmental Panel on Climate Change (IPCC):

“a measure of the net change in the energy balance of the Earth system in response to some external perturbation, with positive RF leading to a warming and negative RF to a cooling” and is measured in watts per meter squared (W/m²) [9].

The electricity sector has accounted for approximately 28% of all GHG emissions in the US in 2016 as shown in Fig. 1.3. More specifically, it is responsible for roughly 34% of all CO₂ emissions in the US making it the largest emitter of CO₂ in the nation. This is due to the fact that CO₂ is released from burning fossil fuel (primarily coal) as a by-product of the production of electric energy. Therefore, the electricity sector is considered a prime target whenever policy makers are designing policies with the goal of curbing CO₂ emissions.

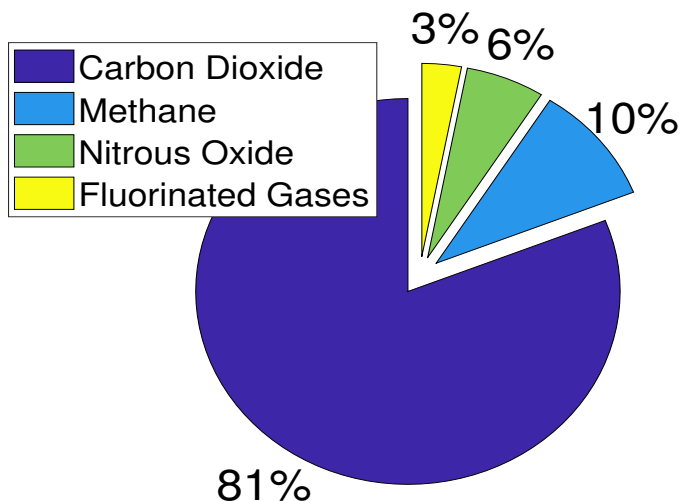


Figure 1.2: US Greenhouse Gas Emissions in 2016 by gas type [10].

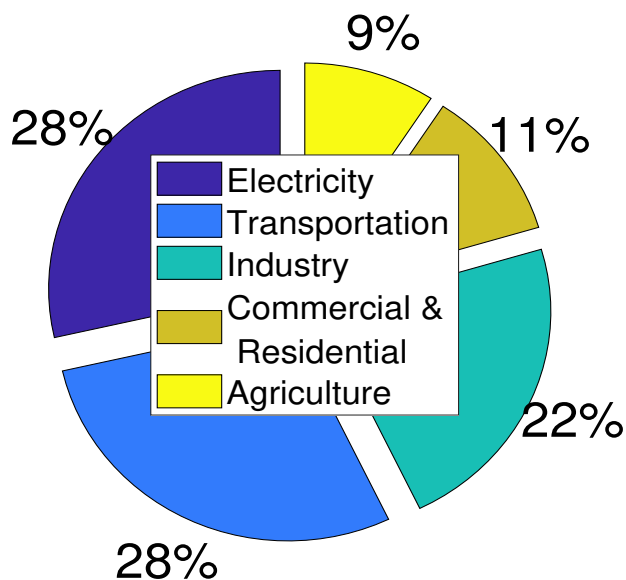


Figure 1.3: US Greenhouse Gas Emissions in 2016 by sectoral output. The graph was generated using data obtained from the United States Environmental Protection Agency (EPA) [10].

1.3 Market-Based Approaches to Reduce CO₂ Emissions

Market-based regulatory instruments work by setting an explicit price on carbon emissions, thereby encouraging a behavioral change through price signals instead of explicit directives [11]. In doing so, market-based policies expose all polluters to the same marginal abatement cost, and incentivize the innovation of new low-polluting technologies [12]. Therefore, economists usually argue in their favor claiming that they achieve the desired outcome at lower costs when compared to other policies. Carbon taxes and cap-and-trade policies are the most common market-based strategies that are implemented.

Although both of the aforementioned policies share some similarities (for example, both put a price on carbon emissions, generate revenue, and require monitoring [13]), they differ with regards to the method of implementation. A cap-and-trade policy sets a hard limit on

the permissible level of emissions while simultaneously establishing an auxiliary market for emission allowance trading. The European Union Emissions Trading System (EU ETS) [14] is an example of a real-world application of a cap-and-trade policy, and is the world largest emission trading market covering over three-quarter of international carbon trading.

Conversely, A carbon tax is a form of a Pigouvian tax [15] which works to internalize the cost of negative externalities (environmental damages in this case) associated with any market activity. Therefore, this policy sets a known explicit price on carbon emissions which acts to reduce the gap between the private cost and the social cost of producing electricity¹. British Columbia, Canada, for example, has been using this policy since 2008, and as of 1 April 2018, the carbon tax rate is \$35 per tonne of carbon dioxide equivalent [16].

There is an ongoing debate on which of the market-based approaches is the superior option. Cap-and-trade advocates are concerned about the environmental uncertainty associated with the implementation of carbon taxes, whereas supporters of carbon taxes usually point out the price uncertainty in the allowance market linked to the cap-and-trade policy. Even though there doesn't seem to be an unequivocal winner since the issue of whether to use pricing or quantities to regulate an economic variable is a longstanding one [17], a carbon tax policy has been gaining traction recently because of the advantages it has over its counterpart [18]. Notably, its implementation does not induce price volatility as experienced with a cap-and-trade policy. Moreover, a carbon tax is not as complex since it does not require an additional market place for trading purposes, nor does it necessitate the extra cost related to operating the market.

1.4 Outline of the Dissertation

Chapter 2: Optimally Designed Subsidies for Achieving Carbon Emissions Targets in Electric Power Systems

¹Without an explicit price on carbon emissions, the marginal cost of producing electrical energy incurred by carbon-emitting producers (private cost) does not account for the environmental damage caused by those producers (social cost).

Chapter 2 addresses one of the major impediments to the implementation of carbon pricing in electric power systems—the added cost to consumers due to the levied tax. In this chapter, we propose a novel multilevel complementary model that designs an optimal tax/subsidy policy to achieve any feasible reduction in carbon emissions. Through the use of linearization techniques, this non-linear multilevel model is transformed to a mixed-integer linear program that can be solved using commercial tools. Results obtained from applying the developed model demonstrate the effectiveness of the proposed approach in reducing carbon emissions without overburdening consumers with excessive tax rates and high prices of electric energy.

Chapter 3: Market Power in the Presence of Carbon Taxes in Electricity Markets

This chapter aims to investigate how strategic producers modify their offers in the day-ahead electricity market in response to the implementation of carbon taxes, and how this change would impact the level of carbon emissions. A Stackelberg game is used to model the interaction between the strategic producer and the electricity market. The Stackelberg game is formulated as a bilevel optimization in which the upper-level represents the strategic producer whose objective is to maximize its profit and the lower-level represents the day-ahead market clearing process with the objective of maximizing the social welfare. Numerical results from a 24-bus case study demonstrate that the strategic offers of producers will indeed be affected by the imposition of a carbon tax, and consequently, carbon emissions will duly change.

Chapter 4: The Impact of Carbon Pricing on the Optimal Participation of Electric Vehicle Aggregators in the Day-ahead Energy Market

In Chapter 4, we present our third and final framework of this dissertation. In this chapter, a complementary optimization model is developed to find the optimal bidding/offering strategy in carbon-taxed electricity markets for an aggregator managing a large fleet of electric vehicles. Numerical results from a 24-bus case study show how different carbon penalty

rates affect the optimal charging and discharging profiles scheduled by the aggregator. Results also show how different participation strategies implemented by the aggregator lead to different carbon emissions outcomes due to the added load from electrifying the transportation sector.

Chapter 5: Conclusion and Future Work

Chapter 5 summarizes the key findings of the proposed frameworks and provides suggestions for future work.

Chapter 2

OPTIMALLY DESIGNED SUBSIDIES FOR ACHIEVING CARBON EMISSIONS TARGETS IN ELECTRIC POWER SYSTEMS

2.1 Introduction

2.1.1 Motivation

As highlighted in Chapter 1, there is a dire need to regulate carbon emissions from the electricity sector and imposing a carbon tax is one of the well-established methods of doing so. Since the added carbon tax works by internalizing the cost of environmental damages, it will lead to an increase in the total cost of generating electricity incurred by carbon-emitting producers. Additionally, the demand for electricity is highly inelastic in the short run [19], so the higher costs caused by the levied taxes will inevitably be passed on to consumers in the form of higher prices for electric energy. Therefore, it is necessary to find alternative solutions to reduce CO₂ emissions without overwhelming consumers.

2.1.2 Proposed Solution

The framework presented in this chapter aims to achieve any feasible CO₂ reduction target by utilizing the revenue collected from the levied carbon tax. The tax revenue is optimally recycled to offer low-carbon electricity producers financial incentives in the form of production subsidies. The subsidies are provided to relatively clean producers that will otherwise not participate in the day-ahead energy market due to their higher costs.

A multilevel optimization approach is taken to formulate the problem where each level represents a different objective function. The goal of the upper level (UL) is to optimally solve for the tax rate required to maintain revenue neutrality and ensure that the subsidy

scheme does not leave a budget deficit. The middle level (ML) represents the regulating authority that is minimizing the cost of production subsidies offered to producers. The lower level (LL) is modeling the day-ahead energy market clearing process where the objective is to minimize the production cost of generating units while adhering to the constraints of electric power systems. One important feature of this work is the fact that the subsidies are offered on a time-varying and producer specific basis. A key advantage of this method in contrast with offering subsidies at a fixed rate or not offering them at all (i.e. imposing a tax only) is that it notably reduces the carbon tax rate required to maintain CO₂ emissions below a specific level.

2.2 Literature Survey

2.2.1 The Effectiveness and Associated Socio-Economic Costs of Carbon Taxes

The use of carbon taxes to mitigate CO₂ emissions and the effects of their implementation have been researched extensively. Park and Baldick investigated the effects of enacting different policies to reduce CO₂ emissions on the generation capacity expansion planning problem in [20]. The authors found that among the policies assessed, imposing a carbon tax is more efficient in term of CO₂ emissions reduction. Benavides *et al.* investigated the implications of applying a carbon tax on the Chilean electricity generation sector in [21]. Their studies demonstrate that, while a carbon tax is an effective method to reduce CO₂ emissions, it will also be accompanied by an increase in the price of electricity and a decrease in the annual GDP growth rate. Similarly, Vera and Sauma [22] found that CO₂ emissions is expected to reduce by 1% and the marginal cost of power production will increase by 3.4% with the introduction of a \$5/tCO₂e carbon tax in Chile. In [23], the authors explored the impacts of carbon taxes on the Chinese economy by proposing a dynamic recursive general equilibrium model. Their analysis showed that carbon taxes levied reduce CO₂ emissions depending on the tax rate considered. The reductions, however, come at the cost of decreasing the country's GDP—the higher the rate, the larger the decrease. The authors

suggested incorporating complementary policies to mitigate the negative consequences of the added taxes. Eser *et al.* [24] studied the impact of carbon taxes on the power systems in central Europe. The authors concluded that although the EU 40% greenhouse gas emissions reduction target for 2030 can be achieved, a high carbon tax rate of 40€/tCO_{2e} is required, which would lead to higher wholesale electricity prices.

Wang *et al.* [25] examined the distributional effects of carbon taxes on households and economic sectors. The authors highlighted the regressiveness of a carbon tax (with the electricity sector being more regressive than others) and how it would have a larger impact on the lower income households. The main reason for this regressivity can be attributed to the fact that poor households spend a greater portion of their income on fossil fuels compared to higher income households. Dissou and Siddiqui [26] further complemented the studies on the distributional impacts of carbon taxes by assessing the change in factor prices in addition to the change commodity prices. Their research shows that a U-shaped relationship exists between carbon taxes and inequality meaning that a low tax rate is actually progressive. In contrast, for higher tax rates, the opposite is observed and carbon taxes become regressive. Hence, achieving the same emissions reduction target with a much lower tax rate may come with the added benefit of decreasing inequality.

2.2.2 The Case for Revenue Recycling and Financial Incentives

In [27], Murray and Rivers assessed the effects of the revenue-neutral carbon tax implemented in British Columbia, Canada. The authors showed that the tax reduced emissions with relatively small impacts on inequality and on the aggregate economy. Additionally, the public perception was generally in favor of the carbon tax. In their study of the carbon tax in Portugal [28], Pereira *et al.* argued that in order to deliver on the triple dividend the policy aimed to achieve, all of revenue collected from the carbon tax must be recycled back into the economy. The authors in [29] used a dynamic energy-environment-economy computable general equilibrium model to study the impacts of imposing carbon taxes on the level of CO₂ emissions and the economic growth in China. Their research concluded that the effectiveness

of the carbon tax can be enhanced if the tax revenue is used to improve energy efficiency rather than being retained by the government. Liu and Lu [30] compared different revenue recycling schemes on the Chinese economy. Their results show that both studied schemes alleviate the negative impact of carbon taxes on the GDP with a production tax deduction yielding the lowest abatement cost. However, the consumption tax deduction will lead to the largest emissions reduction. Klenert and Mattauch [31] made the case that recycling the carbon tax revenue as uniform lump-sum transfers can be progressive as opposed to linear income tax cuts or lump-sum payments proportional to the households' productivity.

Galinato and Yoder developed a revenue neutral tax/subsidy scheme in [32]. Their studies on the motor fuel and electric power industries show that it is more advantageous to tax high emitters and use the revenue to fund the subsidies for low emitters as opposed to using the general tax fund. The authors in [33] used a top-down economy-energy-environment model to study multiple instruments commonly used for mitigating CO₂ emissions. Their work showed that, compared to the tax-only case, using the tax revenue to support non-carbon energy resources would result in a 40% reduction in the cost of climate change mitigation. In [34], Kainuma *et al.* proposed a bilevel model that represents two types of players: policy makers and consumers. Policy makers try to minimize CO₂ emissions by means of imposing carbon taxes on carbon-emitting technologies and offering subsidies to energy-saving technologies, whereas consumers want to minimize the cost of satisfying their consumption needs. The authors discussed the effects of offering subsidies in addition to carbon taxes and concluded that CO₂ emissions reduction targets can be achieved with lower tax rates when subsidies are properly allocated among the considered sectors. The authors in [35] presented a bilevel model with the goal of designing incentive policies to stimulate renewable energy investment in the generation capacity planning problem. Their studies showed that offering subsidies in conjunction with taxes is more efficient and leads to a decrease in the taxes and subsidies required to satisfy a given objective.

2.2.3 Multilevel Optimization

The concept of multilevel programming has been applied to model and solve many power systems problems. For example, Wei *et al.* [36] presented a bilevel model with the goal of setting optimal carbon tax rates levied on generating units in accordance with their CO₂ emissions. Moreover, this technique has been used in [37] to develop different offering strategies for electricity producers in the day-ahead energy market. Wang *et al.* [38] proposed a bilevel model in which generating companies make strategic generation capacity expansion decisions based on incomplete information. Garcés *et al.* provided a framework that addresses the transmission expansion planning problem within a market environment using a bilevel model in [39]. A bilevel model with the goal of minimizing consumer payment in electricity markets was presented in [40,41]. Electric grids vulnerability to deliberate attacks has been studied in [42–44], and modeling the participation of energy storage systems in electricity markets using a bilevel optimization can be found in [45–47].

2.3 Contributions

The contributions of the framework presented in this chapter are threefold.

1. A computationally tractable trilevel model is proposed to design optimal producer-specific, time-varying production subsidies for the electricity sector. In particular, the model takes into account realistic constraints associated with electricity markets. The designed subsidies work in conjunction with carbon taxes to achieve specified emissions targets at much lower tax rates while maintaining revenue neutrality.
2. The proposed nonlinear trilevel model is then transformed into an equivalent bilevel mixed-integer program that can be solved iteratively using suitable off-the-shelf software.
3. Comprehensive studies with numerical results and sensitivity analysis are presented in order to demonstrate the proposed model's effectiveness and efficiency in comparison

with a carbon tax only method.

2.4 Chapter Organization

The remainder of this chapter is structured as follows. Section 2.5 describes the formulation of the proposed trilevel model. Section 2.6 explains the procedure used to transform the trilevel model to a bilevel optimization and the approach taken to solve the resultant bilevel problem. Numerical results from a 14-bus illustrative example and a 24-bus case study are presented and discussed in Section 2.7. Finally, relevant conclusions are duly drawn in Section 2.8.

2.5 Model Formulation

As shown in Fig 2.1, the proposed trilevel model consists of an UL problem, a ML problem and a LL problem. The UL problem determines the tax rate to impose on carbon-emitting generating units based on the amount of subsidies and the dispatch decision obtained from the ML and LL respectively. The ML determines the optimal amount of subsidies offered to clean units considering endogenous dispatch decisions from the LL problem. Finally, the day-ahead electric energy market clearing process is modeled in the LL problem where all the generators' dispatch results are found considering the added tax and subsidy obtained from the UL and ML problems respectively.

2.5.1 Upper-Level Problem

$$\min P^{CO_2} \tag{2.1a}$$

subject to:

$$\Delta t \sum_{t \in \mathcal{T}} \sum_{g \in \mathcal{G}} \sum_{b \in \mathcal{B}} p_{t,g,b} S_{t,g,b} \leq \Delta t \sum_{t \in \mathcal{T}} \sum_{g \in \mathcal{G}} \sum_{b \in \mathcal{B}_g} e_g h_{g,b} P^{CO_2} p_{t,g,b} \tag{2.1b}$$

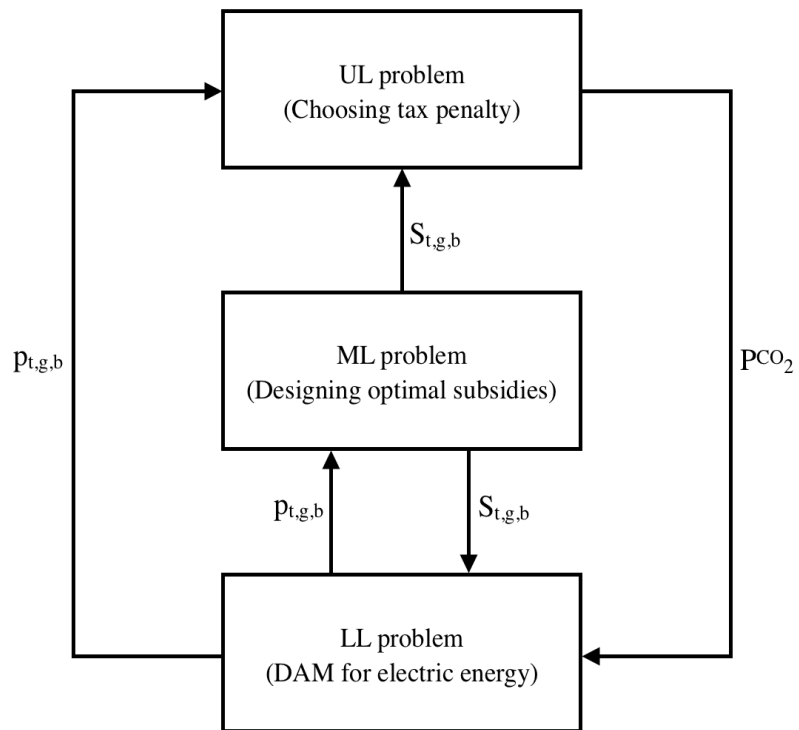


Figure 2.1: An illustration depicting how the different levels interact in the proposed trilevel model

The UL objective function (2.1a) minimizes the carbon tax penalty, P^{CO_2} , imposed on carbon-emitting generating units. Constraint (2.1b) enforces the tax revenue collected to be greater or equal to the total cost of subsidies.

2.5.2 Middle-Level Problem

$$\min_{S_{t,g,b}} \Delta t \sum_{t \in \mathcal{T}} \sum_{g \in \mathcal{G}} \sum_{b \in \mathcal{B}} p_{t,g,b} S_{t,g,b} \quad (2.2a)$$

subject to

$$0 \leq S_{t,g,b} \leq \bar{S}; \forall t \in \mathcal{T}, \forall g \in \mathcal{G}, \forall b \in \mathcal{B} \quad (2.2b)$$

$$\sum_{t \in \mathcal{T}} \sum_{g \in \mathcal{G}} \sum_{b \in \mathcal{B}_g} \Delta t e_g h_{g,b} p_{t,g,b} \leq E^{max} \quad (2.2c)$$

The ML problem (2.2) represents the regulating authority. The objective function (2.2a) is the total cost of production subsidies being offered to generating units. Constraints (2.2b) enforce the subsidy rate to be non-negative and lower than a rate cap. Constraint (2.2c) enforces the upper bound on the level of CO₂ emissions to ensure that it is below a specified target.

2.5.3 Lower-Level Problem

The LL problem models the day-ahead energy market clearing process where the objective is to supply the load at minimal cost as expressed in (2.3a). Note that a piecewise linear cost curve is assumed for each generator and that the imposed carbon tax (as done in [48, 49]), as well as the production subsidies offered by the regulating authority, are incorporated into the generating unit's cost function.

$$\min_{\Psi^{LL}} \Delta t \sum_{t \in \mathcal{T}} \sum_{g \in \mathcal{G}} \sum_{b \in \mathcal{B}_g} \left[c_g h_{g,b} + e_g h_{g,b} P^{CO_2} - S_{t,g,b} \right] p_{t,g,b} \quad (2.3a)$$

where $\Psi^{LL} = \{p_{t,g}, p_{t,g,b}, pf_{t,l}, \theta_{t,n}\}$ is the set of the primal LL decision variables. The LL constraints are defined below and the dual variables associated with each constraint is shown in between parentheses following a colon.

2.5.3.1 Nodal Power Balance

The power injected into each bus must equal the power flowing out of the bus for all time periods.

$$\sum_{g \in \mathcal{G}} A_{g,n}^{gen} p_{t,g} - \sum_{l \in \mathcal{L}} A_{l,n}^{line} p_{f,t,l} = D_{t,n} : (\lambda_{t,n}); \forall t \in \mathcal{T}, \forall n \in \mathcal{N} \quad (2.3b)$$

2.5.3.2 Network Constraints

As explained in [50], a lossless DC linear approximation is adopted to model the transmission network used for the day-ahead electric energy market in the LL problem. Equation (2.3c) defines the real power flow in each transmission line. Constraints (2.3d) enforce the capacity limits of each transmission line.

$$p_{f,t,l} = B_l \sum_{n \in \mathcal{N}} A_{l,n}^{line} \theta_{t,n} : (\gamma_{t,l}); \forall t \in \mathcal{T}, \forall l \in \mathcal{L} \quad (2.3c)$$

$$-\bar{F}_l \leq p_{f,t,l} \leq \bar{F}_l : (\mu_{t,l}^{min}, \mu_{t,l}^{max}); \forall t \in \mathcal{T}, \forall l \in \mathcal{L} \quad (2.3d)$$

2.5.3.3 Dispatch Constraints

Constraints (2.3e) enforce the upper and lower bounds of each generating unit. Equation (2.3f) states that the output of each generating unit is the summation of all block outputs. Constraints (2.3g)–(2.3h) enforce the ramping limits of each generating unit.

$$0 \leq p_{t,g,b} \leq \bar{P}_{g,b} : (\zeta_{t,g,b}^{min}, \xi_{t,g,b}^{max}); \forall t \in \mathcal{T}, \forall g \in \mathcal{G}, \forall b \in \mathcal{B}_g \quad (2.3e)$$

$$\sum_{b \in \mathcal{B}_g} p_{t,g,b} = p_{t,g} : (\chi_{t,g}); \forall t \in \mathcal{T}, \forall g \in \mathcal{G} \quad (2.3f)$$

$$p_{t+1,g} - p_{t,g} \leq R_g^{up} : (\zeta_{t,g}^{up}); \forall t = 1 \dots n_T - 1, \forall g \in \mathcal{G} \quad (2.3g)$$

$$p_{t,g} - p_{t+1,g} \leq R_g^{dn} : (\zeta_{t,g}^{dn}); \forall t = 1 \dots n_T - 1, \forall g \in \mathcal{G} \quad (2.3h)$$

2.5.3.4 Angle Stability Constraints

The upper and lower angle bounds of each bus are imposed in (2.3i) and the reference bus is defined in (2.3j).

$$-\pi \leq \theta_{t,n} \leq \pi : (\rho_{t,n}^{min}, \rho_{t,n}^{max}); \forall t \in \mathcal{T}, \forall n \in \mathcal{N} \quad (2.3i)$$

$$\theta_{t,n=\text{ref}} = 0 : (\sigma_t); \forall t \in \mathcal{T} \quad (2.3j)$$

2.6 Solution Methodology

2.6.1 Transformation to a Bilevel Problem

The first step is to reformulate the trilevel model to a bilevel optimization which can be done by replacing the ML and LL problems with their single-level equivalent. This is possible since the LL problem (2.3) is linear and continuous, and thus, can be replaced by its KKT optimality conditions as explained in [51, 52]. Note that the bilinear term $p_{t,g,b}S_{t,g,b}$ in the LL objective function does not render the LL problem nonlinear because it involves multiplication of variables from different levels, namely, the ML and LL, and variables from one level are considered parameters in the other.

2.6.1.1 MPEC

The Mathematical Problem with Equilibrium Constraints (MPEC) form of the single-level equivalent is given by (2.4a)–(2.4o) as follows:

$$\min (2.2a) \quad (2.4a)$$

subject to

$$(2.2b) - (2.2c), (2.3b) - (2.3c), (2.3f), \text{ and } (2.3j) \quad (2.4b)$$

$$\sum_{l \in \mathcal{L}} B_l A_{l,n}^{line} \gamma_{t,l} - (\sigma_t)_{n=\text{ref}} - \rho_{t,n}^{min} + \rho_{t,n}^{max} = 0; \forall t \in \mathcal{T}, \forall n \in \mathcal{N} \quad (2.4c)$$

$$\sum_{n \in \mathcal{N}} A_{l,n}^{line} \lambda_{t,n} - \gamma_{t,l} + \mu_{t,l}^{max} - \mu_{t,l}^{min} = 0; \forall t \in \mathcal{T}, \forall l \in \mathcal{L} \quad (2.4d)$$

$$c_{g,b} h_{g,b} + e_g h_{g,b} P^{CO_2} - S_{t,g,b} + \chi_{t,g} + \xi_{t,g,b}^{max} - \xi_{t,g,b}^{min} = 0; \forall t \in \mathcal{T}, \forall g \in \mathcal{G}, \forall b \in \mathcal{B}_g \quad (2.4e)$$

$$\sum_{n \in \mathcal{N}} A_{g,n}^{gen} \lambda_{t,n} + \chi_{t,g} + \zeta_{t+1,g}^{dn} - \zeta_{t,g}^{dn} + \zeta_{t,g}^{up} - \zeta_{t+1,g}^{up} = 0; \forall t < n_T, \forall g \in \mathcal{G} \quad (2.4f)$$

$$\sum_{n \in \mathcal{N}} A_{g,n}^{gen} \lambda_{n_T,n} + \chi_{n_T,g} - \zeta_{n_T,g}^{dn} + \zeta_{n_T,g}^{up} = 0; \forall g \in \mathcal{G} \quad (2.4g)$$

$$0 \leq \mu_{t,l}^{min} \perp (pf_{t,l} + \bar{F}_l) \geq 0; \forall t \in \mathcal{T}, \forall l \in \mathcal{L} \quad (2.4h)$$

$$0 \leq \mu_{t,l}^{max} \perp (\bar{F}_l - pf_{t,l}) \geq 0; \forall t \in \mathcal{T}, \forall l \in \mathcal{L} \quad (2.4i)$$

$$0 \leq \xi_{t,g,b}^{min} \perp p_{t,g,b} \geq 0; \forall t \in \mathcal{T}, \forall g \in \mathcal{G}, \forall b \in \mathcal{B}_g \quad (2.4j)$$

$$0 \leq \xi_{t,g,b}^{max} \perp (\bar{P}_{g,b} - p_{t,g,b}) \geq 0; \forall t \in \mathcal{T}, \forall g \in \mathcal{G}, \forall b \in \mathcal{B}_g \quad (2.4k)$$

$$0 \leq \zeta_{t,g}^{up} \perp (R_g^{up} - p_{t+1,g} + p_{t,g}) \geq 0; \forall t < n_T, \forall g \in \mathcal{G} \quad (2.4l)$$

$$0 \leq \zeta_{t,g}^{dn} \perp (R_g^{dn} - p_{t,g} + p_{t+1,g}) \geq 0; \forall t < n_T, \forall g \in \mathcal{G} \quad (2.4m)$$

$$0 \leq \rho_{t,l}^{min} \perp (\theta_{t,n} + \pi) \geq 0; \forall t \in \mathcal{T}, \forall n \in \mathcal{N} \quad (2.4n)$$

$$0 \leq \rho_{t,l}^{max} \perp (\pi - \theta_{t,n}) \geq 0; \forall t \in \mathcal{T}, \forall n \in \mathcal{N} \quad (2.4o)$$

2.6.1.2 Linearizing the MPEC

The MPEC shown above contains the following sources of nonlinearities:

1. The bilinear term $\sum_{t \in \mathcal{T}} \sum_{g \in \mathcal{G}} \sum_{b \in \mathcal{B}} p_{t,g,b} S_{t,g,b}$ in the objective function (2.4a)
2. The complementary slackness conditions (2.4h)–(2.4o)

In order to transform the MPEC into a single-level mixed-integer linear program, we first apply the equality associated with the strong duality theorem [53] which will yield an equivalent linear form of the bilinear term stated above as shown in (2.5). Then, we utilize the technique proposed in [54] to replace the complementary slackness conditions of the form $0 \leq a \perp b \geq 0$ with a set of mixed-integer linear conditions as follows: $a \geq 0, b \geq 0, a \leq uM, b \leq (1-u)M$, where u is an auxiliary binary variable and M is a large positive constant. Guidelines for choosing a suitable value for M can be found in [55, 56].

$$\begin{aligned}
\sum_{t \in \mathcal{T}} \sum_{g \in \mathcal{G}} \sum_{b \in \mathcal{B}} p_{t,g,b} S_{t,g,b} &= \sum_{t \in \mathcal{T}} \sum_{g \in \mathcal{G}} \sum_{b \in \mathcal{B}_g} (c_g + e_g P^{CO_2}) h_{g,b} p_{t,g,b} \\
&+ \sum_{t \in \mathcal{T}} \sum_{l \in \mathcal{L}} \bar{F}_l (\mu_{t,g}^{min} + \mu_{t,g}^{max}) + \sum_{t \in \mathcal{T}} \sum_{g \in \mathcal{G}} \sum_{b \in \mathcal{B}_g} \bar{P}_{g,b} \xi_{t,g,b}^{max} \\
&+ \sum_{t=1}^{n_T-1} \sum_{g \in \mathcal{G}} R_g^{up} \zeta_{t,g}^{up} + \sum_{t=1}^{n_T-1} \sum_{g \in \mathcal{G}} R_g^{dn} \zeta_{t,g}^{dn} \\
&+ \sum_{t \in \mathcal{T}} \sum_{n \in \mathcal{N}} \pi (\rho_{t,g}^{min} + \rho_{t,g}^{max}) - \sum_{t \in \mathcal{T}} \sum_{n \in \mathcal{N}} D_{t,n} \lambda_{t,n} \tag{2.5}
\end{aligned}$$

2.6.1.3 Complete Bilevel Model

Fig. 2.2 shows the final form of the bilevel model which is represented mathematically by the following:

$$\min \quad (2.1a) \tag{2.6a}$$

subject to

$$(2.1b) \tag{2.6b}$$

$$p_{t,g,b} \text{ and } S_{t,g,b} \in \operatorname{argmin} \left\{ \quad \right. \quad (2.5) \quad (2.7a)$$

subject to

$$(2.2b) - (2.2c), (2.3b) - (2.3j), \text{ and } (2.4c) - (2.4g) \quad (2.7b)$$

$$\mu_{t,l}^{\min} \leq u_{t,l}^{\mu^1} M; \forall t \in \mathcal{T}, \forall l \in \mathcal{L} \quad (2.7c)$$

$$pf_{t,l} + \bar{F}_l \leq (1 - u_{t,l}^{\mu^1}) M; \forall t \in \mathcal{T}, \forall l \in \mathcal{L} \quad (2.7d)$$

$$\mu_{t,l}^{\max} \leq u_{t,l}^{\mu^2} M; \forall t \in \mathcal{T}, \forall l \in \mathcal{L} \quad (2.7e)$$

$$\bar{F}_l - pf_{t,l} \leq (1 - u_{t,l}^{\mu^2}) M; \forall t \in \mathcal{T}, \forall l \in \mathcal{L} \quad (2.7f)$$

$$\xi_{t,g,b}^{\min} \leq u_{t,g,b}^{\xi^1} M; \forall t \in \mathcal{T}, \forall g \in \mathcal{G}, \forall b \in \mathcal{B}_g \quad (2.7g)$$

$$p_{t,g,b} \leq (1 - u_{t,g,b}^{\xi^1}) M; \forall t \in \mathcal{T}, \forall g \in \mathcal{G}, \forall b \in \mathcal{B}_g \quad (2.7h)$$

$$\xi_{t,g,b}^{\max} \leq u_{t,g,b}^{\xi^2} M; \forall t \in \mathcal{T}, \forall g \in \mathcal{G}, \forall b \in \mathcal{B}_g \quad (2.7i)$$

$$\bar{P}_{g,b} - p_{t,g,b} \leq (1 - u_{t,g,b}^{\xi^2}) M; \forall t \in \mathcal{T}, \forall g \in \mathcal{G}, \forall b \in \mathcal{B}_g \quad (2.7j)$$

$$\zeta_{t,g}^{up} \leq u_{t,g}^{\zeta^1} M; \forall t < n_T, \forall g \in \mathcal{G} \quad (2.7k)$$

$$R_g^{up} - p_{t+1,g} + p_{t,g} \leq (1 - u_{t,g}^{\zeta^1}) M; \forall t < n_T, \forall g \in \mathcal{G} \quad (2.7l)$$

$$\zeta_{t,g}^{dn} \leq u_{t,g}^{\zeta^2} M; \forall t < n_T, \forall g \in \mathcal{G} \quad (2.7m)$$

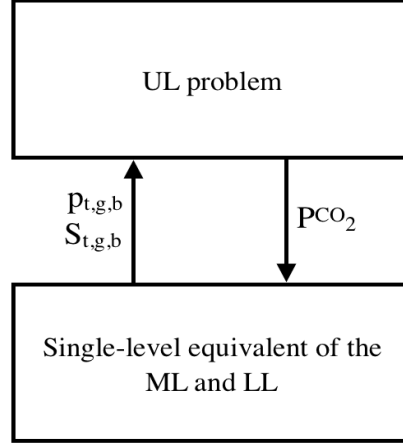


Figure 2.2: An illustration of the interface between the different levels of the resultant bilevel model

$$R_g^{dn} - p_{t,g} + p_{t+1,g} \leq (1 - u_{t,g}^{\zeta^2})M; \forall t < n_T, \forall g \in \mathcal{G} \quad (2.7n)$$

$$\rho_{t,l}^{min} \leq u_{t,n}^{\rho^1}M; \forall t \in \mathcal{T}, \forall n \in \mathcal{N} \quad (2.7o)$$

$$\theta_{t,n} + \pi \leq (1 - u_{t,n}^{\rho^1})M; \forall t \in \mathcal{T}, \forall n \in \mathcal{N} \quad (2.7p)$$

$$\rho_{t,l}^{max} \leq u_{t,n}^{\rho^2}M; \forall t \in \mathcal{T}, \forall n \in \mathcal{N} \quad (2.7q)$$

$$\pi - \theta_{t,n} \geq (1 - u_{t,n}^{\rho^2})M; \forall t \in \mathcal{T}, \forall n \in \mathcal{N} \quad (2.7r)$$

$$\mu^{max}, \mu^{min}, \xi^{max}, \xi^{min}, \zeta^{up}, \zeta^{dn}, \rho^{max}, \rho^{min} \geq 0 \quad (2.7s)$$

$$u^{\mu^1}, u^{\mu^2}, u^{\xi^1}, u^{\xi^2}, u^{\zeta^1}, u^{\zeta^2}, u^{\rho^1}, u^{\rho^2} \in \{0, 1\} \}. \quad (2.7t)$$

2.6.2 Solving the Bilevel Problem

To solve the resultant bilevel problem, we employ a technique similar to the one proposed in [57]. The False Position method [58], an iterative root-finding algorithm, is adopted to find the minimum tax rate needed to finance the total cost of subsidies. The algorithm starts by initializing an interval for the tax rate $[P_{LB}^{CO_2}, P_{UB}^{CO_2}]$ within which the root of the function must exist. It then proceeds by finding the root of the secant line connecting the function values at the upper and lower bounds of the interval. Based on the sign of the function evaluated at the secant line root, the algorithm updates the bounds of the interval and then repeats the process until the root of the function is found. Since the goal is to find the minimum carbon tax penalty that we need to impose such that the tax revenue is larger than the cost of subsidies required to achieve an emissions target, the function evaluated in the algorithm is:

$$f(P^{CO_2}) = R(P^{CO_2}) - C(S_{t,g,b})$$

where $R(P^{CO_2})$ and $C(S_{t,g,b})$ are the tax revenue and the cost of subsidies, respectively, and are defined as follows:

$$R(P^{CO_2}) = \Delta t \sum_{t \in \mathcal{T}} \sum_{g \in \mathcal{G}} \sum_{b \in \mathcal{B}_g} e_g h_{g,b} P^{CO_2} p_{t,g,b}$$

$$C(S_{t,g,b}) = \Delta t \sum_{t \in \mathcal{T}} \sum_{g \in \mathcal{G}} \sum_{b \in \mathcal{B}} p_{t,g,b} S_{t,g,b}$$

The volumes of the cleared power output for each generating unit ($p_{t,g,b}$) and the amount of monetary subsidies given to generating units ($S_{t,g,b}$) used in the calculations above are obtained by solving (2.7). The root of the given function, $f(P^{CO_2})$, would then be the desired tax rate. A detailed flowchart of the algorithm is shown in Fig. 2.3.

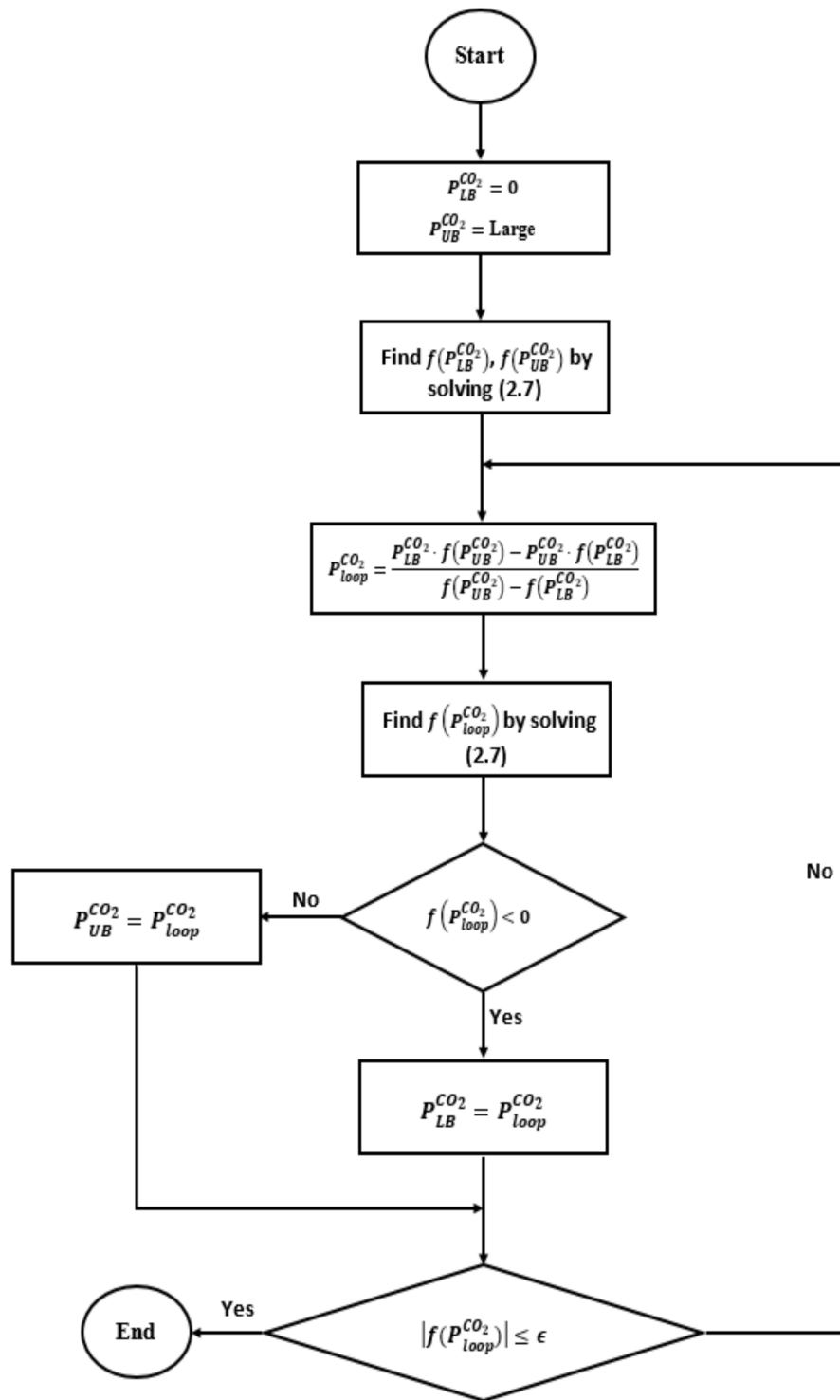


Figure 2.3: Flowchart for finding the optimal tax rate using the False Position method

2.7 Simulation Results

All simulation results are obtained by solving the model using CPLEX v12.5 [59] under GAMS v24.0 [60] as a mixed-integer linear program with a maximum optimality gap of 0.1%. A tolerance of 0.01% was used for the False Position method stopping criteria (ϵ).

2.7.1 Illustrative Example: 14-Bus Test System

The numerical results discussed in this section are based on applying the proposed approach to a modified version of the test system found in [61], which consists of 14 buses, 5 generating units, 20 transmission lines, and load at 11 buses, over a 24-hour scheduling horizon. The generating units used in the test system are shown in Table B.3 and are obtained from [62]. The fuel prices from [63] are used to convert each incremental heat rate block from MBtu to dollars. All other relevant data used for the test system can be found in Appendix B.

2.7.1.1 System Characteristics

Solving an economic dispatch for the system, which is equivalent to solving (2.3) with the tax rate, P^{CO_2} , and the production subsidies, $S_{t,g,b}$, equal to zero, yields the zero tax rate solution. The total CO_2 emissions given that no taxes are being enforced is found to be $4764.54 \text{ tCO}_2\text{e}^1$ which is considered the upper bound on the amount of CO_2 emitted. Finding the minimum emissions that can be realized for the test system requires solving for the minimum emissions dispatch. This is equivalent to solving (2.3), but with substituting the objective function (2.3a) with the one shown in (2.8). The minimum emissions solution yields a value of $4128.02 \text{ tCO}_2\text{e}$ which is a 13.36% reduction in emissions when compared to the minimum cost solution. The black dashed line in Fig. 2.4 shows the required tax rate for different levels of emissions using carbon taxes only. The plot is found by solving (2.3) with $S_{t,g,b}$ equal to

¹ CO_2 emissions are expressed in short tons. 1 short ton is equivalent to 2000 lbs.

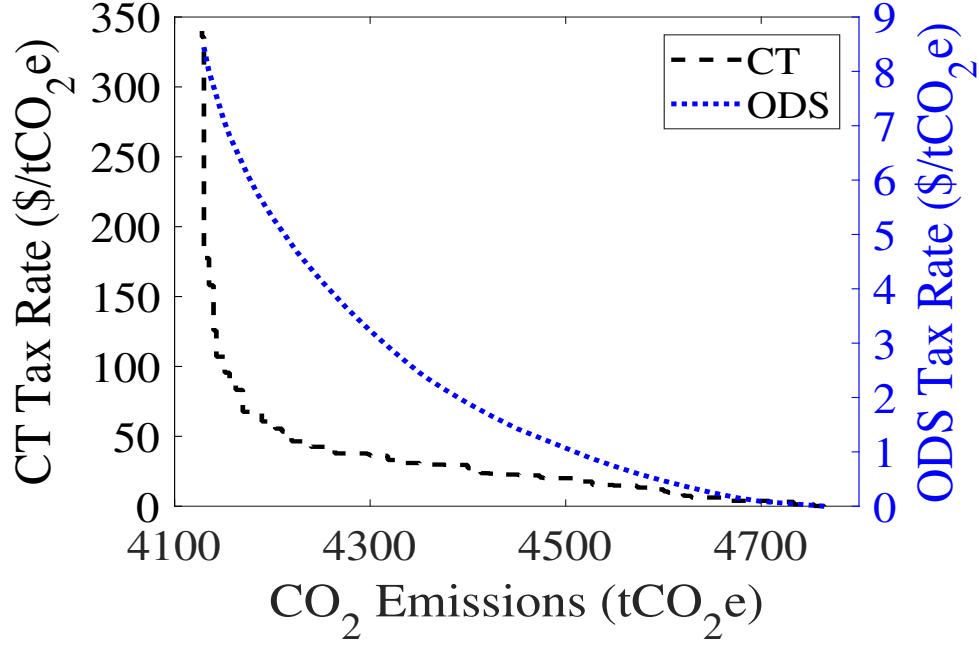


Figure 2.4: Required tax rate as a function of CO₂ emissions

zero and varying P^{CO_2} in increments of $\$0.01/tCO_2e$.

$$\min \Delta t \sum_{t \in \mathcal{T}} \sum_{g \in \mathcal{G}} \sum_{b \in \mathcal{B}_g} e_g h_{g,b} p_{t,g,b} \quad (2.8)$$

2.7.1.2 Discussion

Referring to Fig. 2.4, we can see the tax rate needed in order to achieve a specific emissions level for both the tax only method (CT) and the proposed approach where subsidies are offered (ODS). Note that they are plotted on different axes for the sake of clarity. It is apparent that for both methods the tax rate must increase to reduce emissions. However, the difference when comparing the rate of increase is what makes our approach more effective and a far better option when setting emissions targets. This is particularly noticeable as we approach the minimum emissions limit of the system. For example, reducing emissions by

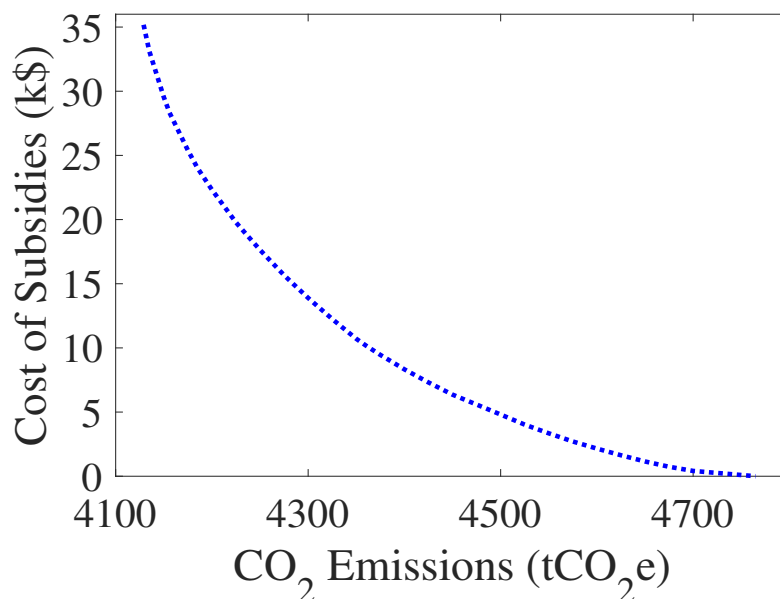


Figure 2.5: Total cost of subsidies as a function of CO₂ emissions

575.36 tCO₂e, which is roughly 90% of the maximum amount that can be reduced, would require a tax rate of \$60.61/tCO₂e when using the CT method. If, however, we would like to realize the minimum emissions solution, a staggering tax rate of \$335.69/tCO₂e must be set when using the CT method. Alternatively, setting the same targets under the ODS method would only require tax rates of \$5.60/tCO₂e and \$8.78/tCO₂e respectively. Therefore, not only does the ODS method require lower taxes to achieve desired reductions, it also does it for the entire range of reduction targets without sizable increases in the tax rate. The increase in taxes in the ODS method is necessary when curbing more emissions due to the increase in the subsidies required to remunerate the lower emitting generating units as can be seen in Fig. 2.5.

The effects each method has on the total cost of consumption², which is the cost con-

²Since carbon taxes are supposed to be revenue-neutral, all revenue collected when analyzing the CT method is recycled back to tax payers in the form of cost reduction. Therefore, the consumption costs shown for the CT method is actually the cost consumers pay to satisfy their load minus the tax revenue.

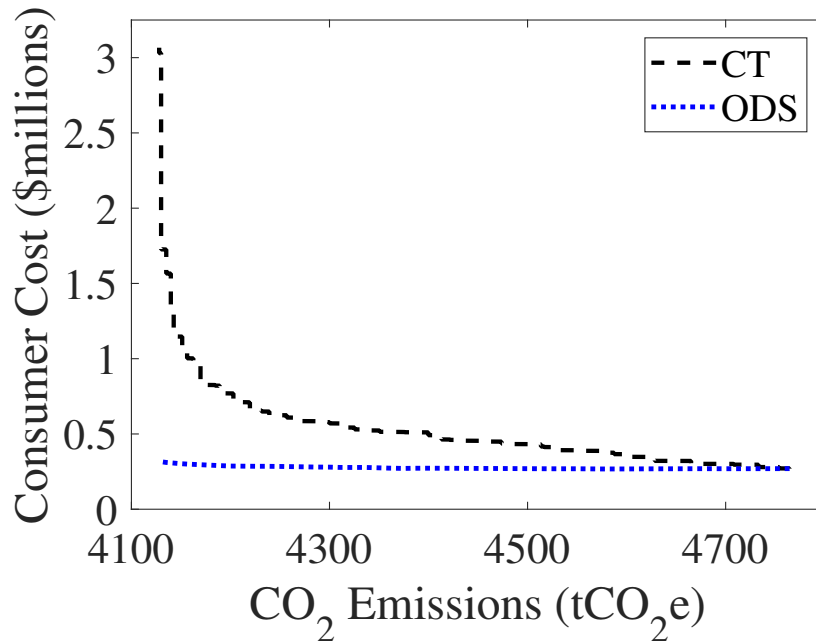


Figure 2.6: Total cost of consumption (with reimbursement) as a function of CO₂ emissions

sumers incur to satisfy their load, can be seen in Fig. 2.6. Under zero tax, both methods yield the same cost of \$269,756.50. However, they quickly diverge as the constraints on the level of emissions get tighter. This is due to the difference in the tax rate required between the two methods. Increasing carbon taxes will bring about higher locational marginal prices (LMPs) which will lead to an increase in the total cost paid by consumers. Consequently, the consumption cost is the highest when setting the emissions level to the lowest level possible. At this level, the total cost incurred under the CT method is \$3,028,915.50 which is a 1022.83% increase in cost when compared to the zero tax consumption cost. Conversely, it is found when using the ODS method that the total cost is \$317,521.87, a 17.71% increase.

Fig. 2.7 shows that the energy share of each generating unit changes as the level of CO₂ emissions is reduced. As we increase the amount of emissions reduced, the cheaper coal generators are phased out and their energy share is shifted to the more expensive but relatively cleaner oil units. Note that there are no CO₂ emissions associated with the nuclear

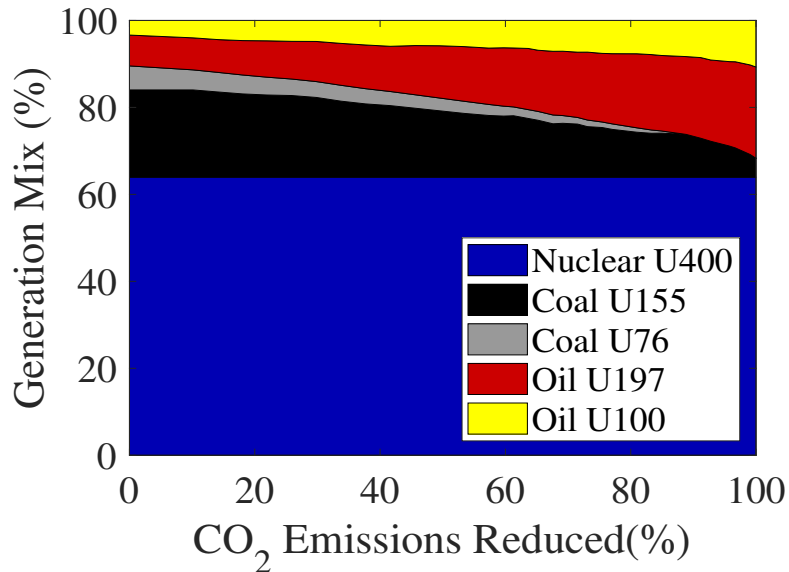


Figure 2.7: Share of total production for each generating unit as a function of CO₂ emissions reduced (relative to the highest achievable reduction target)

generator, hence, its production is constant for all reduction targets.

2.7.2 Case Study: IEEE 24-Bus Reliability Test System

In this section, the proposed model is applied on a modified version of the IEEE 24-bus reliability test system found in [64]. The test system contains 24 conventional generating units and 6 hydro units, 24 buses, 38 transmission lines, and load at 17 buses. All simulations were conducted considering a 24-hour scheduling period.

2.7.2.1 Test Cases

The following scenarios are assessed to validate the efficacy of the proposed scheme. In all scenarios, the target reduction when using the ODS method was set to be the maximum attainable for the test system i.e. the minimum feasible level of CO₂ emissions.

- **Base:** the nominal test case which will be used as the benchmark.

- **Transmission Capacity:** the capacity of all transmission lines is increased/decreased by 35%.
- **Gas Prices:** the price of gas is increased/decreased by 10% to model the fluctuations in the spot price of natural gas [65].
- **Demand Change:** the hourly load of the system is increased/decreased by 2%.
- **Coal Retirement:** the 350MW coal unit located at bus 23 is retired (11.6% of total capacity) to model the expected decrease in coal generation capacity [66,67].

2.7.2.2 Results

The impact each scenario has on the level of CO₂ emissions and the required tax penalty can be seen in Fig. 2.8. Table 2.1 and Fig. 2.13 show the output and profit of generating units respectively. Finally, relevant costs associated with the case study are shown in Fig. 2.10.

System Emissions and Tax Rate

1. **Transmission Capacity:** increasing the capacity of all transmission lines will lead to a modest decrease (0.18%) in CO₂ emissions when no taxes are imposed. This is due to the fact that the output of gas units increases slightly by 27.73MW at the expense of coal units because of the additional capacity of the transmissions corridors. Moreover, the minimum level of emissions decreases by 2.76% resulting in an increase in the tax rate imposed in the ODS method to a value of \$13.12/tCO_{2e} because of the additional subsidies given to cleaner units. In contrast, decreasing the capacity of the lines will further constrain the transmission corridors, and thus, will lead to a small increase (0.79%) in the level of emissions under zero taxes. Even though the amount of emissions curbed is lower in this case, the ODS tax rate increases as in the case of expanded capacity mainly due to:

- (a) The increase in production of oil units by 10.87%.
- (b) The increase in production of single-cycle gas units by 10.07%.

Both (a) and (b) warrant additional subsidies since oil units have the highest fuel cost in the system and single-cycle gas units have higher incremental heat rates when compared to combined-cycle gas units making them less efficient and more costly.

2. **Gas Prices:** the increase in gas prices will shift 194.85MW of output power from gas units to coal units increasing CO₂ emissions by 0.67% when the tax rate is zero. Conversely, when gas prices decrease under zero tax, CO₂ emissions decrease by 5.84% owing to the displacement of 2319.07MW from coal units to gas units. In both test cases, the minimum level of emissions remains unchanged, yet the necessary ODS tax rate varies since the price deviation will affect the marginal cost of production associated with gas units which would consequently induce different amounts of subsidies. The 10% increase (decrease) in gas prices will bring about an increase (decrease) in the ODS tax rate by 14.61% (13.77%) indicating that the required tax rate in the ODS method is sensitive to the price of natural gas the most amongst all other cases.
3. **Demand Change:** as expected, the change in the system load will cause a change in the no tax emissions since the total output of units will vary depending on whether the load increases or decreases. Similarly, load deviations will also impact the reduction target. For a rise in demand, the tax rate decreases because of *i*) the lower reduction target, and *ii*) the levied tax generates more revenue due to the increase in the power output of thermal units that is necessary to serve the additional load. By comparison, a 2% load reduction will increase the tax rate for reasons opposite to the ones explained in the load increase scenario.
4. **Coal Retirement:** the zero tax CO₂ emissions decrease by 10.46% because all of power generated by the coal unit shifts to gas and oil units that are relatively cleaner.

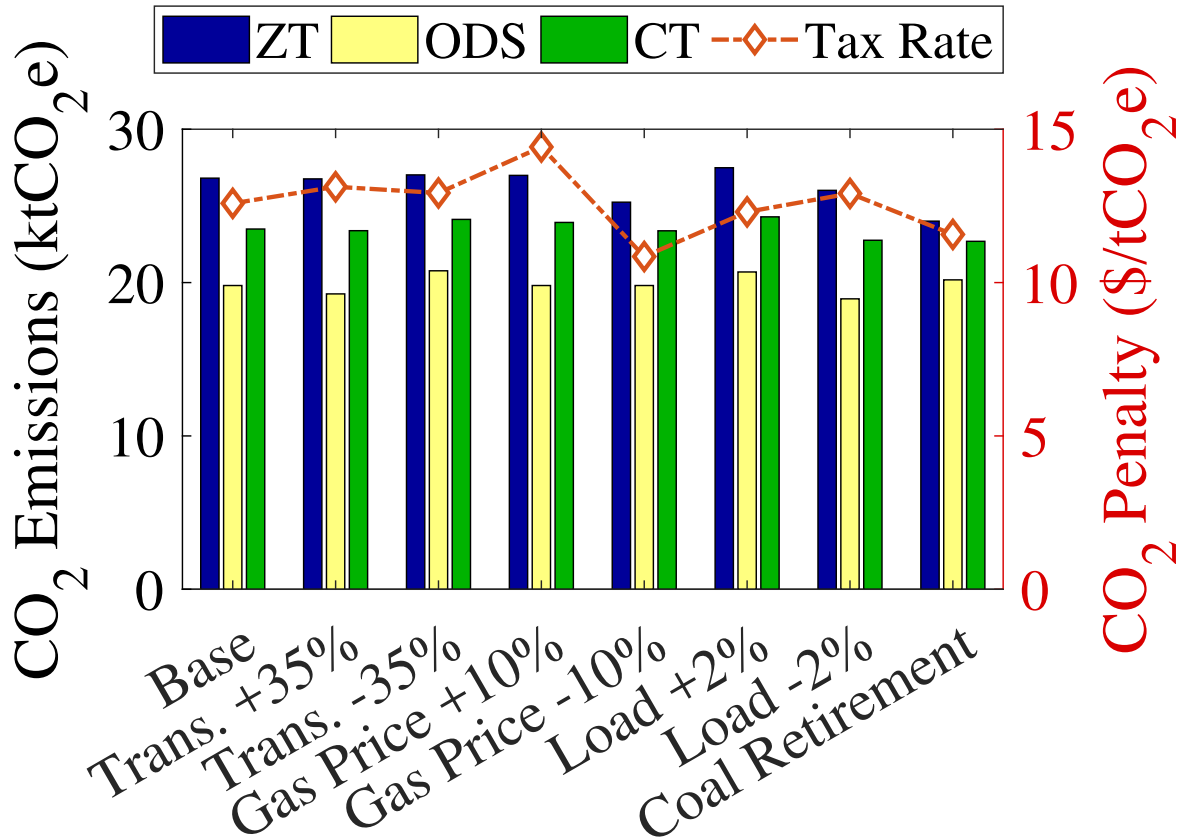


Figure 2.8: The amount of CO₂ emissions under no taxes (ZT), carbon taxes only (CT), and carbon taxes with subsidies (ODS) in addition to the necessary tax rate associated with the ODS method to achieve the reduction target for all test cases. Note that the same tax rate used in the ODS method was also used in the CT method.

In this case, the minimum emissions level is higher when compared to the base case which can be attributed to the increase in production of other coal and oil units that are operating at higher incremental heat rates. Therefore, the tax rate decreases but not by much since oil units require higher amounts of subsidies because of their high costs.

Table 2.1: Production (in MW) by fuel type for all scenarios. Note that the output of nuclear and hydro units is constant at 9,600MW and 7,200MW respectively in all test cases.

		Coal	Gas	Oil
Base	ZT	24499.72	9284.13	0
	ODS	9378.65	23332.22	1072.98
	CT	19532.01	14251.85	0
Trans. +35%	ZT	24471.99	9311.589	0
	ODS	8346.78	24384.98	1052.10
	CT	19410.03	14373.83	0
Trans. -35%	ZT	24600.95	9182.90	0
	ODS	10747.67	21846.61	1189.57
	CT	20316.19	13467.66	0
Gas Price +10%	ZT	24694.57	9089.29	0
	ODS	9378.65	23332.22	1072.98
	CT	20111.49	13672.37	0
Gas Price -10%	ZT	22180.65	11603.20	0
	ODS	9378.65	23332.22	1072.98
	CT	19337.08	14446.77	0
Load +2%	ZT	24784.08	10011.45	0
	ODS	10131.94	23553.47	1110.12
	CT	20012.67	14782.86	0
Load -2%	ZT	24065.19	8706.98	0
	ODS	8629.87	23089.95	1052.36
	CT	19115.65	13656.52	0
Coal Retirement	ZT	17457.39	16219.88	106.58
	ODS	9211.8	23332.22	1239.83
	CT	15495.17	18182.11	106.58

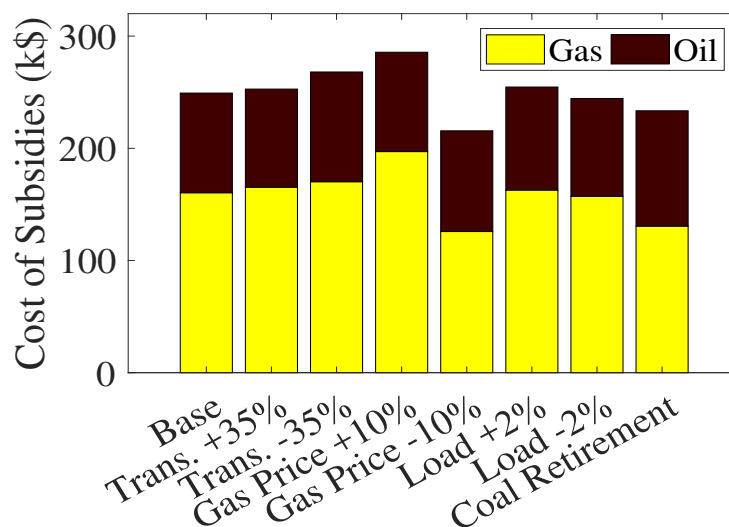


Figure 2.9: Total cost of subsidies under the three schemes for all scenarios.

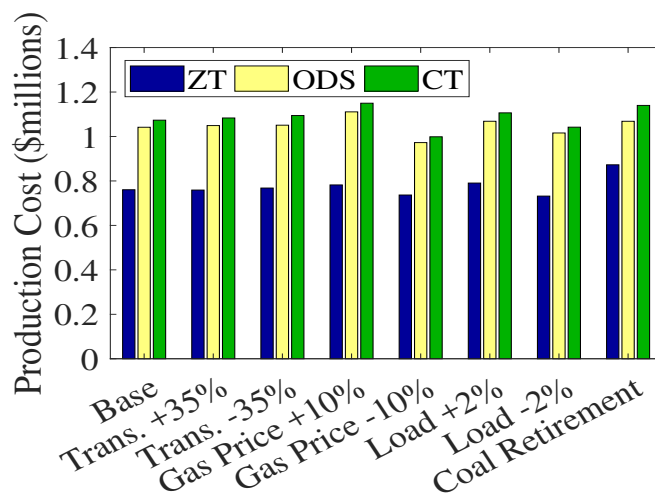
Consumer's Perspective

In all but two cases, the ODS cost of consumption is higher than the one observed for ZT. Interestingly, the lower consumption cost in the the load increase and coal retirement scenarios is due to the lower average price of electricity paid by consumers relative to the base case. To gain a better understanding on the reason behind this phenomenon, we refer to the LMPs shown in Fig 2.11. As can be seen in the plots, there are time periods where the LMPs are higher in ODS and others where they are higher in ZT. In periods where the demand is low, cheaper units are setting the price of electricity, and therefore, the effect of the added tax is much more pronounced making the price higher in ODS for those periods. In high demand periods, however, more expensive units are setting the price of electricity since the cheaper units are already dispatched at full capacity in ZT. This is not the case in ODS since the price is set by the cheaper but high emitting units that are not at full capacity due to the change in dispatch in the ODS scheme necessary for the emissions reduction. On average, the cost increase due to the tax in ODS exceeds the cost reduction gained from the

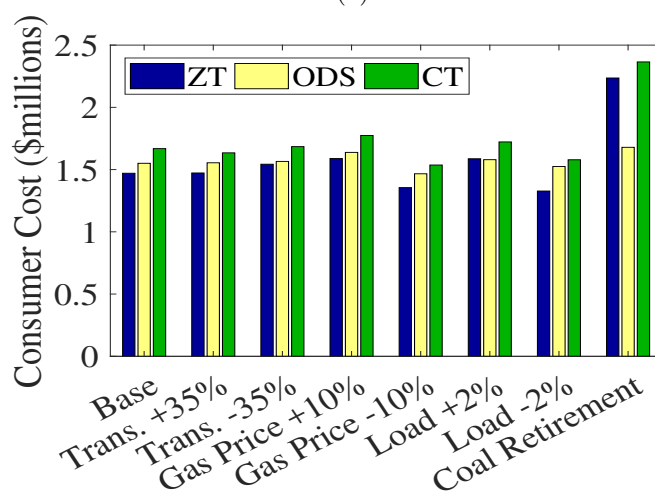
lower LMPs for all but the two cases highlighted above. The difference in cost between ODS and ZT is more noticeable in the case where the coal unit is retired. In this scenario, oil units are used to compensate the lost energy in time periods where the load is high (17-20), and thus, set the price of electricity in those periods leading to a much higher average price of electricity paid by consumers. When compared to CT, ODS emerges as the better option in terms of both the cost of consumption and the cost of abatement which can be seen in Table 2.2 for all cases.

Table 2.2: Abatement cost defined as the extra cost consumers pay per unit reduction of CO₂ emissions when compared to the zero tax case.

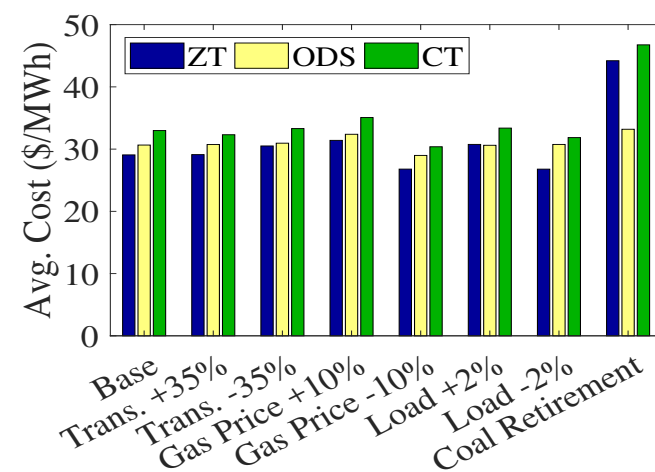
		Abatement Cost (\$/tCO ₂ e)
Base	ODS	11.44
	CT	59.63
Trans. +35%	ODS	10.92
	CT	47.85
Trans. -35%	ODS	3.61
	CT	48.68
Gas Price +10%	ODS	6.90
	CT	60.49
Gas Price -10%	ODS	20.47
	CT	97.29
Load +2%	ODS	-1.07
	CT	42.25
Load -2%	ODS	27.82
	CT	77.18
Coal Retirement	ODS	-145.43
	CT	98.15



(a)

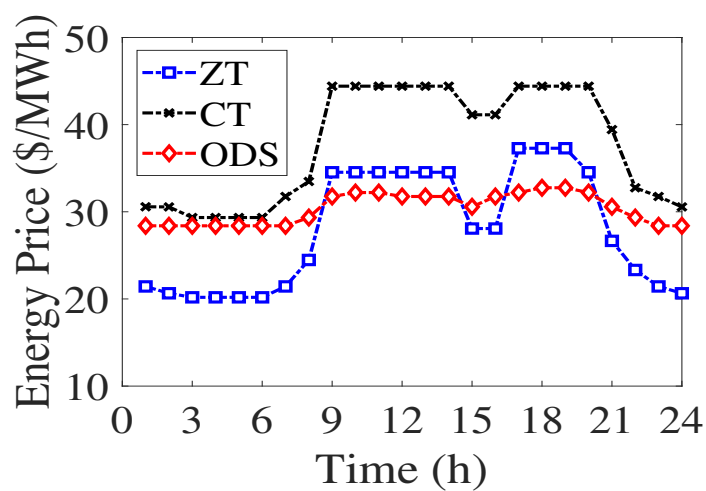


(b)

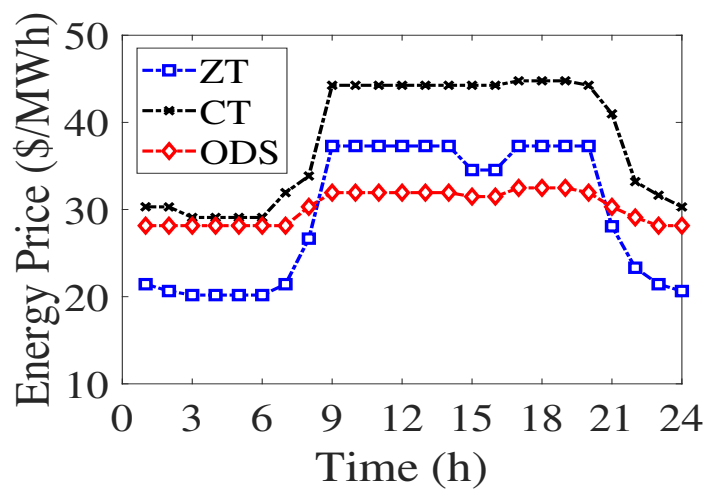


(c)

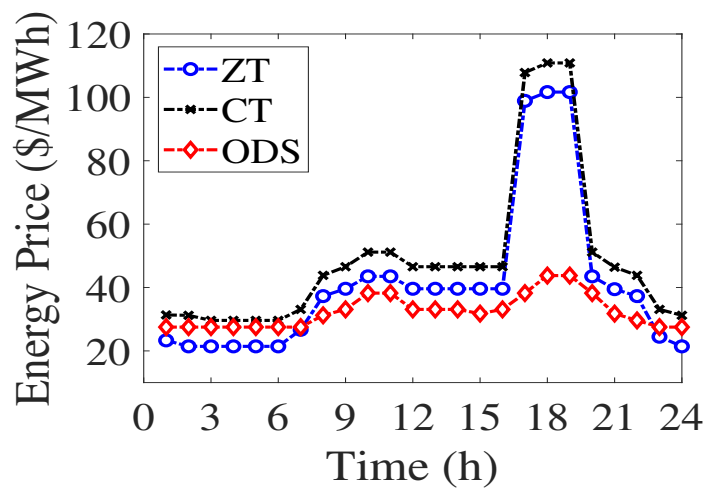
Figure 2.10: (a) Total cost of supplying the load after adjusting for the tax penalty and subsidies, (b) total cost of consumption after consumer reimbursement in the case of CT, and (c) average cost of electricity paid by consumers under the three schemes for all scenarios.



(a) Base



(b) Load +2%



(c) Coal Retirement

Figure 2.11: Average Hourly Locational Marginal Prices

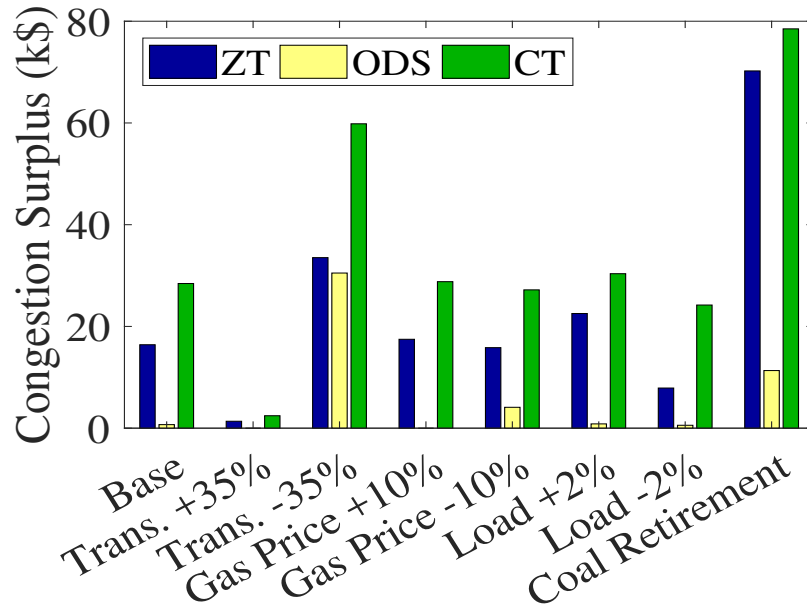


Figure 2.12: Merchandizing surplus under the three schemes for all scenarios.

Furthermore, as shown in Fig 2.12, the ODS method has a positive impact on the congestion surplus since it reduces it for all test cases when compared with the other schemes. Congestion surplus (or merchandizing surplus), defined as the difference between the payments collected from the load and the revenue distributed to generators, has adverse effects on electricity markets as explained in [68]. Therefore, alleviating the negative impacts associated with congestion surplus by reducing it can be seen as an added benefit of this method.

Producer's Perspective

Nuclear and hydro units benefit the most under the proposed method since they see an increase in profit when compared to the no tax case in all scenarios except for the coal retirement case. Coal units, however, are damaged the most since they see their profits decrease substantially when compared to the other schemes. For example, the largest decrease in

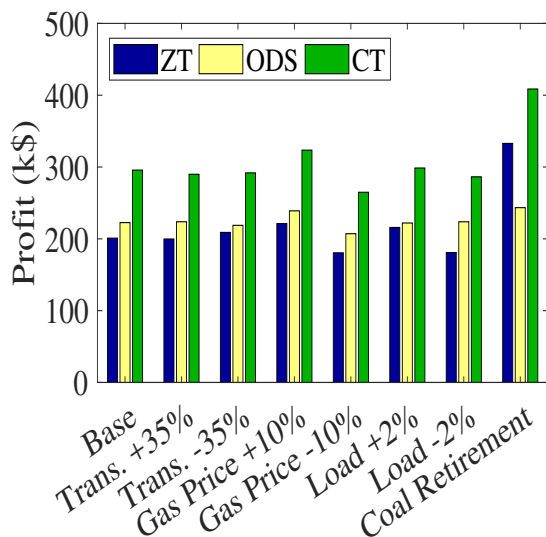
profit (93.22%) occurs when the capacity of transmission lines is increased by 35%. The smallest decrease was found to be 85.90% in the coal retirement scenario. Even though gas units suffer in terms of profit reduction when compared to the ZT case, the difference is not as pronounced as in the case with coal units.

Computational Efficiency

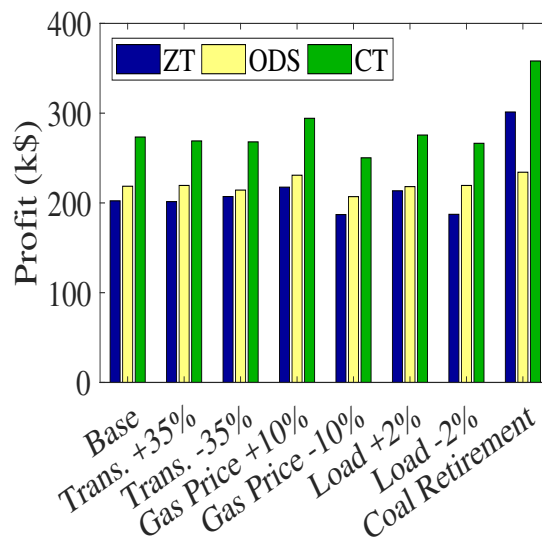
The number of iterations along with the computational time associated with the False Position method for all testing conditions are shown in Table 2.3. The results verify the potency of the chosen algorithm in solving the bilevel model rapidly without requiring many iterations. The maximum number of iterations occurs when the transmission capacity decreases by 35% and was found to be 6 iterations; whereas the longest solve-time occurs in the coal retirement case and was found to be 567.09s. The results of each iteration in the base case can be seen in Fig. 2.14.

Table 2.3: False Position Method Computational Performance

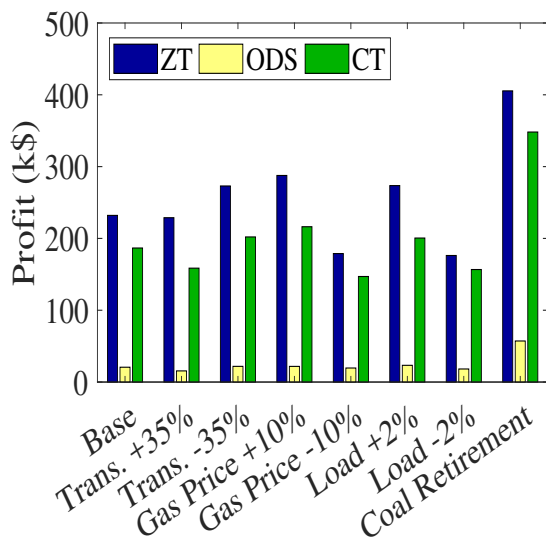
Test Case	No. of Iterations	Computation Time (s)
Base	5	103.46
Transmission Capacity +35%	5	365.26
Transmission Capacity -35%	6	117.54
Gas Price +10%	5	110.79
Gas Price -10%	4	93.15
Load +2%	5	181.6
Load -2%	5	109.74
Coal Retirement	5	567.07



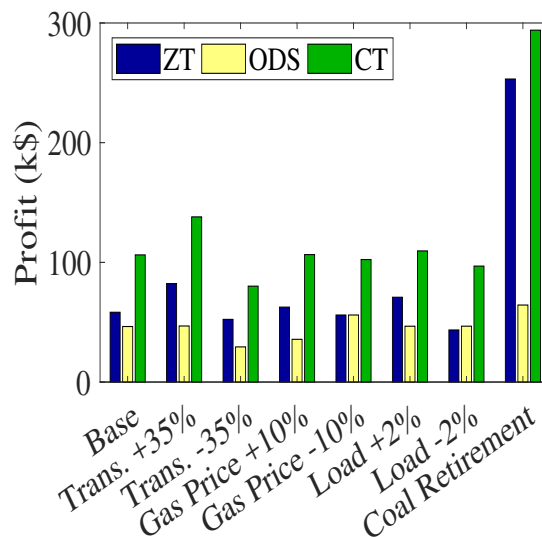
(a) Nuclear



(b) Hydro



(c) Coal



(d) Gas

Figure 2.13: Cumulative profit of all generating units broken down by fuel type. Note that the profits of oil units are zero in all test cases except under ZT and CT in the coal retirement scenario where the profits are \$185.46 and \$202.05 respectively.

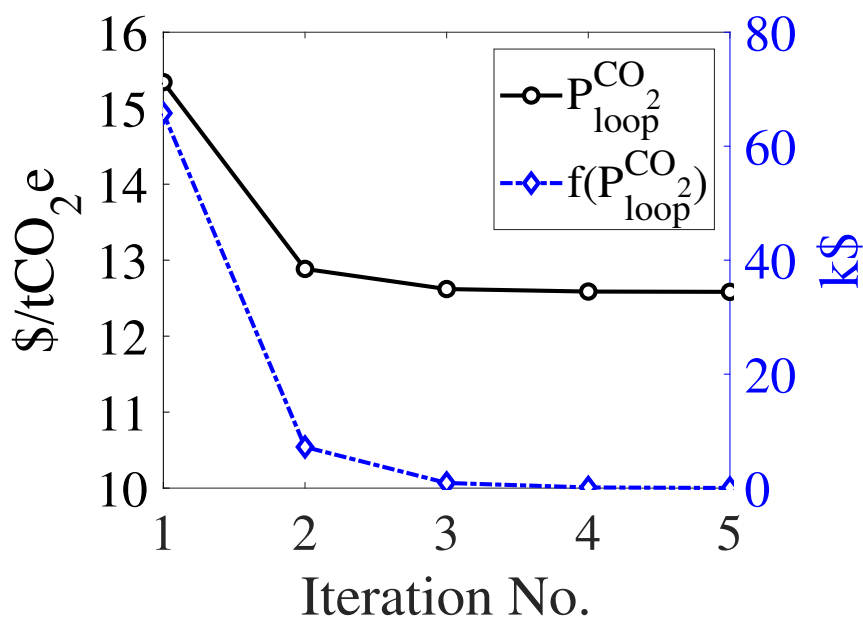


Figure 2.14: Base case results for each iteration of the False Position method.

2.7.2.3 The Flexibility of Subsidies

Thus far, we have assumed that the amount of monetary subsidies is designed and distributed to producers without restrictions. However, this may not always be the case. Therefore, in this section, we will address the implication associated with two types of limitations on the flexibility of subsidies that can occur in practical applications of the proposed method.

Tax Revenue Restrictions

It is not always the case that the total amount of tax revenue collected is appropriated entirely to subsidize non- and low-emitting generating units. The governmental body responsible for allocating the budget may choose to fund other projects³ in addition to the proposed subsidy scheme. To account for this in our mathematical model, we modify constraint (2.1b) of the

³For example, issuing a carbon dividend payable to affected households, reducing budget deficits, repairing environmental damages caused by carbon emissions, and increasing the capacity of installed renewable energy sources such as wind and solar.

upper level problem to be as follows:

$$\Delta t \sum_{t \in \mathcal{T}} \sum_{g \in \mathcal{G}} \sum_{b \in \mathcal{B}} p_{t,g,b} S_{t,g,b} \leq \left[\Delta t \sum_{t \in \mathcal{T}} \sum_{g \in \mathcal{G}} \sum_{b \in \mathcal{B}_g} e_g h_{g,b} P^{CO_2} p_{t,g,b} \right] \kappa_{TR}$$

where κ_{TR} is the percentage of the tax revenue collected from carbon-emitting producers that is allocated to the subsidy scheme.

Figure 2.15 shows how, for the base case, the tax rate changes as the amount of the appropriated funds changes due to the restrictions on the revenue generated from the carbon tax. Initially, when all of the tax revenue is used (i.e. $\kappa_{TR} = 1$), the tax rate that is needed to achieve the desired reduction target using the ODS method is \$12.58/tCO₂e. As we limit the amount of tax revenue that can be used by reducing κ_{TR} , the tax rate starts to increase. In fact, if κ_{TR} is set to be 0.4, the tax rate will then increase to \$25.39/tCO₂e, which is approximately double the rate compared to when $\kappa_{TR} = 1$. Furthermore, if only 10% of the tax revenue is allocated to the subsidy scheme, a tax rate of \$56.44/tCO₂e must be levied to adequately cover the expenses of the ODS method.

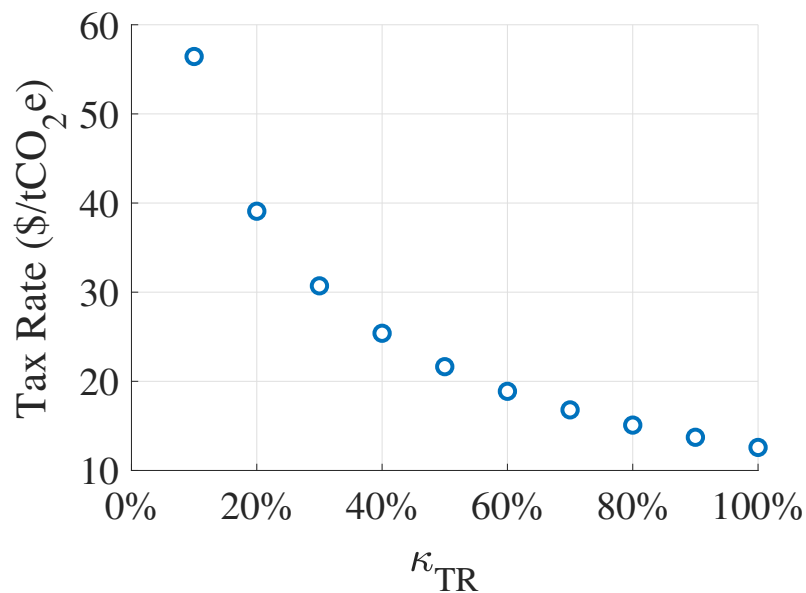


Figure 2.15: Tax rate required for the ODS method for different percentages of κ_{TR} .

The rise in tax rate is due to the fact that more revenue must be generated from the carbon tax to finance the cost of subsidies since we are limiting the amount of money that can be taken from the tax revenue. Interestingly, the cost of subsidies decreases as we reduce κ_{TR} as can be seen in Fig. 2.16(a). This can be attributed to the higher tax rate which penalizes carbon-emitting producers by increasing their marginal cost of production; thus, the amount of subsidies needed to make cleaner units more competitive in the day-ahead market is less. Nonetheless, the higher tax rates have an adverse effect on the total cost incurred by consumers. Figure 2.16(b) shows the average cost of electricity paid by consumers to satisfy their fixed demand. It is noticeable that decreasing κ_{TR} would bring about higher tax rates and consumers pay more for the same level of consumption as a result.

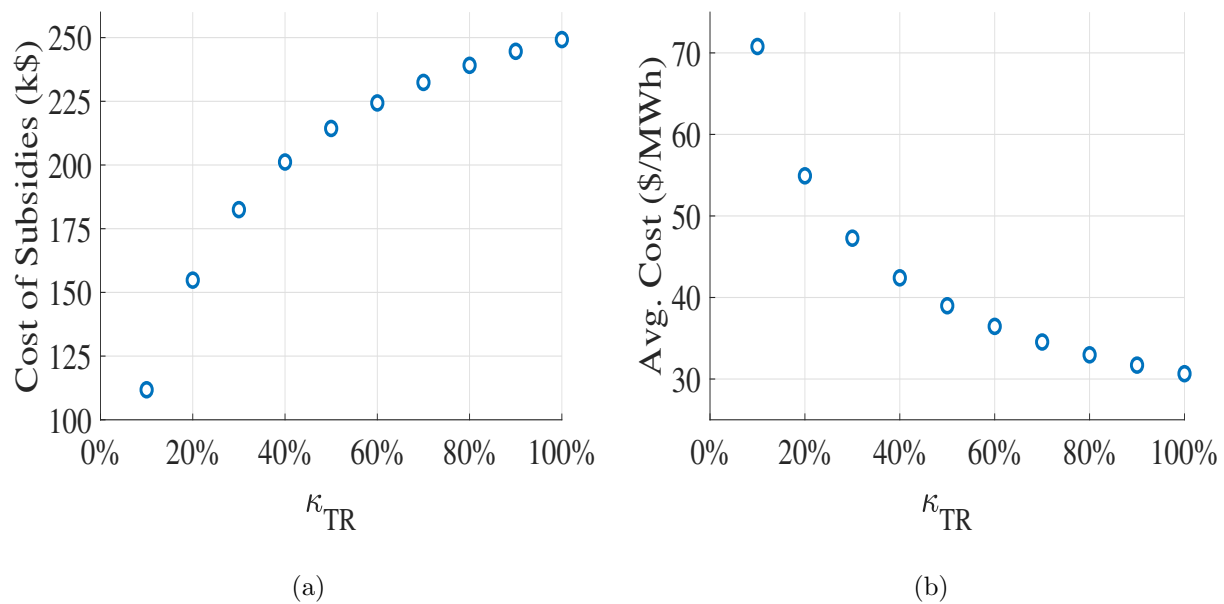


Figure 2.16: (a) Total cost of subsidies, and (b) average cost of electricity paid by consumers for different percentages of κ_{TR} .

Subsidy Design Restrictions

One of the features of the proposed approach is that subsidies are designed to be time-varying, generator specific, and dispensed on a per block basis. Therefore, to assess the impact of subsidy design restrictions on the overall performance of the ODS method, we first study the case where subsidies are non-time-varying (i.e. fixed for all time periods), and then consider the case where they are not offered on a per block basis. Mathematically, this is represented by replacing all occurrences of $S_{t,g,b}$ in Sections 2.5 and 2.6 by $S_{g,b}$ for the first case and $S_{t,g}$ for the latter.

Table 2.4 displays the results associated with the different methods used in the design of subsidies. Fixing the amount of subsidies for all time periods causes the tax rate to increase from \$12.58/tCO₂e to \$13.80/tCO₂e, or 9.70%. Contrary to the case where we limit the percentage of tax revenue allocated to the subsidy scheme, the total cost of subsidies increases with the higher tax rate. This is due to the limited flexibility when optimizing the amount of subsidies distributed since we are constraining it to be equal for all time periods. The average cost increases due to the higher tax rate as well. Moreover, the profits of generating units also rise because of the higher tax rate, and, in the case of gas and oil units, because subsidies are not as flexible, they cover more than the difference between their marginal costs and the marginal cost of the units ahead in the merit order.

Similarly, not designing subsidies on a per block basis for generating units causes tax rate to increase. The increase in this case, however, is much higher when compared to the non-time-varying case (36.73% as opposed to 9.70%). The total cost of subsidies, the average cost of electricity, and the profits of all generating units (except oil) are also higher by comparison.

Table 2.4: Outcomes of the different subsidy design methods for the base case

	Subsidy Design Method		
	$S_{t,g,b}$	$S_{g,b}$	$S_{t,g}$
Tax Rate (\$/tCO ₂ e)	12.58	13.80	17.20
Cost of Subsidies (k\$)	249.23	273.34	340.74
Average Cost (\$/MWh)	30.65	31.70	34.91
Nuclear	222.59	233.43	263.74
Hydro	218.59	226.72	249.45
Profits (k\$)			
Gas	46.39	68.67	178.95
Coal	20.64	21.41	23.55
Oil	0	3.00	2.52

2.8 Summary

This chapter presents a novel model that aims to tackle the issue of cost increases associated with imposing carbon taxes to reduce CO₂ emissions. The proposed scheme takes advantage of the tax revenue generated from the taxes to offer financial incentives to low emitting units in the form of production subsidies. A trilevel optimization is introduced to model the problem and then transformed to a bilevel optimization that can be solved iteratively. Numerical studies were conducted to evaluate the proposed model against levying carbon taxes only. The key findings of this chapter can be summarized as follows:

- The proposed model achieves any feasible reduction target without requiring a high tax rate. In doing so, we avoid burdening consumers with excessive cost increases. A fact that is more palpable as the reduction target approaches the minimum level of emissions.

- For a given reduction target, the required tax rate in the proposed model does not deviate much when predictable system operational changes occur.
- Implementing the proposed scheme comes with additional advantages under certain circumstances. For example, in some cases, consumers see a decrease in costs for the same level of consumption. Furthermore, congestion surplus is seen to be reduced when compared to the other methods.
- The proposed scheme sends proper pricing signals to producers since it rewards non-emitting units by increasing their profits in most cases when compared to the zero tax case. Moreover, it penalizes high-emitting units by substantially reducing their profits, hence, encouraging the shift to clean units.
- The manner in which subsidies is designed and distributed affects the overall performance of the ODS method. Limiting the amount of revenue that can be allocated to subsidize clean generating units increases the required tax rate, and consequently, the total cost incurred by consumers to satisfy their demand for electric energy.

Chapter 3

MARKET POWER IN THE PRESENCE OF CARBON TAXES IN ELECTRICITY MARKETS

3.1 Introduction

Market power refers to the ability of strategic players to change their position in the market with the purpose of leveraging prices for their own benefit. For example, a producer is said to be exercising market power when it increases its selling price (economic withholding) or reduces its output (physical withholding) in order to alter market prices to increase its profit [69]. Such a producer is known as a price maker due to its ability to influence market prices.

In electricity markets, economic withholding can occur if producers inflate their offer prices when participating in the day-ahead market for electric energy, which would cause the supply curve to shift upwards. For example, a producer who owns a generating unit that can produce up to 100 MW at a marginal cost of \$20 per MWh can either participate competitively (i.e. offer 100 MW at its marginal cost of \$20 per MWh) or act strategically and increase its offering price to a value larger than \$20 per MWh. On the other hand, physical withholding occurs when producers limit the capacity at which they participate in the market. This will cause the Market Operator to dispatch the next available unit in the merit order to compensate for the shortage in capacity, which is equivalent to shifting the supply curve to the left. To illustrate this scenario, using the same producer from the previous example, instead of offering 100 MW at a price of \$20 per MWh, the producer would offer 80 MW at the same price of \$20 per MWh. In both withholding cases, the day-ahead market will clear at a higher price when compared to the price with competitive participation (i.e. without economic/physical withholding). As a result, it would cost consumers more

money to serve the same level of demand. Knowing this, producers are highly incentivized to exploit any vulnerability in electricity markets to manipulate energy prices since higher energy prices translate to additional revenue pocketed by producers.

As detailed in [70], electricity markets are considered susceptible to market power for multiple reasons that can be summarized as follows:

1. **The nature of the demand curve:** the demand for electricity is highly inelastic in the short run due to:
 - The majority of consumers pay a fixed retail rate instead of being exposed to real time pricing which is more indicative of actual market conditions such as congestion or unforeseen shortages in supply. Therefore, consumers have no incentive to adjust their consumption patterns.
 - Electric energy is required to be available at specific periods by consumers which restricts inter-temporal substitution of electricity demand.

2. **The nature of the supply curve:** in the short-run, the generation capacity is fixed for a given market. Moreover, the supply curve steepens as the load approaches the capacity limit of the system as shown in Fig. 3.1. Therefore, at peak demand periods, both the supply and the demand are inelastic. This combination enhances the capability of producers to exercise market power to the extent that even suppliers with small market shares may substantially alter market prices.

3. **Transmission line constraints:** the electric power grid is interconnected using a network of transmission lines that serve to transfer bulk electric energy from generation sites to other locations in the grid (e.g. electrical substations). The power flow transferred using those transmission lines must be constrained to be below the operating limits of the lines to ensure a safe and reliable transfer of electric energy. Limitations on transmission capacity, however, can create localized market power where some producers can benefit from the fact that they are the only viable option to serve the load.

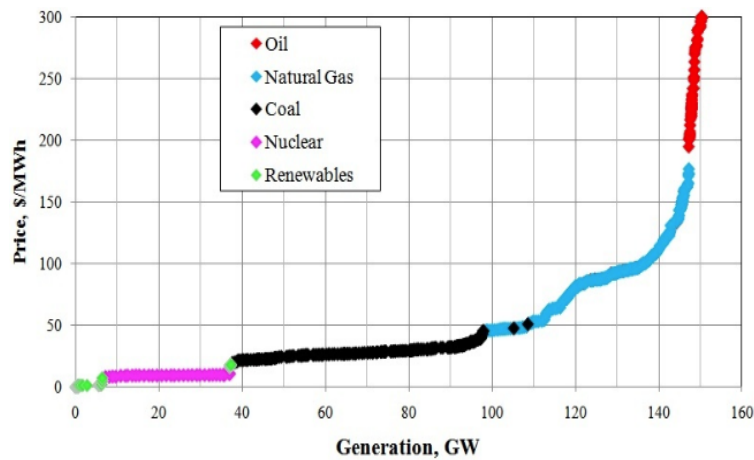


Figure 3.1: The generation stack for the Pennsylvania-Jersey-Maryland (PJM) electric power market [71]. Note that the supply curve depicted in this figure is from approximately 2008. Since then, the type of units may have changed, however, the general shape of the curve is still comparable.

Consequently, those producers would effectively have a monopoly on the production of electric energy in those areas that are isolated due to congestion.

4. **Frequent market interaction:** the cyclical nature of the load (e.g. Fig. 3.2) means that producers will interact on a regular basis with each other during the market clearing process. This unique characteristic of electricity markets opens the door for participants to learn the behavior of one another, which may lead to firms accurately predicting the offers of other firms, or worse, to firms colluding with each other.

Therefore, given that electricity markets are prone to participants engaging in market power behavior, constant market monitoring is crucial. However, this task has proven to be challenging since the actual marginal cost of power producers cannot be known with absolute certainty¹. Nevertheless, market operations are being monitored constantly by regulating

¹The true costs incurred by suppliers due to the production of electric energy are confidential and proprietary information.

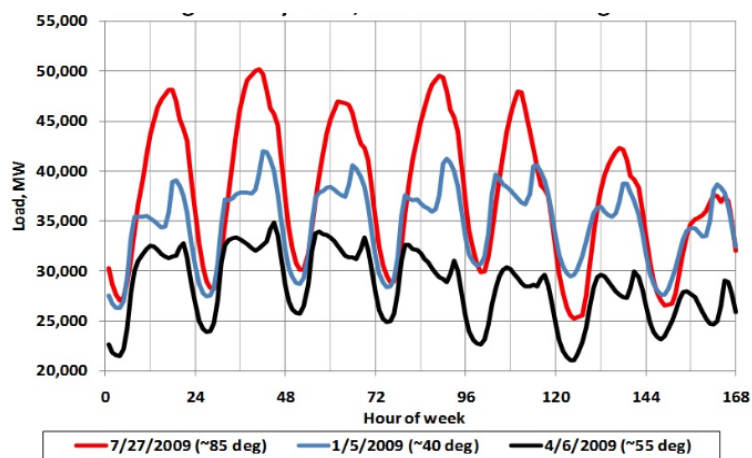


Figure 3.2: The average hourly load for an entire week in the PJM Mid-Atlantic Region [71]. The black, red, and blue traces represent Spring, Summer, and Winter, respectively.

authorities² to detect the presence of market power using specialized indices (e.g. the Herfindahl-Hirschman Index³ (HHI) and the Residual Supply Index⁴ (RSI)) and work on prevention methods and mitigating techniques⁵ [74, 75].

The presence of market power in electricity markets is also a major concern when designing a policy to mitigate CO₂ emissions. In addition to the operational inefficiencies⁶ it causes when compared to perfect competition, market power also affects the potency of en-

²Such as the Federal Energy Regulatory Commission (FERC) [72], state regulators, and specialized organizations tasked with market monitoring (e.g. The California ISO (CAISO) Department of Market Monitoring [73])

³The HHI, commonly used by the FERC, the Department of Justice (DOJ) and the Federal Trade Commission (FTC), is a statistical measure of market concentration. It can be calculated by first squaring the market share of each supplier and then summing the resultant values.

⁴The RSI is used by the CAISO Department of Market Monitoring. It is a measure of how much a particular supplier can manipulate market prices, and is based on how much capacity the system has to serve the load after excluding the capacity of that particular supplier. The RSI of a supplier S can be computed as follows: $RSI(S) = (\text{Total available supply in the system} - \text{Available supply from } S) / \text{Demand}$.

⁵For instance, setting a price cap on offers, increasing the capacity of narrow transmission corridors, limiting entry barriers to the market, and keeping the market share of individual suppliers below a specified value.

⁶Such as the transfer of wealth from consumers to suppliers, higher overall prices, and dispatching more expensive generators that would otherwise not be dispatched.

vironmental policies [76]. This is especially worrisome for price-based policies such as carbon taxes where, unlike mass-based policies, there is no quota set on the level of emissions. In this chapter, we attempt to shed light on this issue by addressing the following questions:

1. Do carbon taxes have an effect on market power? If so, does it depend on how “clean” the strategic producer is relative to the competitive fringe?
2. What are the consequences of exercising market power on the effectiveness of the carbon tax and, by extension, on the level of emissions?

To that end, a single-leader-follower Stackelberg game [77] is used to model the behavior of strategic producers participating in electricity markets. A bilevel optimization approach is taken to formulate the Stackelberg game where the leader, represented by the upper-level problem (UL), is the strategic producer that is maximizing its profit using endogenous formations of locational marginal prices (LMPs). The follower, represented by the lower-level problem (LL), models the day-ahead market for electric energy whose objective is to maximize the social welfare.

3.2 Literature Survey

3.2.1 Market Power in Electricity Markets

3.2.1.1 Empirical Evidence

Kumar and Wen have reported several instances of real-world examples in [75] where it is believed that market power has been exercised. In those cases, there is strong evidence of market power abuse since prices in electricity markets had risen substantially above competitive levels. The National Electricity Market of Australia and the Midwest US market are notable examples where wholesale electricity prices reached \$4814 per MWh on November 25, 1997, and \$7000 per MWh briefly on June 1998, respectively.

Müsgens studies market power in the German wholesale electricity market in [78]. He attempts to quantify market power by first computing a competitive price estimator, which

is based on marginal costs, and then compare the price estimator with observed power prices in the electricity spot market from June, 2000 to June, 2003. He concludes that there is no evidence for market power from June, 2000 to August, 2001 since the observed market prices matches with his price estimator. However, from September, 2001 to June, 2003, he found that prices are, on average, 50% higher than estimated cost. Müsgens mentions increased market concentration and adaptive learning from repeated market participation as potential reasons for the increase in market power that led to the price discrepancy.

3.2.1.2 Academic Works

Ruiz and Conejo [79] present a bilevel optimization that solves for the optimal offers for a strategic power producer. Their results show that the proposed technique is capable of identifying the strategic offers that result in maximum profit. The strategic participation of price-making wind power producers in electricity markets is discussed in [80–82]. Recognizing the limitations of the dc power flow approximation, the authors in [83] include an ac power flow model to account for the issues that arise from reactive power and voltage constraints in their analysis of imperfect competition in active power markets. Chitkara *et al.* study the strategic participation of generating companies in the reactive power market in [84]. They also examine the effects of a price cap on the strategic behavior of the generating companies.

From the perspective of the demand, Kazempour *et al.* [85] model the strategic behavior of a large consumer. They conclude that a strategic consumer can lower the clearing price of the market by under-bidding, which would result in an increase in the expected utility of said consumer. Moreover, Daraeepour *et al.* [86] show that the market power of a strategic consumer participating in the reserve market with high levels of wind penetration increases proportionally to its operating reserves capacity.

The authors in [87] studied how the social welfare is affected by the strategic behavior of energy storage systems, and present a novel market power mitigation pricing scheme. Their proposed pricing scheme is designed to stimulate strategic energy storage systems to operate in a socially optimal manner, thus achieving the claimed benefits from their presence in

electricity markets.

3.2.2 *Environmental Regulation and Market Power*

Kolstad and Wolak [88] investigate the ability of electricity suppliers in the California power market to exercise market power in the presence of the NO_x emissions permit market. Their empirical studies present evidence that large producers were able to inflate permit prices by over-consuming allowances which consequently raise the marginal cost of other firms, a behavior that contributed to the 2001 California electricity crisis [89]. Using a complementary approach, Chen and Hobbs [90] model the interaction of electricity markets with permit markets for NO_x under both perfect and Cournot competition. Their results show that the strategic behavior of Cournot firms would alter the prices of tradable permits prompting a change in the output of the competitive fringe due to the change in their marginal cost of production. Because of the shortcomings associated with heuristic algorithms, Chen *et al.* further examine the same issue using a Stackelberg game in [91]. They conclude that, compared to the pure Cournot model, the strategic producer in the Stackelberg model is able to extract more rent from the market, thus highlighting its ability to exercise market power.

In their study of strategic behavior in electricity markets under a CO_2 cap-and-trade policy, Limpitton and Chen [92] demonstrate that emissions increase with market power while energy consumption decreases. Papavasiliou *et al.* [93] compare the competitive effects of renewable portfolio standards (RPS) and carbon taxes in transmission constrained electricity markets under a Cournot duopoly. They conclude that taxes are market-power neutral whereas RPS increase the market power of clean generating units. Downward [94] uses a Cournot model to study the impact of a carbon tax on a two-node electricity system. His work presented an interesting case where the imposition of a carbon tax resulted in higher emissions. The cause of this anomaly was attributed to the strategic behavior of generators and the congestion of transmission lines. A comparison between a mass-based and a performance-based standard for curbing CO_2 emissions under imperfect competition

can be found in [95]. The authors of [96] studied the effect that different environmental policy instruments have on the behavior of oligopolistic firms in a generation expansion model. Their analysis shows that the non-renewable electricity market exhibits an increase in market power, effectively raising energy prices compared to the perfect competition case.

3.2.3 Stackelberg Games in Electric Power Systems

In addition to using Stackelberg games for modeling strategic offering/bidding in electricity markets, these type of games are also utilized to model different kind of interactions in electric power systems. For example, Jenabi *et al.* [97] use a bilevel optimization to model a Stackelberg game where the upper level problem represents a Transmission Operator (TO) looking to optimize investment in transmission either to maximize profits or social welfare, and the lower level problem models the market clearing process. Moreover, Zugno *et al.* [98] use a Stackelberg game to model the interaction between a single energy retailer and consumers. The retailer (the leader) participates in electricity markets with the goal of maximizing his profits by developing a dynamic pricing scheme that is relayed to consumers (the followers) in order to achieve an optimal load pattern. Similarly, the authors of [99] study the interaction between smart grids and an ensemble of Plug-in Electric Vehicles (PHEV) to find an optimal price and charging schedule.

Furthermore, it is possible to have Stackelberg games that involve more than a single leader, where the leader not only factors in the optimal response of the follower(s), but also must incorporate the optimal decisions of other leaders. These mutli-leader follower games have dedicated reformulation techniques⁷ since solving these types of games has proven to be a challenging task in the optimization and game theory communities [100–102]. Examples of such application in the power systems literature can be found in [103–105].

⁷For example, reformulating the problem as an Equilibrium Problem with Equilibrium Constraints (EPEC).

3.3 Contribution

Since other models may underestimate the market power of strategic producers, in this chapter, we attempt to fill the existing gap in the literature by utilizing a leader-follower Stackelberg game. We use a detailed representation of the electric power system to examine the effects price makers have on electricity markets that are carbon regulated via carbon taxes. In doing so, we aim to achieve the following:

1. Investigate the effects carbon taxes have on the capability and extent of generating units to exercise market power. This is done by analyzing how much strategic producers can change market prices to their advantage, which would be reflected on the cost incurred by consumers.
2. Study the environmental consequences that may arise from the change in the offer prices of strategic producers. More specifically, we look at the change in the level of carbon emissions.

3.4 Chapter Organization

The rest of the chapter is organized as follows. The Stackelberg game is explained in Section 3.5. Section 3.6 describes the bilevel optimization used to model the game and conduct the study. Section 3.7 explains the solution methodology used to transform the bilevel optimization to its corresponding Mathematical Problem with Equilibrium Constraints (MPEC) and its single-level equivalent MILP. Section 3.8 presents numerical results from a 24-bus case study. Section 3.9 provides concluding remarks about the key findings of this chapter.

3.5 The Stackelberg Game

The Stackelberg game is a multi-level, hierarchical model that is comprised of two key players: the leader and the follower. The leader benefits by making the first move when optimizing his

objective considering the response of the follower. The follower would then react optimally to the optimal strategy chosen by the leader.

In our model, we consider a single leader, the strategic producer, and a single follower, the Independent System Operator (ISO). The strategic producer looks to construct a strategic offering scheme with the objective of maximizing the total profits accrued from participating in the day-ahead market for electric energy. The strategic offers are developed while taking into consideration the outcome of the market clearing process performed by the ISO.

The ISO, who functions as both a System Operator to maintain reliability and Market Operator to establish market prices, collects all demand bids by the load, supply offers from non-strategic producers, and supply offers from the strategic producer. Then, the ISO would proceed to clear the day-ahead market for electric energy by maximizing the social welfare considering system constraints. The outcome of market clearing process would then be the hourly market price at each node in the system, and the power output of the strategic producer and all non-strategic producers for each time period. The interaction between the two players of the Stackelberg game is shown in Fig. 3.3.

The following assumptions are made in our model:

1. There is only a single producer who is participating strategically in the market. The strategic producer, however, may own more than one generating unit.
2. The objective of the strategic producer is to maximize its short-term⁸ profits.
3. The strategic producer does not collude with other producers.
4. The strategic producer has perfect information about other market participants (i.e. other producers and large consumers) and system parameters (e.g. system topology and transmission line limits).

⁸The focus of this chapter is on the effects of exercising market power in the short-run. This is the case since the FERC has found that, barring any barriers to entry, long-term power markets are “workably competitive” [106].

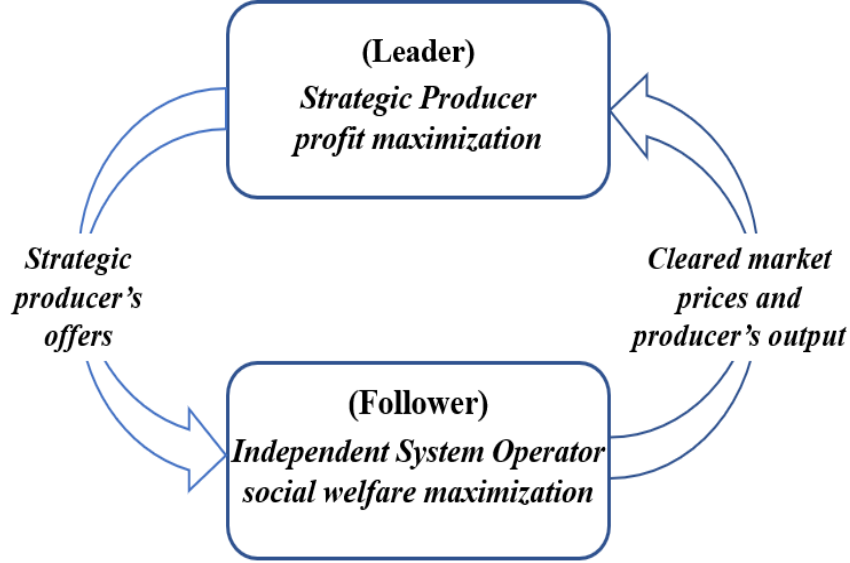


Figure 3.3: Flowchart depicting the interaction between the two players in the Stackelberg game.

5. All other market participants are participating competitively in the market (i.e. offer/bid their true marginal cost/utility).

3.6 Mathematical Model

The bilevel optimization used to model the Stackelberg game is described mathematically in (3.1)–(3.2) below. The UL problem is defined in (3.1), and its primal set of variables is $\Xi^{UL} = \{\beta_{t,g \in \Omega^{SG}, b}, \Xi^{LL}\}$ where Ξ^{LL} is the set of primal and dual variables for the LL problem. The LL problem is defined in (3.2) and involves the following set of variables,

$$\Xi^{LL} = \left\{ p_{t,g,b}, p_{t,l}, \theta_{t,n}, \lambda_{t,n}, \gamma_{t,l}, \mu_{t,l}^{\min}, \mu_{t,l}^{\max}, \xi_{t,g,b}^{\min}, \xi_{t,g,b}^{\max}, \rho_{t,n}^{\min}, \rho_{t,n}^{\max}, \sigma_t \right\}.$$

The dual variables associated with each constraint in the LL problem is shown between parentheses following a colon.

$$\min \Delta t \sum_{t \in \mathcal{T}} \sum_{g \in \Omega^{SG}} \sum_{b \in \mathcal{B}_g} \left[c_g h_{g,b} + e_g h_{g,b} P^{CO_2} - \sum_{n \in \mathcal{N}} m_{g,n}^{gen} \lambda_{t,n} \right] p_{t,g,b} \quad (3.1a)$$

subject to the following constraints:

$$0 \leq \beta_{t,g,b} \leq \bar{\beta}; \forall t \in \mathcal{T}, \forall g \in \Omega^{SG}, \forall b \in \mathcal{B} \quad (3.1b)$$

$$\sum_{b \in \mathcal{B}_g} p_{t+1,g,b} - \sum_{b \in \mathcal{B}_g} p_{t,g,b} \leq R_g^{up}; \forall t = 1 \dots n_T - 1, \forall g \in \Omega^{SG} \quad (3.1c)$$

$$\sum_{b \in \mathcal{B}_g} p_{t,g,b} - \sum_{b \in \mathcal{B}_g} p_{t+1,g,b} \leq R_g^{dn}; \forall t = 1 \dots n_T - 1, \forall g \in \Omega^{SG} \quad (3.1d)$$

$p_{t,g,b}, \lambda_{t,n} \in$

$$\operatorname{argmin} \left\{ \Delta t \sum_{t \in \mathcal{T}} \sum_{b \in \mathcal{B}_g} \sum_{g \in \Omega^{NS}} \left[c_g h_{g,b} + e_g h_{g,b} P^{CO_2} \right] p_{t,g,b} + \sum_{t \in \mathcal{T}} \sum_{b \in \mathcal{B}_g} \sum_{g \in \Omega^{SG}} \beta_{t,g,b} p_{t,g,b} \right. \quad (3.2a)$$

subject to the following constraints:

$$\sum_{g \in \mathcal{G}} \sum_{b \in \mathcal{B}_g} m_{g,n}^{gen} p_{t,g,b} - \sum_{l \in \mathcal{L}} m_{l,n}^{line} p_{f,t,l} = D_{t,n} : (\lambda_{t,n}); \forall t \in \mathcal{T}, \forall n \in \mathcal{N} \quad (3.2b)$$

$$p_{f,t,l} = B_l \sum_{n \in \mathcal{N}} m_{l,n}^{line} \theta_{t,n} : (\gamma_{t,l}); \forall t \in \mathcal{T}, \forall l \in \mathcal{L} \quad (3.2c)$$

$$-\bar{F}_l \leq p_{f,t,l} \leq \bar{F}_l : (\mu_{t,l}^{min}, \mu_{t,l}^{max}); \forall t \in \mathcal{T}, \forall l \in \mathcal{L} \quad (3.2d)$$

$$0 \leq p_{t,g,b} \leq \bar{P}_{g,b} : (\xi_{t,g,b}^{min}, \xi_{t,g,b}^{max}); \forall t \in \mathcal{T}, \forall g \in \mathcal{G}, \forall b \in \mathcal{B}_g \quad (3.2e)$$

$$-\pi \leq \theta_{t,n} \leq \pi : (\rho_{t,n}^{min}, \rho_{t,n}^{max}); \forall t \in \mathcal{T}, \forall n \in \mathcal{N} \quad (3.2f)$$

$$\left. \theta_{t,n=ref} = 0 : (\sigma_t); \forall t \in \mathcal{T} \right\} \quad (3.2g)$$

The UL problem (3.1a)–(3.1c) represents the strategic producer. The objective function (3.1a) minimizes the cost of production, including the cost of emissions, minus the revenue obtained from supplying electric energy in the day-ahead market. The variable $\lambda_{t,n}$ represents the actual market clearing price of electric energy and is found endogenously. Constraints (3.1b) enforce the strategic offer to be non-negative and lower than an offer cap. The up and down ramping limits of each generating unit owned by the strategic producer is enforced in (3.1c)–(3.1d).

The LL problem (3.2a)–(3.2g) models the day-ahead energy market clearing process where the objective is to maximize the social welfare. This is equivalent to the formulation of (3.2a) because we minimize minus the social welfare assuming inelastic demand, which is the same as minimizing the cost of supplying the load considering offers from both strategic and competitive producers. Equation (3.2b) enforces the power balance at each bus. Note that the price of electric energy used in the UL objective function (3.1a) is defined as the dual variable of the nodal balance constraint (3.2b). Equation (3.2c) defines the real power flow in each transmission line assuming a lossless dc power flow. Constraints (3.2d) enforce the capacity limits of each transmission line. Constraints (3.2e) enforce the upper and lower bounds of each generating unit. The upper and lower angle stability bounds at each bus are imposed in (3.2f). Finally, the reference bus is defined in (3.2g).

3.7 Solution Technique

In a similar vein to what was done in Chapter 2, the LL problem is replaced with its Karush-Kuhn-Tucker (KKT) optimality conditions since it is linear and continuous. Note that the bilinear term $(\beta_{t,g \in \Omega^{SG}, b} p_{t,g \in \Omega^{SG}, b})$ in the LL objective function does not make the LL problem nonlinear because it involves multiplication of variables from different levels, and variables from one level are considered parameters in the other. The MPEC form of the bilevel optimization is shown below:

$$\min \quad (3.1a) \tag{3.3a}$$

subject to the following constraints:

$$(3.1b) - (3.1d), (3.2b), (3.2c), \text{ and } (3.2g) \quad (3.3b)$$

$$\sum_{l \in \mathcal{L}} B_l m_{l,n}^{line} \gamma_{t,l} - (\sigma_t)_{n=\text{ref}} - \rho_{t,n}^{min} + \rho_{t,n}^{max} = 0; \forall t \in \mathcal{T}, \forall n \in \mathcal{N} \quad (3.3c)$$

$$\sum_{n \in \mathcal{N}} m_{l,n}^{line} \lambda_{t,n} - \gamma_{t,l} + \mu_{t,l}^{max} - \mu_{t,l}^{min} = 0; \forall t \in \mathcal{T}, \forall l \in \mathcal{L} \quad (3.3d)$$

$$c_{g,b} h_{g,b} + e_g h_{g,b} P^{CO_2} - \sum_{n \in \mathcal{N}} m_{g,n}^{gen} \lambda_{t,n} + \xi_{t,g,b}^{max} - \xi_{t,g,b}^{min} = 0; \forall t \in \mathcal{T}, \forall g \in \Omega^{NS}, \forall b \in \mathcal{B}_g \quad (3.3e)$$

$$\beta_{t,g,b} - \sum_{n \in \mathcal{N}} m_{g,n}^{gen} \lambda_{t,n} + \xi_{t,g,b}^{max} - \xi_{t,g,b}^{min} = 0; \forall t \in \mathcal{T}, \forall g \in \Omega^{SG}, \forall b \in \mathcal{B}_g \quad (3.3f)$$

$$0 \leq \mu_{t,l}^{min} \perp (pf_{t,l} + \bar{F}_l) \geq 0; \forall t \in \mathcal{T}, \forall l \in \mathcal{L} \quad (3.3g)$$

$$0 \leq \mu_{t,l}^{max} \perp (\bar{F}_l - pf_{t,l}) \geq 0; \forall t \in \mathcal{T}, \forall l \in \mathcal{L} \quad (3.3h)$$

$$0 \leq \xi_{t,g,b}^{min} \perp p_{t,g,b} \geq 0; \forall t \in \mathcal{T}, \forall g \in \mathcal{G}, \forall b \in \mathcal{B}_g \quad (3.3i)$$

$$0 \leq \xi_{t,g,b}^{max} \perp (\bar{P}_{g,b} - p_{t,g,b}) \geq 0; \forall t \in \mathcal{T}, \forall g \in \mathcal{G}, \forall b \in \mathcal{B}_g \quad (3.3j)$$

$$0 \leq \rho_{t,l}^{min} \perp (\theta_{t,n} + \pi) \geq 0; \forall t \in \mathcal{T}, \forall n \in \mathcal{N} \quad (3.3k)$$

$$0 \leq \rho_{t,l}^{max} \perp (\pi - \theta_{t,n}) \geq 0; \forall t \in \mathcal{T}, \forall n \in \mathcal{N} \quad (3.3l)$$

Two sources of nonlinearities arise in the MPEC. The first being the complementary slackness conditions, and the linearization of which has been addressed previously in Chapter 2. The second is the bilinear term in the objective function that involves the multiplication of the cleared power output of the strategic producer and the LMPs $(\lambda_{t,n} p_{t,g \in \Omega^{SG}, b})$. To obtain an exact linear equivalent of the bilinear term, we utilize the strong duality theorem along with some of the identities associated with the complementary slackness conditions as follows:

1. Using the strong duality theorem we get the following identity:

$$\begin{aligned}
\sum_{t \in \mathcal{T}} \sum_{g \in \Omega^{SG}} \sum_{b \in \mathcal{B}} \beta_{t,g,b} p_{t,g,b} &= - \sum_{t \in \mathcal{T}} \sum_{g \in \Omega^{NS}} \sum_{b \in \mathcal{B}_g} (c_g + e_g P^{CO_2}) h_{g,b} p_{t,g,b} \\
&\quad - \sum_{t \in \mathcal{T}} \sum_{l \in \mathcal{L}} \bar{F}_l (\mu_{t,g}^{min} + \mu_{t,g}^{max}) - \sum_{t \in \mathcal{T}} \sum_{g \in \mathcal{G}} \sum_{b \in \mathcal{B}_g} \bar{P}_{g,b} \xi_{t,g,b}^{max} \\
&\quad - \sum_{t \in \mathcal{T}} \sum_{n \in \mathcal{N}} \pi (\rho_{t,g}^{min} + \rho_{t,g}^{max}) + \sum_{t \in \mathcal{T}} \sum_{n \in \mathcal{N}} D_{t,n} \lambda_{t,n} \quad (3.4)
\end{aligned}$$

2. From 3.3f, we can replace $\beta_{t,g,b}$ in (3.4) with the following:

$$\beta_{t,g,b} = \sum_{n \in \mathcal{N}} m_{g,n}^{gen} \lambda_{t,n} - \xi_{t,g,b}^{max} + \xi_{t,g,b}^{min}$$

3. From 3.3i and 3.3j, we know that:

$$p_{t,g,b} \xi_{t,g,b}^{min} = 0$$

$$p_{t,g,b} \xi_{t,g,b}^{max} = \bar{P}_{g,b} \xi_{t,g,b}^{max}$$

4. Finally, we substitute the results from steps (2) and (3) back in (3.4) to get the following linear equivalent form:

$$\begin{aligned}
\sum_{t \in \mathcal{T}} \sum_{g \in \Omega^{SG}} \sum_{b \in \mathcal{B}} \sum_{n \in \mathcal{N}} m_{g,n}^{gen} \lambda_{t,n} p_{t,g,b} &= - \sum_{t \in \mathcal{T}} \sum_{g \in \Omega^{NS}} \sum_{b \in \mathcal{B}_g} (c_g + e_g P^{CO_2}) h_{g,b} p_{t,g,b} \\
&\quad - \sum_{t \in \mathcal{T}} \sum_{l \in \mathcal{L}} \bar{F}_l (\mu_{t,g}^{min} + \mu_{t,g}^{max}) - \sum_{t \in \mathcal{T}} \sum_{g \in \Omega^{NS}} \sum_{b \in \mathcal{B}_g} \bar{P}_{g,b} \xi_{t,g,b}^{max} \\
&\quad - \sum_{t \in \mathcal{T}} \sum_{n \in \mathcal{N}} \pi (\rho_{t,g}^{min} + \rho_{t,g}^{max}) + \sum_{t \in \mathcal{T}} \sum_{n \in \mathcal{N}} D_{t,n} \lambda_{t,n} \quad (3.5)
\end{aligned}$$

3.8 Case Study: IEEE 24-Bus Reliability Test System

3.8.1 Test System Data and Setup

A modified version of the IEEE Reliability Test System available from [64] is used to conduct the study. This test system contains 24 buses, 38 transmission lines, and load at 17 buses.

A total of 8 firms^{9,10} (shown in Table 3.1) with different generation capacities and fuel types participate in the market. For the sake of simplicity throughout this case study, we assume that generators submit single-block offers to the day-ahead market. The following tax rates are considered: zero tax, \$20/ton, \$40/ton, \$60/ton, and \$80/ton. All of the ensuing simulation results are obtained by solving the model using CPLEX under the GAMS modeling environment with the maximum optimality gap set to be 1%.

3.8.2 *Effect on Consumption Cost*

Figure 3.4 shows the effect each firm has on the total cost incurred by consumers when offering strategically. As expected, the consumption cost increases when a strategic firm exercises market power. However, for all firms other than Firm 4, introducing a carbon tax to the system reduces the relative increase in consumption cost. This shows that levying a carbon tax diminishes the ability to exercise market power for some market participants. In fact, for Firms 2 and 8, offering strategically when the tax rate is \$80/ton has no effect whatsoever on the consumption cost. Moreover, their ability to increase the total cost paid by consumers declines as the tax rate increases.

To better understand the driving factors behind this, Fig. 3.5 shows the merit order of the participating firms used by the ISO to dispatch generating units in the day-ahead market and how this order changes for different tax rates. In this simulated market setting, a strategic firm can alter market prices to its advantage by raising its offer price to be just under the marginal cost of a more expensive unit in the merit order. In periods where the strategic firm is infra-marginal, raising its offer price will also reduce its output because the current marginal unit is not at full capacity. Conversely, in periods where the strategic firm

⁹The HHI for the participating firms can be calculated as follows: $HHI = 3.18^2 + 12.07^2 + 20.25^2 + 15.29^2 + 18.47^2 + 0.95^2 + 13.90^2 + 15.89^2 = 1587.67$. This value indicates that the market is moderately concentrated since, per the DOJ guidelines, the HHI is just above the threshold of competitive markets (1500) but lower than the threshold of highly concentrated markets (2500).

¹⁰The RSI of the firms are 1.21, 1.11, 1, 1.07, 1.03, 1.25, 1.08, and 1.06. All of the suppliers' RSI values are larger than one, indicating that no individual supplier is pivotal according to [74]. Note that the peak demand was used in the calculation of the RSI.

Table 3.1: Data for the participating firms

	Bus	Fuel Type	Capacity (MW)	Fuel Price (\$/MBtu)	IHR (MBtu/MWh)	CO ₂ Emissions (ton/MBtu)
Firm 1	Unit 1 1	Oil CT	40	10.35	10.14	0.08
	Unit 2 2					
Firm 2	Unit 1 1	Coal	152	2.11	9.97	0.105
	Unit 2 2					
Firm 3	Unit 1 7	Gas CC	255	3.89	6.00	0.059
	Unit 2 18					
Firm 4	Unit 1 13	Gas CT	220	3.89	10.30	0.059
	Unit 2 23		165			
Firm 5	Unit 1 15	Coal	155	2.11	8.54	0.105
	Unit 2 16		310			
Firm 6	Unit 1 15	Oil ST	24	10.35	10.33	0.085
Firm 7	Unit 1 23	Coal	350	2.11	8.90	0.105
Firm 8	Unit 1 21	Nuclear	400	0.81	8.97	0

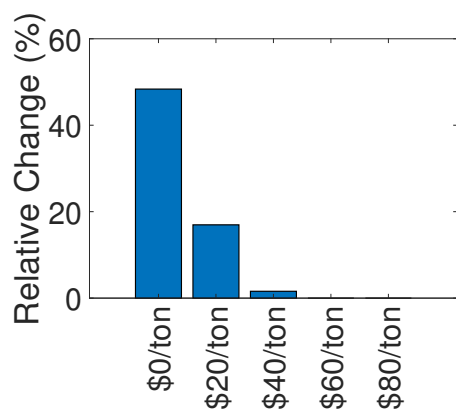
is marginal, it can either raise its offer price to the marginal cost of the next unit in the merit order without reducing its output, or, if it is more profitable, decide to forego some of its production and raise its offer price even more to the marginal cost of the following unit. Hence, when Firm 2 is the strategic firm, as the tax rate increases to \$20/ton and to \$40/ton, the difference between its marginal cost and the marginal cost of the next firm decreases. This is the case since Firm 4 owns gas units and the tax increase does not increase its marginal cost as much as it does for Firm 2. For higher tax rates, Firm 2 becomes extra-marginal and has no influence on market prices. As for the case when Firm 8 is the strategic firm, as tax rates increase, it becomes less profitable to forego some of its production for the sake of higher prices.

As is the case with Firm 4, other firms benefit from higher tax rates. For low tax rates, Firm 4 is extra-marginal, and hence, cannot alter market prices. However, it becomes marginal for some periods when the tax is \$60/ton and both marginal and infra-marginal when the tax is \$80/ton. In this case, imposing carbon taxes results in an increase in market power as shown in Fig. 3.4(c).

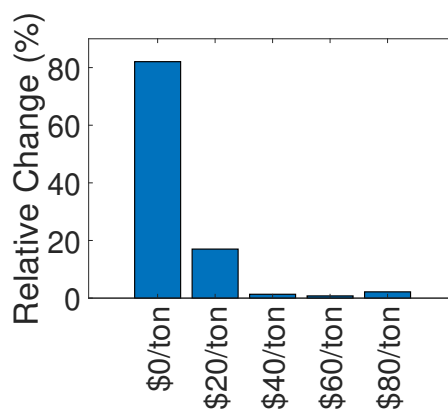
3.8.3 *Effect on Emissions*

Fig. 3.6 shows how the level of CO₂ emissions changes, with respect to perfect competition, when each firm is exercising market power for the considered tax rates. The strategic behavior of firms does indeed affect the potency of the imposed carbon tax. Whether the change is desirable or undesirable, i.e. CO₂ emissions decrease or increase respectively, depends on *i*) the emissions rate of the type of unit(s) owned by the strategic firm, and *ii*) the emissions rate of the type of unit(s) owned by the firms that are compensating the decrease in generation resulting from the strategic behavior of the strategic firm.

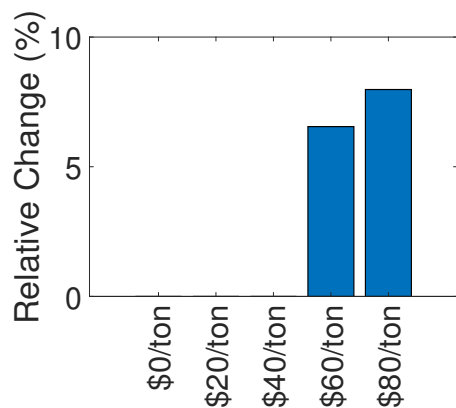
For example, Firm 8 owns nuclear units, which means that a decrease in its total output will result in an increase in the level of CO₂ emissions no matter which unit is dispatched to compensate for the loss in generation. This is the case since the nuclear unit, unlike other units, does not release any CO₂ emissions. In the case where Firm 8 is the strategic firm



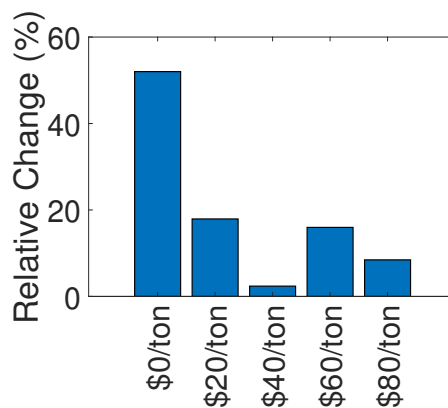
(a) Firm 2



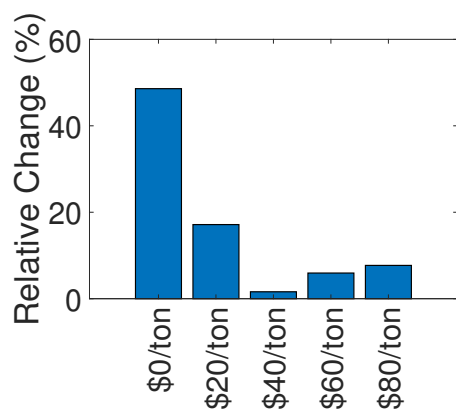
(b) Firm 3



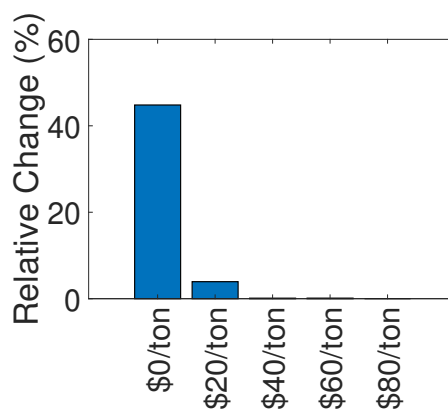
(c) Firm 4



(d) Firm 5



(e) Firm 7



(f) Firm 8

Figure 3.4: The percentage change, relative to a perfectly competitive market, in the cost incurred by consumers given that a single firm is offering strategically.

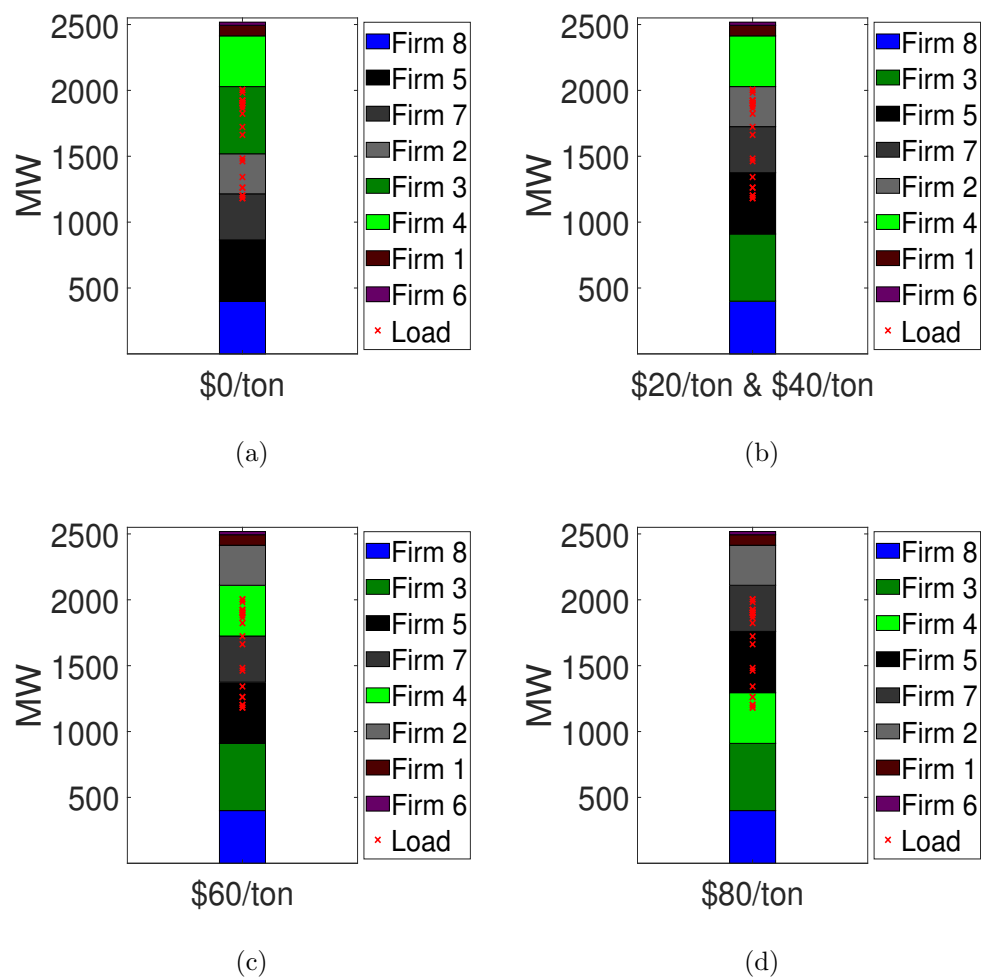


Figure 3.5: The generation capacity of the participating firms ordered by merit for different tax rates, and the system-wide hourly load.

(Fig. 3.6(f)), we notice that the largest decrease in production (roughly 14%) occurs when no carbon tax is imposed. Even though this constitutes a substantial reduction in output, CO₂ emissions increase only by 2.22% because relatively clean gas units owned by Firm 3 are dispatched to offset the shortage in generation as shown in Fig. 3.7(d). As we begin imposing and increasing the carbon tax, we can see that the difference in CO₂ emissions and Firm 8's output between the strategic offering case and the perfect competition case starts to diminish until it reaches zero.

Similarly, Firms 3 and 4 own gas units that have a lower emissions rate when compared to units owned by other firms (except Firm 8). Therefore, a reduction in their output resulting from offering strategically will lead to an increase in the level of CO₂ emissions. When Firm 3 is the strategic firm, Fig. 3.6(b) shows that the reduction in output is roughly the same (about 14%) for both a zero tax rate and a tax rate of \$20/ton. However, the change in CO₂ emissions is significantly different (0.77% and 5.32% for \$0/ton and \$20/ton respectively). This is due to the fact that under a zero tax rate, gas units owned by Firm 4 are dispatched to make up for the loss in generation as can be seen in Fig. 3.7(a). Consequently, the net increase in emissions is relatively low. By comparison, when imposing a tax rate of \$20/ton, coal units owned by Firms 2, 5, 7 are dispatched to balance the shortage in generation. The difference in dispatches in the two tax scenarios is due to the change in the merit order used by the ISO to dispatch units caused by levying a carbon tax as shown in Fig. 3.5. Under a zero tax rate, coal units have the competitive edge over gas units which means they are dispatched first. Hence, to compensate for the lower output caused by Firm 3 acting strategically, other gas units are dispatched since all coal units that are lower in cost are already dispatched. Whereas under a tax rate of \$20/ton, some coal units are no longer fully dispatched because of the tax penalty, making them available for dispatch to offset the loss in production when Firm 3 offers strategically. When the tax rate is above \$20/ton, strategic offering results in smaller changes in dispatch. Alternatively, when Firm 4 is the strategic firm, we observe that its strategic behavior affects the level of emissions only when the tax rate is \$80/ton. Under this tax rate, the reduction in Firm 4's output is compensated by

Firms 5 and 7 which causes an increase in CO₂ emissions.

Finally, for Firms 2, 5, and 7, the relative change in CO₂ emissions depends on the type of units used to offset the reduction in generation. Since these firms own high-polluting coal units, a decrease in their output will most likely result in a reduction in CO₂ emissions. However, there are some instances where the opposite is observed. For example, when Firm 5 is the strategic firm and the tax rate is \$20/ton, CO₂ emissions rise by 1.11% even though the output of the units owned by Firm 5 decreases by 19% compared to the case with perfect competition. Fig. 3.7(b) shows that this results from the dispatch of coal units that emit more tons of CO₂ per MWh than the units owned by Firm 5.

Since the amount of tax revenue collected from carbon-emitting producers is proportional to the level of emissions in the system, the strategic behavior of participating firms also impacts how much revenue is generated when imposing a carbon tax. Table 3.2 shows the tax revenue in the cases of strategic participation and competitive participation and the difference in revenue between the methods for each firm for all the considered tax rates. The tax revenue exhibit a positive net change when behaving strategically for all but two cases: *i*) when Firm 5 is the strategic firm and the tax rate is \$60/ton, and *ii*) when Firm 7 is the strategic firm and the tax rate is \$60/ton. The shortfall in revenue is of significant concern since, as discussed in Chapter 2, all revenue collected from the carbon tax is appropriated to fund other projects (e.g. issuing a carbon dividend payable to affected households). Hence, even the environmental benefit that may arise in some cases of strategic behavior in the form of reduced CO₂ emissions also comes with the downside of reduced revenue.

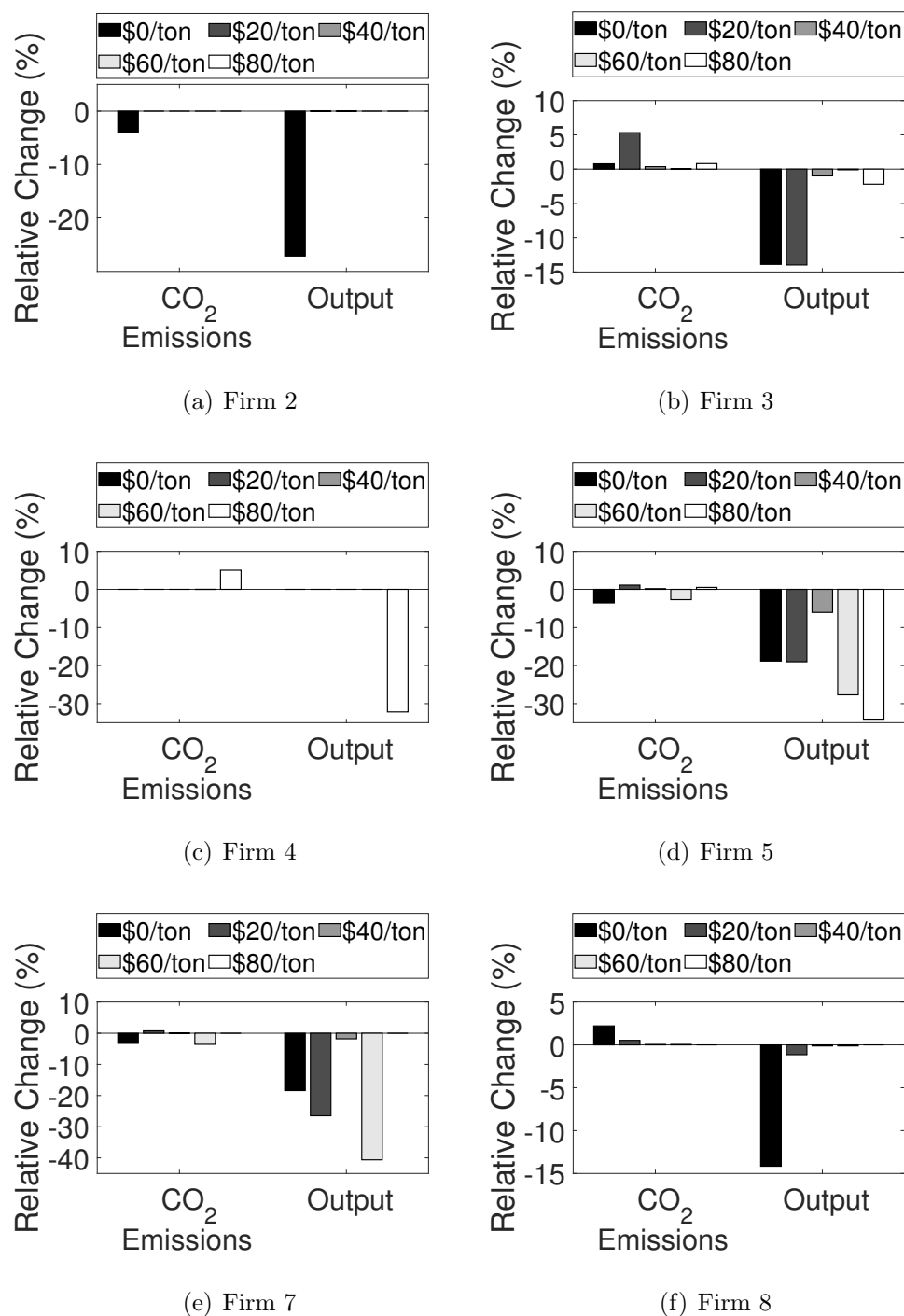


Figure 3.6: The percentage change, relative to a perfectly competitive market, in the strategic firm's output, and the system-wide CO₂ emissions given that a single firm is offering strategically.

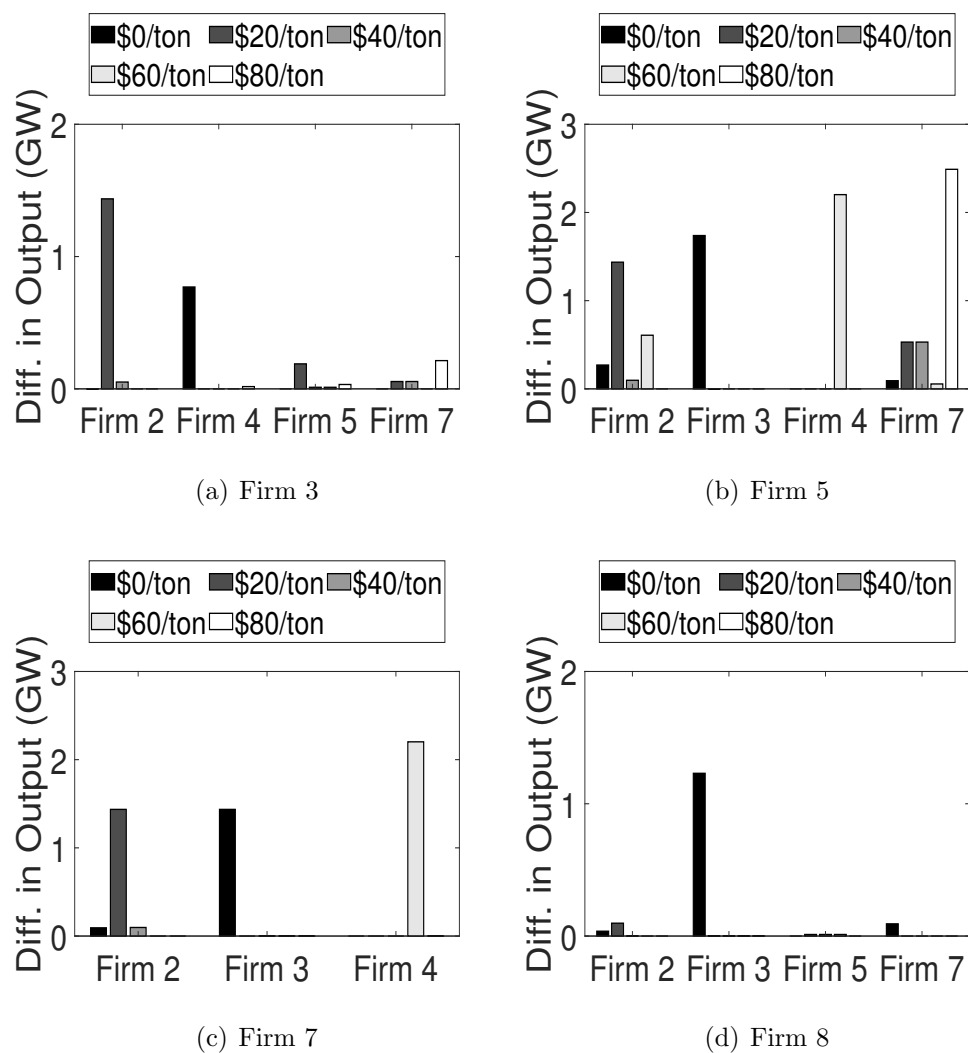


Figure 3.7: The change in total production over the scheduling horizon, relative to a perfectly competitive market, for non-strategic firms given that a single firm is offering strategically. Note that firms that are not shown in a subplot exhibit a zero net change.

Table 3.2: Tax revenue (in k\$) generated for different tax rates considering strategic and competitive behaviors of firms. Note that the difference in tax revenue between participating strategically and participating competitively is zero for firms that are not shown.

	Tax rate (\$/ton)	Strategic	Competitive	Net Change
Firm 3	20	447.24	424.66	22.58
	40	852.28	849.31	2.97
	60	1,208.08	1,207.69	0.39
	80	1,463.82	1,452.14	11.68
Firm 4	20	424.66	424.66	0
	40	849.31	849.31	0
	60	1,207.69	1,207.69	0
	80	1,525.10	1,452.14	72.96
Firm 5	20	429.35	424.66	4.70
	40	850.68	849.31	1.37
	60	1,175.07	1,207.69	-32.62
	80	1,459.56	1,452.14	7.42
Firm 7	20	427.88	424.66	3.23
	40	849.75	849.31	0.44
	60	1,164.56	1,207.69	-43.13
	80	1,452.14	1,452.14	0
Firm 8	20	426.90	424.66	2.25
	40	849.74	849.31	0.43
	60	1,208.33	1,207.69	0.64
	80	1,452.14	1,452.14	0

3.9 Summary

In this chapter, a Stackelberg game is used to study market power in electricity markets that are regulated with carbon taxes. The Stackelberg game is modeled using a bilevel optimization which is then transformed to a single-level MILP equivalent using the KKT optimality conditions, the strong duality theorem, and linearization techniques. Application of this model to a 24-bus test system leads to the following major conclusions:

- In some cases, carbon taxes diminish the ability of firms that are infra-marginal and marginal to exercise market power as measured by the relative increase in the total cost of consumption. Firms that are extra-marginal for low tax rates but become marginal or infra-marginal for higher taxes benefit from their tax-induced position in the market. Therefore, for these firms, a carbon tax increases their market power.
- The level of CO₂ emissions changes when firms offer strategically to maximize their profits. The change is positive if emissions are reduced or negative otherwise and depends primarily on the emissions rate of the units owned by the strategic firm and the emissions rate of the units dispatched to offset the shortage in production caused by the strategic offering of the strategic firm.
- The change in CO₂ emissions also brings about a change in the amount of tax revenue collected from the levied tax. The change can be positive (i.e. an excess of what is expected) or negative (i.e. a shortfall of what is expected) and the direction of change depends on whether CO₂ emissions increased or decreased since the tax revenue is directly proportional to CO₂ emissions.

Chapter 4

THE IMPACT OF CARBON PRICING ON THE OPTIMAL PARTICIPATION OF ELECTRIC VEHICLE AGGREGATORS IN THE DAY-AHEAD ENERGY MARKET

4.1 Introduction

As shown previously in Fig. 1.3, the transportation sector accounted for roughly 28% of greenhouse gas (GHG) emissions in the US in 2016. Therefore, jointly with the electricity sector, the transportation sector accounts for a substantial portion of GHG emissions and should be addressed accordingly. Light-duty vehicles¹ (LDVs) are responsible for approximately 60% of the energy use and GHG emissions of the transportation sector in the US [107]. Hence, replacing internal combustion engine (ICE) vehicles that depend on burning fossil fuel for movement—a highly polluting process [108, 109]—with electric vehicles (EVs) that use electric energy stored in batteries for motion will lead to significant reductions in GHG emissions in addition to other benefits².

The push to decarbonize the transportation sector has been propelled by a myriad of EV support policies³ that are in place globally. By promoting widespread adoption of EVs, these policies accelerated the transition to electric driving. In 2017, the global number of EVs—including both battery electric vehicles (BEVs) and plug-in hybrid electric vehicles (PHEVs)—has crossed the 3 million mark to be roughly 3.1 million vehicles [111]; a staggering increase of more than seventeenfold when compared to the global number of EVs in 2012.

¹Passenger cars and light trucks.

²For example, an increase in energy security and sustainability due to the decrease in dependence on oil, specifically, foreign oil.

³Such as access to HOV lanes, purchase rebates, waiver on fees, and purchase and registration tax exemptions [110].

By 2030, the global stock of EVs is projected to grow to 125 million considering existing and planned support policies. The projected number becomes even larger (220 million) if new ambitious policies are set with the goal of mitigating global GHG emissions [111].

Integrating a large number of EVs into the electric grid comes with multiple challenges to electric utilities (e.g. see [112]). Since most EV owners tend to charge their vehicles when returning home from work, the bulk of the added demand due to the charging of EVs coincides with the system-wide peak demand [113,114]. Therefore, if left uncontrolled, accommodating a sizable number of EVs successfully requires serious investments in power grid assets (e.g. generation capacity, transmission/distribution lines, and transformers) to prevent shortages in supply, branch congestion, power losses, and large voltage drops [115–118]. On the other hand, harnessing the flexibility of EVs by properly managing their load via smart charging and discharging techniques would not only defer costs associated with revamping the power grid, but also enable EVs to provide numerous grid-support services such as facilitating the integration of renewable energy sources (e.g. increase the capacity and limit the curtailment of wind and solar photovoltaics), peak-shaving and valley-filling, and providing ancillary services (e.g. frequency regulation) [119–123].

In order to adequately manage the EV load and provide the aforementioned support services for the power grid, EVs must actively participate in electricity markets. The notion of EVs participating in electricity markets is made possible due to the advent of the smart grid and advancements made in communication technologies which enable a more proactive role from the demand side in electricity markets [124,125]. However, due to the small capacity of individual EVs, a collection of EVs must be aggregated together to meet the minimum capacity⁴ requirement for load participation set by independent system operators (ISOs). Therefore, there is a need for an aggregation agent (referred to as an aggregator hereafter) to manage the participation of EV fleets in electricity markets.

In this chapter, we focus on modeling the optimal participation of EV aggregators in the

⁴For example, 100 kW in PJM [126], 100 kW in ERCOT [127], and 500 kW in CAISO [128].

day ahead market for electric energy under carbon pricing in the form of a carbon tax. In doing so, we attempt to address the following research questions:

1. What are the optimal charging and discharging profiles that minimizes the net costs incurred by the aggregator?
2. What are the environmental impacts (i.e. the amount of carbon emissions) that would result from the optimal participation the EV aggregator?
3. What are the effects of carbon pricing on the optimal charging and discharging schedules, and by extension, the level of system-wide carbon emissions?

To that end, a bilevel optimization approach is taken to formulate the model, where the upper-level (UL) is the aggregator with the objective of minimizing the total cost of net demand for electricity whereas the lower-level (LL) represents the day ahead market clearing process for electric energy. One of the biggest advantages of using a bilevel model is the fact that locational marginal prices (LMPs) are formulated endogenously within the model, which eliminates the need of using exogenous, forecasted prices for electric energy. This is advantageous since exogenous prices do not account for the effects of the EV demand which may lead to suboptimal strategies [129, 130].

4.2 Literature Survey

4.2.1 Electric Vehicles in Electric Power Systems

The optimal participation of EV aggregators in electricity markets has been the subject of multiple research papers commonly found in the literature. For example, Sortomme and El-Sharkawi [131] develop a smart charging algorithm for unidirectional Vehicle-to-Grid (V2G) regulation. The authors further extend their model to account for *i*) EV aggregators supplying spinning reserves to the system in addition to regulation services, and *ii*) the effects of unexpected trips made by EV owners in [132]. Addressing the limitations of unidirectional strategies when compared to their bidirectional counterparts (e.g. smaller reserves

and regulation capacities and inability to exploit arbitrage opportunities), Sortomme and El-Sharkawi [133] develop an optimal charging and ancillary services schedule considering bidirectional capabilities of EVs. Bessa *et al.* [134] present an optimization approach considering a variable maximum charging power in the battery model for EV aggregators participating in the day-ahead energy market as well as secondary reserve sessions, and apply the technique to the Portuguese control area in the Iberian market. Since previous works consider a relatively small-scale penetration of EVs (e.g. 10,000 vehicles) and/or mainly focus on primary and secondary ancillary services, Ortega-Vazquez *et al.* [135] investigate the impact that a large EV fleet has on energy and reserve prices by explicitly modeling the participation of EV aggregators in the energy and tertiary regulation markets simultaneously.

Taking into account uncertainties associated with market conditions and EV characteristics, Vagropoulos and Bakirtzis [136] develop an optimal bidding strategy for EV aggregators participating as price takers in both the day-ahead energy market and the regulation market via stochastic optimization. The authors argue that the market rules concerning instructed and uninstructed deviations have a substantial impact on the bidding strategy of the aggregator, and consequently, the overall costs associated with the strategy. Whereas Ansari *et al.* [137] model market uncertainties using fuzzy optimization when developing optimal bidding strategies for EV aggregators. Sarker *et al.* [138] model the optimal participation of EV aggregators in both the day-ahead energy and reserves markets considering the probability of the aggregator's capacity offers being accepted in the day-ahead ancillary market, and the probability of deployment in the real-time. Wu *et al.* [139] present a novel game theoretic approach to model the competition between several EV aggregators where each aggregator is looking to develop an optimal bidding strategy in the day-ahead energy and ancillary service markets.

Controlling the charging and discharging of a massive number of EVs will undoubtedly have an impact on electricity prices. Therefore, Kristoffersen *et al.* [140] use a multivariate regression algorithm to account for the dependency between electricity prices and the demand when developing charging and discharging strategies for EV aggregators. Moreover, Vayá

and Andersson [129] propose a bilevel optimization model in which the aggregator bids strategically in the day-ahead energy market to secure the energy needs of EVs. The model considers endogenous formations of energy prices when optimizing the charging schedule of the aggregator, which guarantees that the effect of the EV demand on prices is taken into account. The authors further extend their model to include uncertainties related to driving patterns in [130].

The value of coordination with a large EV fleet is shown in [141] where Al-Awami and Sortomme show how EV aggregators who possess their own generation assets can benefit from increased profits and reduced trading risks when coordinating Vehicle-to-Grid (V2G) services with energy trading. The authors of [142] use a stochastic optimization to model the coordination between EVs and wind power producers with the goal of mitigating imbalance concerns that arise from imperfect wind forecasts and EV driving patterns. Takavoli *et al.* [143] use a stochastic bilevel optimization model to find the optimal offering strategy of a strategic producer—who owns both conventional and wind units—that participates in the day-ahead energy and real-time regulation markets while coordinating with unidirectional V2G services.

Sarker *et al.* [144] propose a multistage, non-iterative decentralized approach where consumers adjust their EV charging schedule—along with other flexible household loads—in response to monetary incentives offered by the aggregator who seeks to maximize profits. Mattlet and Maun [145] present a bilevel model where dynamic pricing signals are designed to change the charging profile of EVs to avoid overloading transformers power rating by reducing the peak-to-average ratio.

4.2.2 *Electric Vehicles and GHG Emissions*

Rangaraju *et al.* [146] look at the life cycle environmental emissions of EVs and compare them with petrol and diesel vehicles considering real-world energy consumption patterns based on empirical data and the Belgian electricity mix. The authors show that, within the confines of the Belgian data, off-peak charging leads to significant reductions in the emissions of CO₂

and CO₂ equivalents (SO₂, NO_x, and particulate matters). This is attributed to the fact that during off-peak hours, the load is mainly supplied by nuclear plants, renewables, and natural gas generating units; all of which are no- or low-polluting energy sources. Casals *et al.* [147] compare the Global Warming Potential (GWP) of EVs under different driving conditions with their conventional ICE vehicles counterpart in several European countries. The authors conclude that most of the studied countries offer immediate reductions in GHG emissions due to their relatively low-polluting electricity generation mix. However, the authors also note that some of the countries covered in the analysis need to undertake a decarbonizing effort since their respective electricity sectors still feature high-polluting generation fleets.

Weis *et al.* [148] investigate the impact that controlled (via a central dispatcher) and uncontrolled vehicle charging has on emissions and cost in the US PJM region. Their results demonstrate that controlled charging can reduce system costs by 23% to 34% due to shifting the EV load to off-peak hours where low-cost coal plants are the marginal units. This shift, however, results in increased emissions caused by the high-emitting nature of coal generating units. Hoehne and Chester [149] propose a framework where the charging and discharging of plug-in electric vehicles are optimized to minimize carbon emissions taking into account time varying marginal emissions rates. The authors present cases where utilizing V2G capabilities of EVs for arbitraging can cause an increase carbon emissions when compared to standard, unidirectional EV use. Conversely, Sioshansi and Denholm [150] find that exploiting the V2G potential of EVs to offer ancillary services in addition to arbitrage brings about reductions in carbon emissions. The main reason behind this result is the fact that there are fewer generators that are committed and partially loaded in order to provide spinning reserves to the system. This is the case since EVs are now utilized to supply some of the capacity required for spinning reserves.

In [151], Peterson *et al.* examine the CO₂ and NO_x emissions that result from integrating a large fleet of plug-in hybrid electric vehicles in the PJM interconnection and the New York Independent System Operator (NYISO) electric region for different charging strategies considering a carbon tax rate of \$50/ton. Freeman *et al.* [152] investigate the economic benefits

of arbitraging via V2G under two different carbon tax rates: \$50/mt and \$250/mt. Their analysis shows that even though the cost of charging increases with the implementation of a carbon tax, the average annual cost savings that result from engaging in arbitrage increase when compared to the case without a carbon tax. Therefore, the authors conclude that there exist situations where carbon mitigating policies encourage EV owners to participate in providing V2G services to the grid by making it more financially attractive.

4.3 Contribution

Each of the methods used to develop the optimal bidding and offering strategy in all of the surveyed work suffers from one or more of the following limitations:

1. Uses exogenous prices to schedule the optimal charging and discharging profiles, which would underestimate the effects that the EV aggregator has on energy prices.
2. Considers only a unidirectional mode of operation of the EV fleet, which neglects the arbitrage capability of EVs.
3. Neglects technical constraints related to the operation of power systems such as line limits of the network and ramping constraints of generating units, or in some cases, neglects the power system entirely.
4. Neglects the impact that battery degradation has on the EV fleet.
5. Does not consider the additional costs associated with carbon pricing.

Therefore, our first contribution is to expand existing models and include the previous shortcomings to offer a more rigorous participation strategy for EV aggregators.

Furthermore, EVs are hailed as an environmentally friendly alternative to ICE vehicles because there are no tailpipe emissions associated with them. However, this does not mean that EVs are emissions-free. The manufacturing and disposal processes of the batteries in

addition to the electric energy required to charge the batteries have their environmental impact. Therefore, our second contribution is to provide an adequate assessment of the carbon emissions associated with the optimal strategy carried out by the EV aggregator when participating in electricity markets. Finally, our third contribution comes in the form of investigating the effects that carbon taxes have on the optimal bids and offers made by the aggregator and the resulting impacts on the potency of those taxes to mitigate carbon emissions.

4.4 Chapter Organization

The rest of the chapter is organized as follows. The EV aggregator and market framework is explained in Section 4.5. Section 4.6 describes the bilevel optimization used to model the aggregator's participation in the day-ahead market. Section 4.7 explains both the solution methodology used to transform the bilevel optimization to its corresponding Mathematical Problem with Equilibrium Constraints (MPEC), and the linearization techniques used to convert the MPEC to its single-level equivalent MILP. Section 4.8 presents numerical results from a 24-bus case study. Finally, concluding remarks about the key findings of this chapter are provided in Section 4.9.

4.5 Market Framework

4.5.1 Electric Vehicle Aggregator

The aggregator is a profit-seeking business entity that acts as an intermediary between owners of EVs and wholesale electricity markets with the primary objective of procuring the energy needs of consumers to fulfil their transportation requirements. Since EVs are mostly parked for extended periods of time, aggregators can group a large number of EVs that, collectively, are considered to be a large storage resource and exploit the inherent flexibility of that storage resource. In this framework, we consider a centralized approach where aggregators have direct control of charging and discharging of EVs, as opposed to a decentralized approach

where EV owners respond to pricing signals from aggregators while maintaining autonomy of their charging and discharging schedules [144, 145, 153–156].

After contracting a large number of EVs, the aggregator can then proceed to participate in the day-ahead market for electric energy in one of the following ways:

- Competitively (i.e. a price taker) where the aggregator does not have the ability to influence market prices. In this case, the aggregator submits demand volume bids at the market bid price cap and non-priced supply offers.
- Strategically (i.e. a price maker) where it is assumed that the aggregator has accumulated a significant market share that it is now possible to affect market prices. Under this scenario, the aggregator submits demand bids and supply offers strategically in the day-ahead market.

In both instances, the aggregator benefits both from the reduced cost due to purchasing energy for charging purposes in bulk from the market, and the additional revenue stream from selling energy back to the grid when discharging. In return, the aggregator is expected to share the cost savings fairly with contracted customers in the form of reduced electric energy rates and/or recurring payments. The manner in which this is done, however, is out of the scope of this work. Therefore, to receive the previously stated benefits, EV owners are encouraged to contract with an aggregator that participates in electricity markets on their behalf.

In this work, we make the following assumptions when modeling the aggregator’s participation in the day-ahead energy market:

1. There is only a single EV aggregator who is participating in the market
2. The EV aggregator has complete knowledge of the arrival and departure times, initial state-of-charge (SOC), and total energy required for motion for all of the aggregated EVs.

3. The objective of the EV aggregator is to minimize the short-term net costs incurred from participating in the market.
4. The EV aggregator has perfect information about other market participants (i.e. other producers and large consumers) and system parameters (e.g. system topology and transmission line limits).
5. All other market participants are participating competitively in the market (i.e. offer/bid their true marginal cost/utility).

4.5.2 Day-ahead Market

A pool-based energy market is considered where all of the participants in the day-ahead market (i.e. generating units, and load serving entities) are expected to submit their demand bids and supply offers to the ISO⁵. The ISO would proceed by aggregating all of the bids and offers, and then, clearing the market by maximizing the social welfare subject to the technical constraints of the system. The results of this process are the cleared demand and supply quantities, and the market clearing price (i.e. the price of electric energy) which is used to remunerate accepted offers and invoice accepted bids.

⁵The ISO functions both as a System Operator and a Market Operator in this market setting.

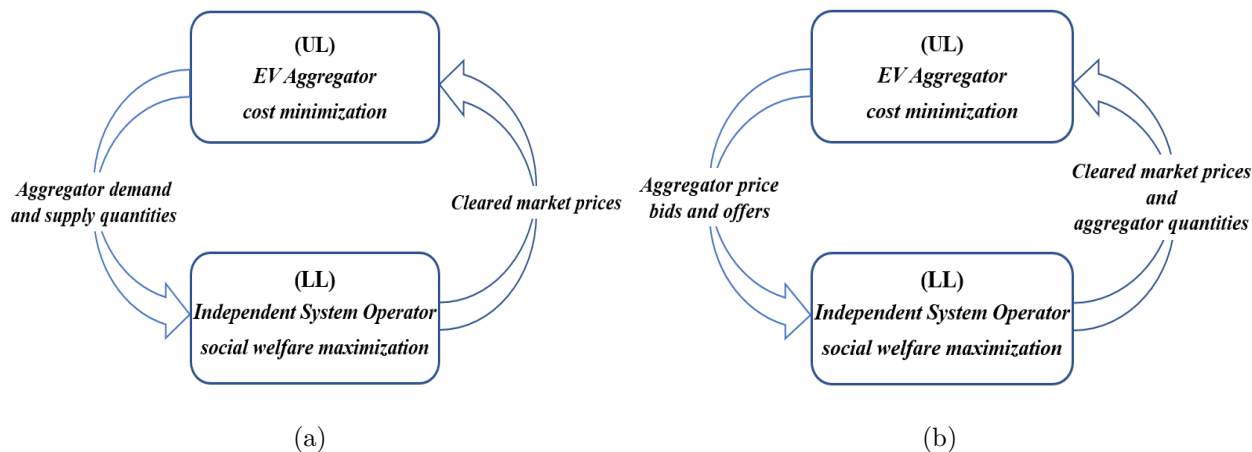


Figure 4.1: Flowchart depicting the interaction between the different levels of the bilevel optimization when the aggregator is participating (a) competitively, and (b) strategically.

4.6 Mathematical Model Formulation

Figure 4.1 illustrates the bilevel formulation used to optimize the participation of the EV aggregator in the day-ahead energy market. The manner in which the aggregator participates in the market (i.e. competitive or strategic) will result in a different mathematical model as shown below. In both models, the UL problem takes the perspective of the EV aggregator who aims to minimize the net cost of the charging and discharging schedule of the large EV fleet. However, the approach taken to achieve the desired objective is different for each model. In the competitive case, the output of the UL is the optimal quantities that the aggregator bids and offers in the day-ahead market. Whereas in the strategic case, the output of the UL problem is the optimal bid and offer prices.

The LL problem takes the perspective of the ISO whose goal is to maximize the social welfare. The LMPs that are used in the UL to calculate the cost in both the competitive and strategic cases as well as the cleared bid and offer quantities that the UL uses in the strategic case are the outcomes of the LL market clearing process. Note that the dual variables associated with each constraint in the LL problem is shown between parentheses following a colon.

4.6.1 Competitive EV Aggregator

The model for the competitive EV aggregator can be formulated as follows:

$$\min_{p_{t,v}^{chg}, p_{t,v}^{dis}, soc_{t,v}} \Delta t \cdot \sum_{t \in \mathcal{T}} \sum_{v \in \mathcal{V}} \left(p_{t,v}^{chg} - \eta_v^{dis} \cdot p_{t,v}^{dis} \right) \cdot \lambda_{t,n(v)} + \Delta t \cdot \sum_{t \in \mathcal{T}} \sum_{v \in \mathcal{V}} \left| \frac{m_v}{100} \right| \cdot C_v^{bat} \cdot p_{t,v}^{dis} \quad (4.1a)$$

subject to the following constraints:

$$soc_{t,v} = soc_{t-1,v} + \Delta t \cdot \left(\eta_v^{chg} \cdot p_{t,v}^{chg} - p_{t,v}^{dis} \right) - E_v \cdot \frac{S_{t,v}}{\sum_{t' \in \mathcal{T}} S_{t',v}}; 1 < t \leq n_t, \forall v \in \mathcal{V} \quad (4.1b)$$

$$soc_{t,v} = SoC_v^{init} + \Delta t \cdot \left(\eta_v^{chg} \cdot p_{t,v}^{chg} - p_{t,v}^{dis} \right) - E_v \cdot \frac{S_{t,v}}{\sum_{t' \in \mathcal{T}} S_{t',v}}; t = 1, \forall v \in \mathcal{V} \quad (4.1c)$$

$$\underline{SoC}_v \leq soc_{t,v} \leq \overline{SoC}_v; \forall t \in \mathcal{T}, \forall v \in \mathcal{V} \quad (4.1d)$$

$$soc_{t=n_T,v} = soc_{t=0,v}; \forall v \in \mathcal{V} \quad (4.1e)$$

$$0 \leq p_{t,v}^{chg} \leq \alpha_{t,v} \cdot \bar{P}_v; \forall t \in \mathcal{T}, \forall v \in \mathcal{V} \quad (4.1f)$$

$$0 \leq p_{t,v}^{dis} \leq \alpha_{t,v} \cdot \bar{P}_v; \forall t \in \mathcal{T}, \forall v \in \mathcal{V} \quad (4.1g)$$

where $\lambda_{t,n(v)} \in$

$$\operatorname{argmin} \left\{ \Delta t \cdot \sum_{t \in \mathcal{T}} \sum_{b \in \mathcal{B}_g} \sum_{g \in \mathcal{G}} (c_g \cdot h_{g,b} + e_g \cdot h_{g,b} \cdot P^{CO_2}) \cdot p_{t,g,b} - \Delta t \cdot \sum_{t \in \mathcal{T}} \sum_{v \in \mathcal{V}} \bar{B} \cdot p_{t,v}^{chg} \right. \quad (4.2a)$$

subject to the following constraints:

$$\sum_{g \in \mathcal{G}} \sum_{b \in \mathcal{B}_g} m_{g,n}^{gen} \cdot p_{t,g,b} - \sum_{l \in \mathcal{L}} m_{l,n}^{line} \cdot p_{f,t,l} = D_{t,n} + \sum_{v \in \mathcal{V}_n} \left(p_{t,v}^{chg} - \eta_v^{dis} \cdot p_{t,v}^{dis} \right) : (\lambda_{t,n}); \quad \forall t \in \mathcal{T}, \forall n \in \mathcal{N} \quad (4.2b)$$

$$p_{f,t,l} = B_l \cdot \sum_{n \in \mathcal{N}} m_{l,n}^{line} \cdot \theta_{t,n} : (\gamma_{t,l}); \forall t \in \mathcal{T}, \forall l \in \mathcal{L} \quad (4.2c)$$

$$-\bar{F}_l \leq pf_{t,l} \leq \bar{F}_l : (\mu_{t,l}^{min}, \mu_{t,l}^{max}); \forall t \in \mathcal{T}, \forall l \in \mathcal{L} \quad (4.2d)$$

$$0 \leq p_{t,g,b} \leq \bar{P}_{g,b} : (\xi_{t,g,b}^{min}, \xi_{t,g,b}^{max}); \forall t \in \mathcal{T}, \forall g \in \mathcal{G}, \forall b \in \mathcal{B}_g \quad (4.2e)$$

$$\sum_{b \in \mathcal{B}_g} p_{t+1,g,b} - \sum_{b \in \mathcal{B}_g} p_{t,g,b} \leq R_g^{up} : (\zeta_{t,g}^{up}); \forall t = 1 \dots n_T - 1, \forall g \in \mathcal{G} \quad (4.2f)$$

$$\sum_{b \in \mathcal{B}_g} p_{t,g,b} - \sum_{b \in \mathcal{B}_g} p_{t+1,g,b} \leq R_g^{dn} : (\zeta_{t,n}^{dn}); \forall t = 1 \dots n_T - 1, \forall g \in \mathcal{G} \quad (4.2g)$$

$$-\pi \leq \theta_{t,n} \leq \pi : (\rho_{t,n}^{min}, \rho_{t,n}^{max}); \forall t \in \mathcal{T}, \forall n \in \mathcal{N} \quad (4.2h)$$

$$\left. \theta_{t,n=\text{ref}} = 0 : (\sigma_t); \forall t \in \mathcal{T} \right\} \quad (4.2i)$$

The objective function of the aggregator (4.1a) minimizes the total costs incurred by the aggregator when participating in the day-ahead market, and it consists of two terms. The first term is the cost of the energy purchased for charging purposes minus the revenue obtained from selling energy—after factoring in the discharge efficiency—in the day-ahead market. The second term represents the cost associated with battery degradation. The act of charging and discharging the batteries of the EV fleet degrades their life, and thus, must be accounted for as an extra cost in the objective function. We use a linear approximation to model the cost of battery cycling as explained in [157]. Equations (4.1b) and (4.1c) determine the energy state-of-charge of EVs, which depends on the state-of-charge in the preceding time period, the charging power, the charging efficiency, the discharging power, and the energy required for transportation. Constraints (4.1d) bound the state-of-charge to be within its upper and lower limits during all time periods to avoid damaging the battery and rapid degradation [158]. Constraint (4.1e) ensures that the state-of-charge at the end of the scheduling horizon is equal to the level at the beginning of the horizon. Without this constraint, every EV with an initial state-of-charge larger than the minimum would have its battery discharged until it reaches

the minimum state-of-charge to benefit from the revenue gained by selling energy back to the grid. However, this action violates the energy neutrality of the EVs since the difference between the initial and final state-of-charge is free energy that was not purchased in the optimization horizon. Constraints (4.1f) and (4.1g) ensure that the charging and discharging rates do not violate their minimum and maximum limits. Note that the formulation used to model the EVs guarantees that—without having to use computationally burdensome auxiliary binary variables—simultaneous charging and discharging of a single EV will not occur for economic reasons as explained in [159].

The LL problem maximizes the social welfare, which is equivalent to the formulation of (4.2a) because we minimize minus the social welfare assuming all demand other than the aggregator is inelastic. This is the same as minimizing the cost of supplying the load minus the bids of the aggregator who, in the competitive case, is submitting demand volume bids at the market price bid cap, \bar{B} . Note that the supply offers from the aggregator are not included in the objective function since the aggregator submits zero-priced supply offers when participating competitively. Equation (4.2b) enforces the power balance at each bus; the dual variable of the nodal balance constraint is the price of electric energy used in the UL objective function (4.1a). Equation (4.2c) defines the real power flow in each transmission line assuming a lossless dc power flow. Constraints (4.2d) enforce the capacity limits of each transmission line. Constraints (4.2e) enforce the upper and lower bounds of each generating unit. Constraints (4.2f) and (4.2g) enforce the ramping limits of each generating unit. The upper and lower angle stability bounds at each bus are imposed in (4.2h). Finally, the reference bus is defined in (4.2i).

4.6.2 Strategic EV Aggregator

The model for the strategic EV aggregator can be formulated as follows:

$$\min_{B_{t,v}, O_{t,v}, soc_{t,v}} \quad (4.1a) \tag{4.3a}$$

subject to the following constraints:

$$(4.1b) - (4.1e) \tag{4.3b}$$

$$0 \leq B_{t,v} \leq \bar{B}; \forall t \in \mathcal{T}, \forall v \in \mathcal{V} \tag{4.3c}$$

$$0 \leq O_{t,v} \leq \bar{O}; \forall t \in \mathcal{T}, \forall v \in \mathcal{V} \tag{4.3d}$$

where $\lambda_{t,n(v)}$, $p_{t,v}^{chg}$, and $p_{t,v}^{dis} \in$

$$\begin{aligned} \text{argmin} \left\{ \Delta t \cdot \sum_{t \in \mathcal{T}} \sum_{b \in \mathcal{B}_g} \sum_{g \in \mathcal{G}} (c_g \cdot h_{g,b} + e_g \cdot h_{g,b} \cdot P^{CO_2}) \cdot p_{t,g,b} \right. \\ \left. + \Delta t \cdot \sum_{t \in \mathcal{T}} \sum_{v \in \mathcal{V}} O_{t,v} \cdot \eta_v^{dis} \cdot p_{t,v}^{dis} - \Delta t \cdot \sum_{t \in \mathcal{T}} \sum_{v \in \mathcal{V}} B_{t,v} \cdot p_{t,v}^{chg} \right\} \end{aligned} \tag{4.4a}$$

subject to the following constraints:

$$(4.2b) - (4.2i) \tag{4.4b}$$

$$0 \leq p_{t,v}^{chg} \leq \alpha_{t,v} \cdot \bar{P}_v : \left(\underline{\varphi}_{t,v}^{chg}, \bar{\varphi}_{t,v}^{chg} \right); \forall t \in \mathcal{T}, \forall v \in \mathcal{V} \tag{4.4c}$$

$$0 \leq p_{t,v}^{dis} \leq \alpha_{t,v} \cdot \bar{P}_v : \left(\underline{\varphi}_{t,v}^{dis}, \bar{\varphi}_{t,v}^{dis} \right); \forall t \in \mathcal{T}, \forall v \in \mathcal{V} \} \tag{4.4d}$$

The UL objective function in addition to the constraints related to the state-of-charge dynamics and limits do not change in the strategic model when compared to its competitive model counterpart. However, the constraints associated with the charging and discharging rates are no longer modeled in the UL problem since the charging and discharging powers are now LL variables and are determined via the market clearing process. Hence, these constraints are included in the LL as shown in (4.4c) and (4.4d). Additional constraints enforcing the strategic bid and offer prices to be non-negative and below a market cap are presented in (4.3c) and (4.3d). Furthermore, the LL objective function (4.4a) is modified to account for the strategic bids and offers of the EV aggregator. Finally, the constraints associated with the power balance, power flow, angle stability, and the generating units in the LL remain the same as they are in the competitive model.

4.7 Solution Methodology

Since both the competitive and strategic models are linear and continuous, the LL problem for each model is replaced with its KKT optimality conditions as previously discussed in Chapters 2 and 3. The MPEC form of the bilevel models for the competitive and the strategic cases are shown in (4.5) and (4.6), respectively.

4.7.1 MPEC for the competitive model

$$\min \quad (4.1a) \tag{4.5a}$$

subject to the following constraints:

$$(4.1b) - (4.1g), (4.2b), (4.2c), \text{ and } (4.2i) \tag{4.5b}$$

$$\sum_{l \in \mathcal{L}} B_l \cdot m_{l,n}^{line} \gamma_{t,l} - (\sigma_t)_{n=\text{ref}} - \rho_{t,n}^{min} + \rho_{t,n}^{max} = 0; \forall t \in \mathcal{T}, \forall n \in \mathcal{N} \tag{4.5c}$$

$$\sum_{n \in \mathcal{N}} m_{l,n}^{line} \cdot \lambda_{t,n} - \gamma_{t,l} + \mu_{t,l}^{max} - \mu_{t,l}^{min} = 0; \forall t \in \mathcal{T}, \forall l \in \mathcal{L} \tag{4.5d}$$

$$\begin{aligned} c_{g,b} \cdot h_{g,b} + e_g \cdot h_{g,b} \cdot P^{CO_2} - \sum_{n \in \mathcal{N}} m_{g,n}^{gen} \cdot \lambda_{t,n} - \zeta_{t+1,g}^{dn} + \zeta_{t,g}^{dn} - \zeta_{t,g}^{up} + \zeta_{t+1,g}^{up} \\ + \xi_{t,g,b}^{max} - \xi_{t,g,b}^{min} = 0; \forall t < n_T, \forall g \in \mathcal{G}, \forall b \in \mathcal{B}_g \end{aligned} \tag{4.5e}$$

$$\begin{aligned} c_{g,b} \cdot h_{g,b} + e_g \cdot h_{g,b} \cdot P^{CO_2} - \sum_{n \in \mathcal{N}} m_{g,n}^{gen} \cdot \lambda_{n_T,n} + \zeta_{n_T,g}^{dn} - \zeta_{n_T,g}^{up} \\ + \xi_{n_T,g,b}^{max} - \xi_{n_T,g,b}^{min} = 0; \forall g \in \mathcal{G}, \forall b \in \mathcal{B}_g \end{aligned} \tag{4.5f}$$

$$0 \leq \mu_{t,l}^{min} \perp (pf_{t,l} + \bar{F}_l) \geq 0; \forall t \in \mathcal{T}, \forall l \in \mathcal{L} \tag{4.5g}$$

$$0 \leq \mu_{t,l}^{max} \perp (\bar{F}_l - pf_{t,l}) \geq 0; \forall t \in \mathcal{T}, \forall l \in \mathcal{L} \tag{4.5h}$$

$$0 \leq \xi_{t,g,b}^{min} \perp p_{t,g,b} \geq 0; \forall t \in \mathcal{T}, \forall g \in \mathcal{G}, \forall b \in \mathcal{B}_g \quad (4.5i)$$

$$0 \leq \xi_{t,g,b}^{max} \perp (\bar{P}_{g,b} - p_{t,g,b}) \geq 0; \forall t \in \mathcal{T}, \forall g \in \mathcal{G}, \forall b \in \mathcal{B}_g \quad (4.5j)$$

$$0 \leq \zeta_{t,g}^{up} \perp \left(R_g^{up} - \sum_{b \in \mathcal{B}_g} p_{t+1,g,b} + \sum_{b \in \mathcal{B}_g} p_{t,g,b} \right) \geq 0; \forall t < n_T, \forall g \in \mathcal{G} \quad (4.5k)$$

$$0 \leq \zeta_{t,g}^{dn} \perp \left(R_g^{dn} - \sum_{b \in \mathcal{B}_g} p_{t,g,b} + \sum_{b \in \mathcal{B}_g} p_{t+1,g,b} \right) \geq 0; \forall t < n_T, \forall g \in \mathcal{G} \quad (4.5l)$$

$$0 \leq \rho_{t,l}^{min} \perp (\theta_{t,n} + \pi) \geq 0; \forall t \in \mathcal{T}, \forall n \in \mathcal{N} \quad (4.5m)$$

$$0 \leq \rho_{t,l}^{max} \perp (\pi - \theta_{t,n}) \geq 0; \forall t \in \mathcal{T}, \forall n \in \mathcal{N} \quad (4.5n)$$

4.7.2 MPEC for the strategic model

$$\min \quad (4.3a) \quad (4.6a)$$

subject to the following constraints:

$$(4.3b) - (4.3d), (4.2b), (4.2c), \text{ and } (4.2i) \quad (4.6b)$$

$$(4.5c) - (4.5n) \quad (4.6c)$$

$$\lambda_{t,n(v)} - B_{t,v} + \bar{\varphi}_{t,v}^{chg} - \underline{\varphi}_{t,v}^{chg} = 0; \forall t \in \mathcal{T}, \forall v \in \mathcal{V} \quad (4.6d)$$

$$\eta_v^{dis} \cdot O_{t,v} - \eta_v^{dis} \cdot \lambda_{t,n(v)} + \bar{\varphi}_{t,v}^{dis} - \underline{\varphi}_{t,v}^{dis} = 0; \forall t \in \mathcal{T}, \forall v \in \mathcal{V} \quad (4.6e)$$

$$0 \leq \underline{\varphi}_{t,v}^{chg} \perp p_{t,v}^{chg} \geq 0; \forall t \in \mathcal{T}, \forall v \in \mathcal{V} \quad (4.6f)$$

$$0 \leq \bar{\varphi}_{t,v}^{chg} \perp \left(\alpha_{t,v} \cdot \bar{P}_v - p_{t,v}^{chg} \right) \geq 0; \forall t \in \mathcal{T}, \forall v \in \mathcal{V} \quad (4.6g)$$

$$0 \leq \underline{\varphi}_{t,v}^{dis} \perp p_{t,v}^{dis} \geq 0; \forall t \in \mathcal{T}, \forall v \in \mathcal{V} \quad (4.6h)$$

$$0 \leq \bar{\varphi}_{t,v}^{dis} \perp \left(\alpha_{t,v} \cdot \bar{P}_v - p_{t,v}^{dis} \right) \geq 0; \forall t \in \mathcal{T}, \forall v \in \mathcal{V} \quad (4.6i)$$

4.7.3 MPEC Linearization

Dealing with the nonlinearities associated with the complementary slackness conditions in the MPEC form of both models has been addressed previously in Chapter 2, where the “Big-M” method is used to obtain linear equivalents. Therefore, the only remaining nonlinear terms in the models concern the objective functions (4.5a) and (4.6a). To obtain an exact linear equivalent of the bilinear terms in the objective functions, we utilize the strong duality theory of linear programming in addition to a number of identities defined in the complementary slackness conditions. Even though the equality corresponding to the strong duality theorem will be different depending on the model⁶, the final linear form of (4.5a) is the same as the one for (4.6a) and is shown in (4.7) below. Detailed steps outlining the process can be found in Appendix C.

$$\begin{aligned}
\sum_{t \in \mathcal{T}} \sum_{v \in \mathcal{V}} \left(p_{t,v}^{chg} - \eta_v^{dis} \cdot p_{t,v}^{dis} \right) \cdot \lambda_{t,n(v)} &= \sum_{t \in \mathcal{T}} \sum_{g \in \mathcal{G}} \sum_{b \in \mathcal{B}_g} (c_g + e_g \cdot P^{CO_2}) h_{g,b} \cdot p_{t,g,b} \\
&+ \sum_{t \in \mathcal{T}} \sum_{l \in \mathcal{L}} \bar{F}_l \cdot (\mu_{t,g}^{min} + \mu_{t,g}^{max}) + \sum_{t \in \mathcal{T}} \sum_{g \in \mathcal{G}} \sum_{b \in \mathcal{B}_g} \bar{P}_{g,b} \cdot \xi_{t,g,b}^{max} \\
&+ \sum_{t=1}^{n_T-1} \sum_{g \in \mathcal{G}} R_g^{up} \cdot \zeta_{t,g}^{up} + \sum_{t=1}^{n_T-1} \sum_{g \in \mathcal{G}} R_g^{dn} \cdot \zeta_{t,g}^{dn} \\
&+ \sum_{t \in \mathcal{T}} \sum_{n \in \mathcal{N}} \pi \cdot (\rho_{t,g}^{min} + \rho_{t,g}^{max}) - \sum_{t \in \mathcal{T}} \sum_{n \in \mathcal{N}} D_{t,n} \cdot \lambda_{t,n} \quad (4.7)
\end{aligned}$$

4.8 Case Study: IEEE 24-bus Reliability Test System

4.8.1 Data Setup

4.8.1.1 EV Data

By implementing the methodology proposed in [160], we generate the driving patterns used in the study (i.e. arrival times, departure times, and energy required for transportation

⁶Since the LL objective function in the competitive model is not identical to the LL objective function in the strategic model, the resulting identities after applying the strong duality theorem for each model—in which the primal and dual LL objective functions are equated—will not be the same.

purposes⁷) based on the data available from the National Household Travel Survey (NHTS) [161]. Since we are considering a large-scale integration of EVs, the resulting number of variables associated with the EV model will render the optimization problem computationally intractable. Therefore, to ease the computational burden, collections of vehicles with similar characteristics (i.e. driving patterns) are aggregated together and represented as a single EV, which is similar to what was done in [135,140]. The energy capacity of the EV battery is set to be 24 kWh (e.g. Nissan Leaf) as in [162] with maximum charging/discharging rate of 3.3 kW which corresponds to Level 2 charging [163]. The minimum and maximum state-of-charge limits are 15% and 95%, while the charging/discharging efficiency is 95% [164]. The initial state-of-charge is uniformly randomized between 30% and 60% of the maximum. Finally, the battery cost of EVs is assumed to be \$300/kWh [158] and the slope used for the degradation model (m_v) is set to -0.015 [157].

4.8.1.2 Power System Data

The proposed model is applied on a modified version of the IEEE Reliability Test System available in [64] considering a 24-hour scheduling horizon. The test system consists of 24 conventional thermal generating units and 6 hydro units for a total of 30 units with a generation capacity of 3018 MW. There are 38 transmission lines, 24 buses, and load (fixed and EV demand) at 17 buses in the test system. All of the ensuing simulation results are obtained by solving the model using CPLEX under the GAMS modeling environment with the maximum optimality gap set to be 0.01%.

4.8.2 Competitive vs. Strategic Participation

Even though the approach for each participation method is different, the results are identical for both cases. Participating strategically or competitively will yield the same total cost and level of CO₂ emissions for all penetration levels. Figure 4.2 shows the locational marginal

⁷We use a conversion factor of 0.33 kWh/mi to calculate the total energy required for motion from the total miles travelled [160].

prices that results from the participation of the EV aggregator, which is the same for both cases. Bidding strategically to procure the energy needs for transportation and arbitrage purposes should not differ from bidding competitively since the EV load is relatively small when compared to the total system load as explained in [130]. However, intuitively, one expects that offering strategically would yield better results as opposed to submitting zero-priced quantity offers. In order to explain this result, we refer to Fig.4.3 which displays a fictitious aggregate supply curve designed for illustrative purposes. Assume that for a given time period t where the total demand of the system is D_t , the aggregator can choose to pre-charge to offer $D_t - q_2$ MW in the case of participating competitively as denoted by the red arrow. Offering slightly more would mean that the price would decrease from p_2 to p_1 since it would shift the supply curve to the right, and therefore, lead to lower revenues. In the case of strategic offering, the aggregator can once again pre-charge and submit an offer price of p_2 to the market. In both cases, we can see that the cleared market price would be p_2 .

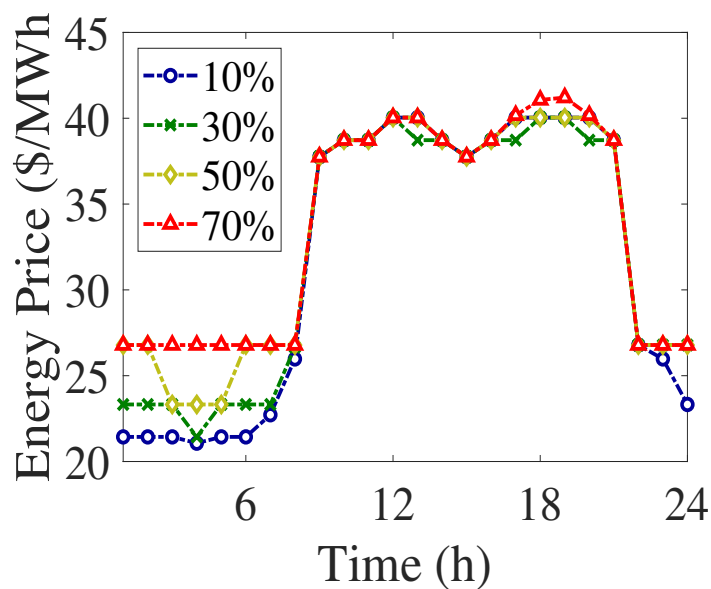


Figure 4.2: The average hourly locational marginal prices for different penetration levels and a zero tax rate.

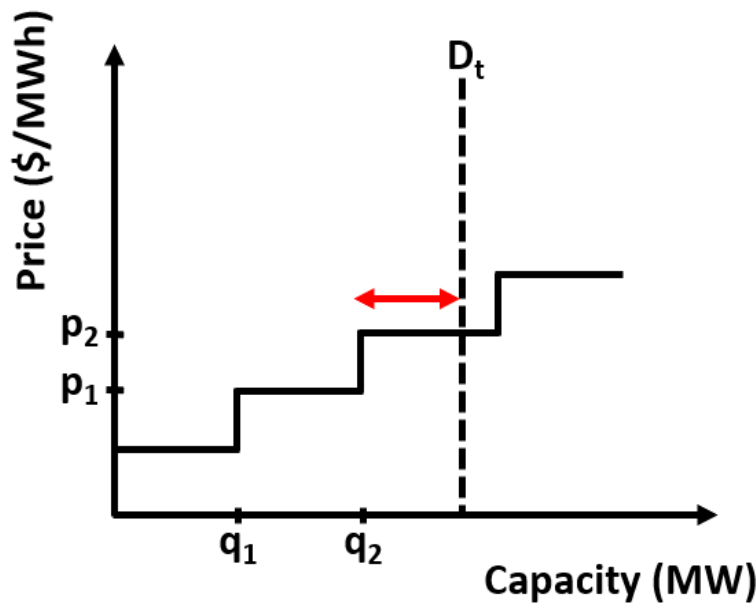


Figure 4.3: Illustrative supply curve.

4.8.3 The Effects on Arbitrage

Figure 4.4 shows how the total energy sold by the aggregator in the day ahead market changes with varying tax rates. Initially, for all penetration levels other than 70%, the amount of energy discharged starts to decrease as we increase the tax rate. This is especially noticeable in the 50% integration case where imposing a tax rate of \$18/ton decreases the total energy discharged by 95.15% (from 757.94 MWh to 44.38 MWh) when compared to its zero-tax counterpart. After the initial decrease in the discharged energy, we can see that it increases until it settle at a specific level for high tax rates. For the highest tax rate considered (i.e. \$150/ton) the total energy sold by the aggregator is 269.61, 112.86, and 51.68 MWh for 10%, 30%, and 50%, respectively. Conversely, for really high penetration of EVs (i.e. 70%) the total energy discharged increases after a specific tax rate (\$42/ton in this case) and settles at a value of 51.68 MWh.

The change in the total energy discharged also comes with a change in the monetary

benefits associated with arbitrage as seen in Fig. 4.5. We can see that the savings⁸ also decreases when we start imposing a carbon tax. This is due to the reduction in the amount of energy sold by the aggregator which decreases the revenue obtained. However, the amount of saving gained by the aggregator increases for high tax rates even though there no change in the level of energy discharges. This is attributed to the higher energy prices due to the higher tax rates which result in higher revenues.

A box plot showing the quartiles of the optimal charging and discharging profiles is shown in Figs. 4.6 and 4.7, respectively. As expected, the bulk of the EV charging is made in off-peak hours where the price of energy is the lowest. On the other hand, most of the discharging occurs during peak hours—where the system demand is high—to pocket the maximum revenue possible from arbitraging.

4.8.4 *The Effects on Carbon Emissions*

4.8.4.1 *Unidirectional Mode*

Charging EVs will increase the level of system-wide CO₂ emissions since additional thermal units are dispatched to satisfy the extra load. The amount added, however, depends on the imposed carbon tax rate. Figure 4.8 shows the additional CO₂ emissions, relative to the zero-tax case, for different penetration levels of EVs considering a unidirectional mode of operation only (i.e. no V2G discharging). We can clearly see that, for any tax rate, the additional load caused by charging EVs will result in an increase in CO₂ emissions when compared to the case where no tax rate is imposed. Moreover, the increase is not trivial, and changes for different rates. For example, when the tax rate is zero, charging EVs will add approximately 473.76, 1518.60, 2623.72, and 3368.78 tons for 10%, 30%, 50%, and 70% penetration levels, respectively. However, imposing a tax rate as small as \$18/ton will result in an increase of 804.75, 2505.52, 4316.64, and 4824.233 tons, respectively. Although the

⁸We define savings as the difference between the total cost incurred by the aggregator with and without arbitrage.

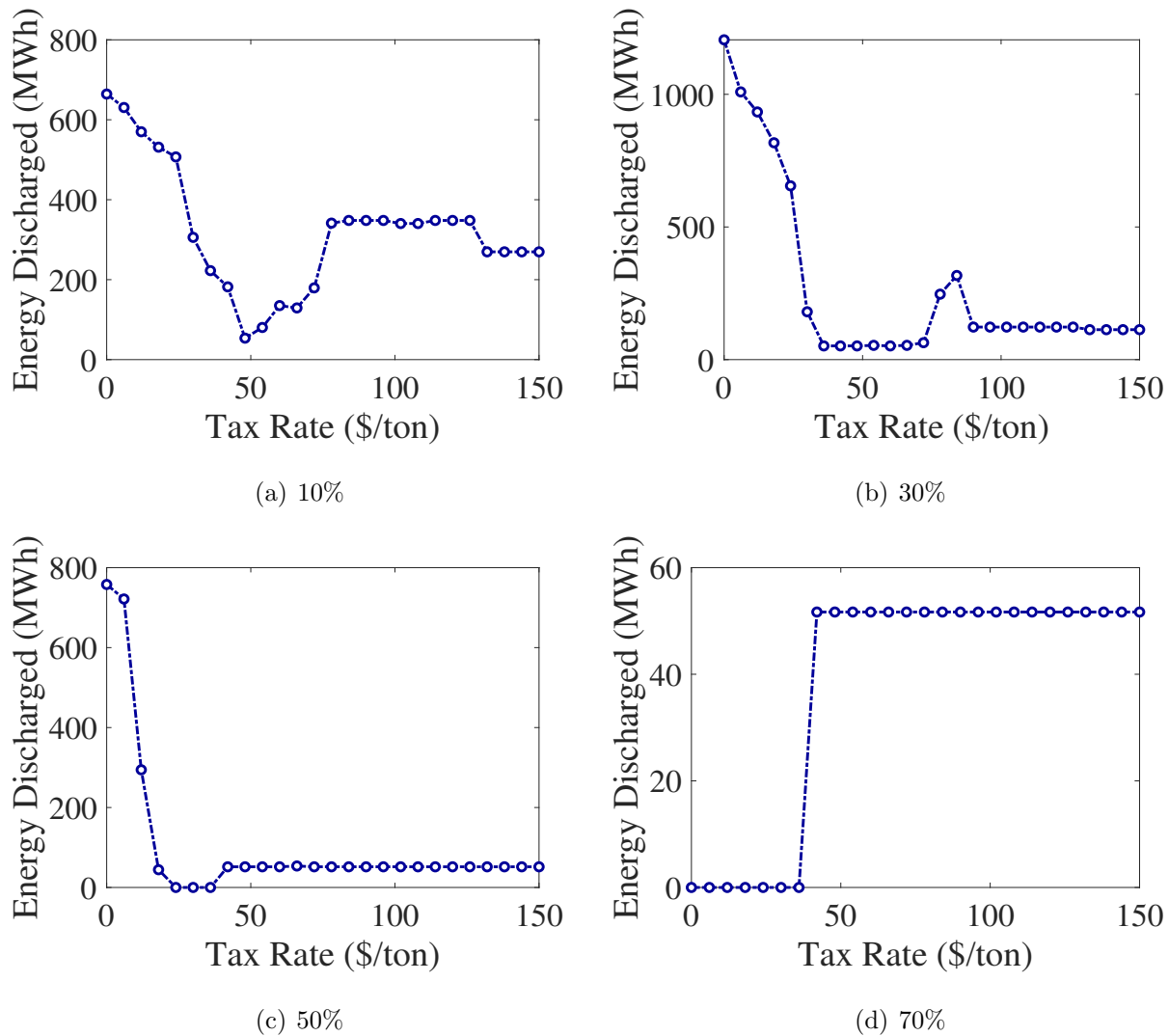


Figure 4.4: The total energy discharged for the entire scheduling horizon by the EV fleet under different tax rates.

variation in the added amount of CO_2 emissions disappears as the the tax rate approaches \$100/ton, the level at which it settles is troubling. For very high tax rates, satisfying the EV demand will add somewhere between 45%-50% more tons of CO_2 emissions relative to the zero-tax rate.

To understand the driving force behind this we refer to Fig. 4.9 where we can see the types of units that are supplying the additional load caused by charging EVs. For all penetration

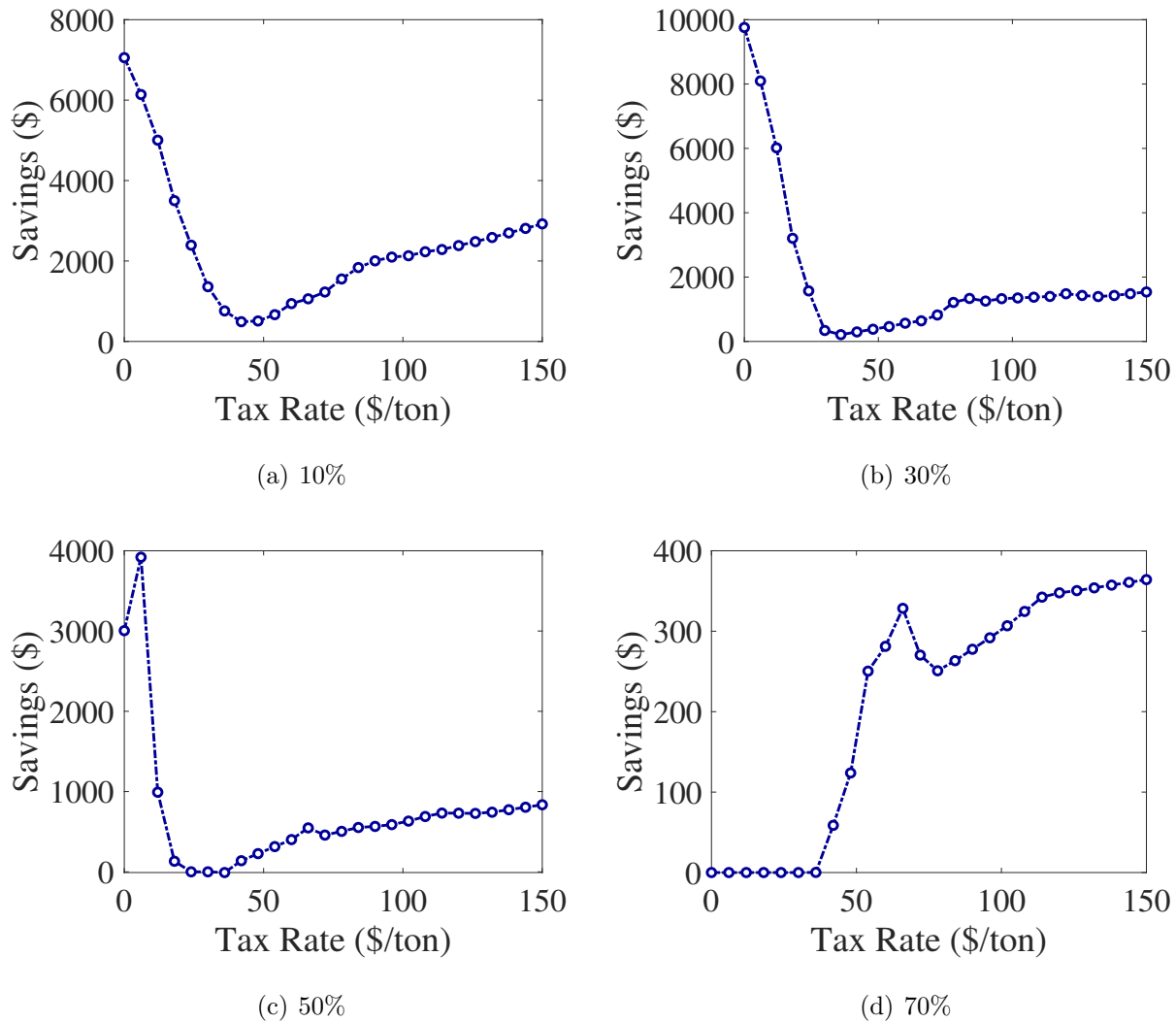


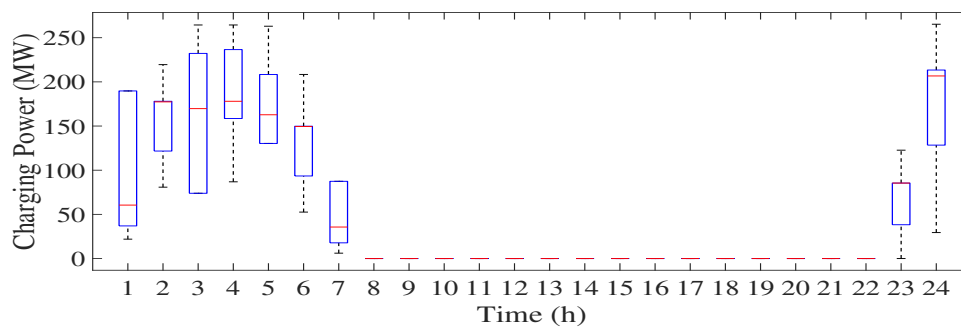
Figure 4.5: Monetary savings gained by the EV aggregator due to engaging in arbitrage.

levels, gas units are dispatched to satisfy the extra demand due to EVs when the tax rate is zero. However, as we start increasing the tax rate, coal units are mostly used to provide the additional power. This is the case since at zero tax, coal units are cheaper than gas units which makes them ahead in the merit order. Therefore, since most of the coal units are dispatched near their capacity, the additional EV load is mostly served by gas units. However, when we impose a carbon tax, the marginal cost of coal units increase because of

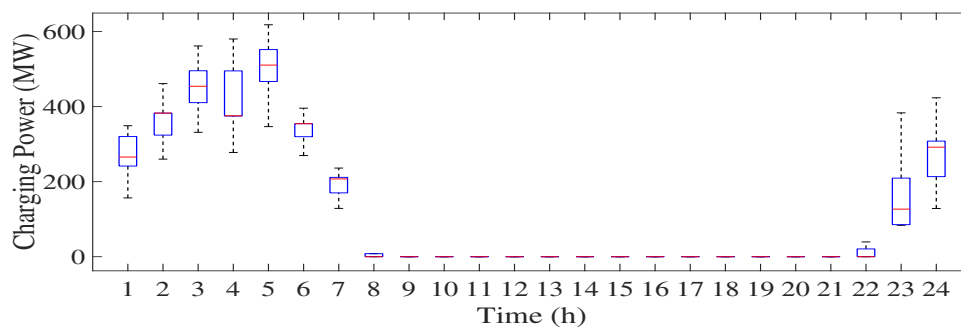
their high-emitting nature, and thus, they no longer precede gas units in the merit order. As a result, the additional EV load is fulfilled predominately by coal units since most gas units are at or near their capacity limit.

4.8.4.2 Bidirectional Mode

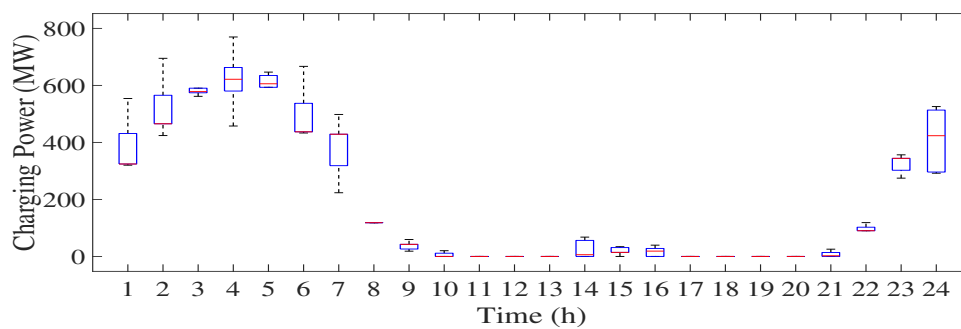
Figure 4.10 shows how the level of CO₂ emissions changes with respect to the unidirectional mode when the aggregator utilizes the arbitrage capabilities of EVs. It is noticeable that when there are no taxes imposed or when the tax rate is low (approximately lower than \$50/ton), V2G will lead to additional CO₂ emissions. This is the case since the optimal charging occurs in hours where the marginal unit are mostly coal units and the price of energy is low. Whereas discharging occurs at peak hours where the prices are high, and in those time periods, gas units are the marginal units. Therefore, EVs displace low-emitting gas units with high-emitting coal units as can be seen in Fig. 4.11. As the tax rate increases, the opposite occurs since coal units become more expensive due to their increased marginal cost, which would make them the marginal units during peak hours.



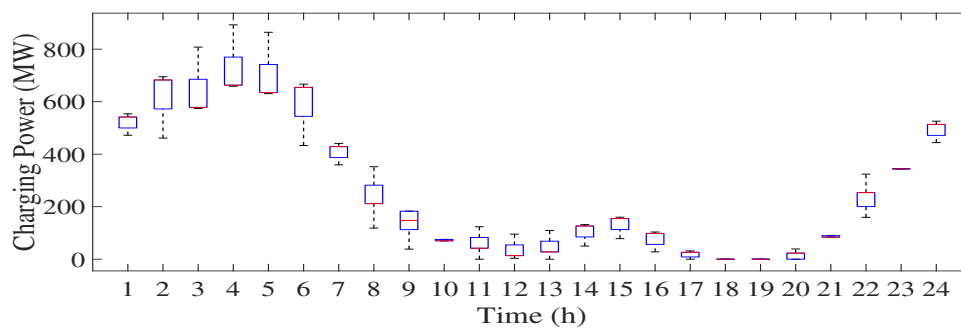
(a) 10%



(b) 30%

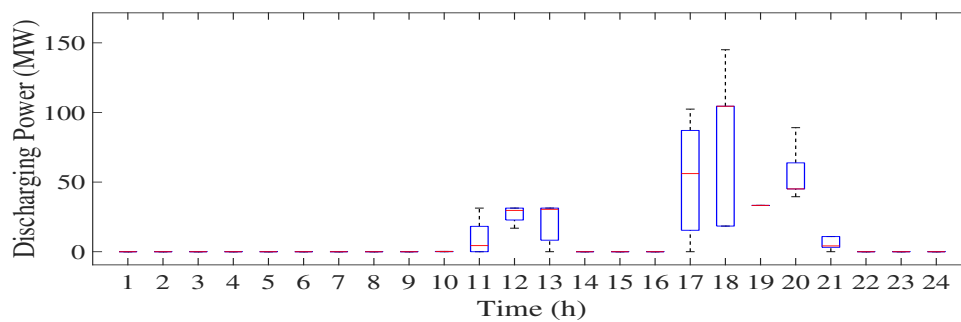


(c) 50%

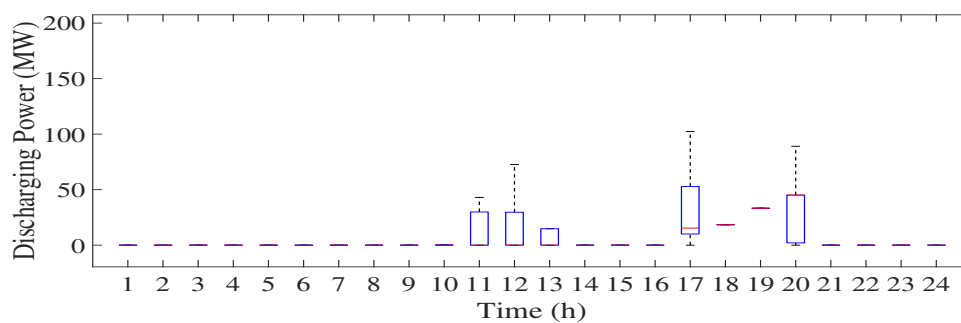


(d) 70%

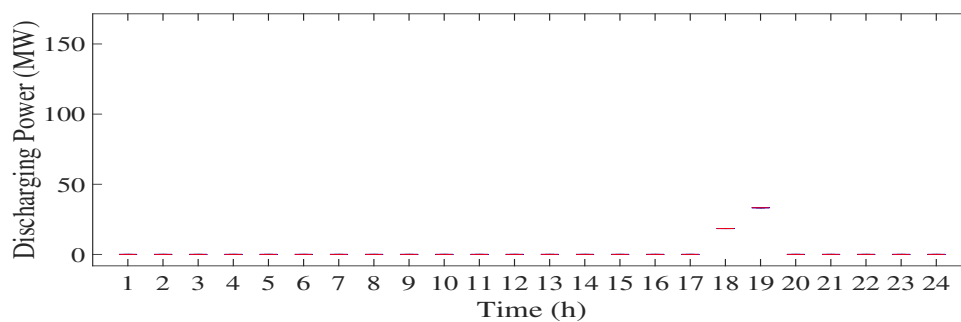
Figure 4.6: Box plot displaying the distribution of the hourly charging profile under varying tax rates.



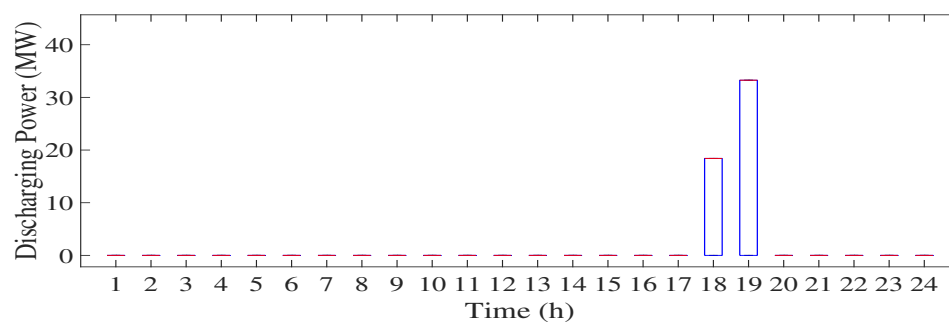
(a) 10%



(b) 30%



(c) 50%



(d) 70%

Figure 4.7: Box plot displaying the distribution of the hourly discharging profile under varying tax rates.

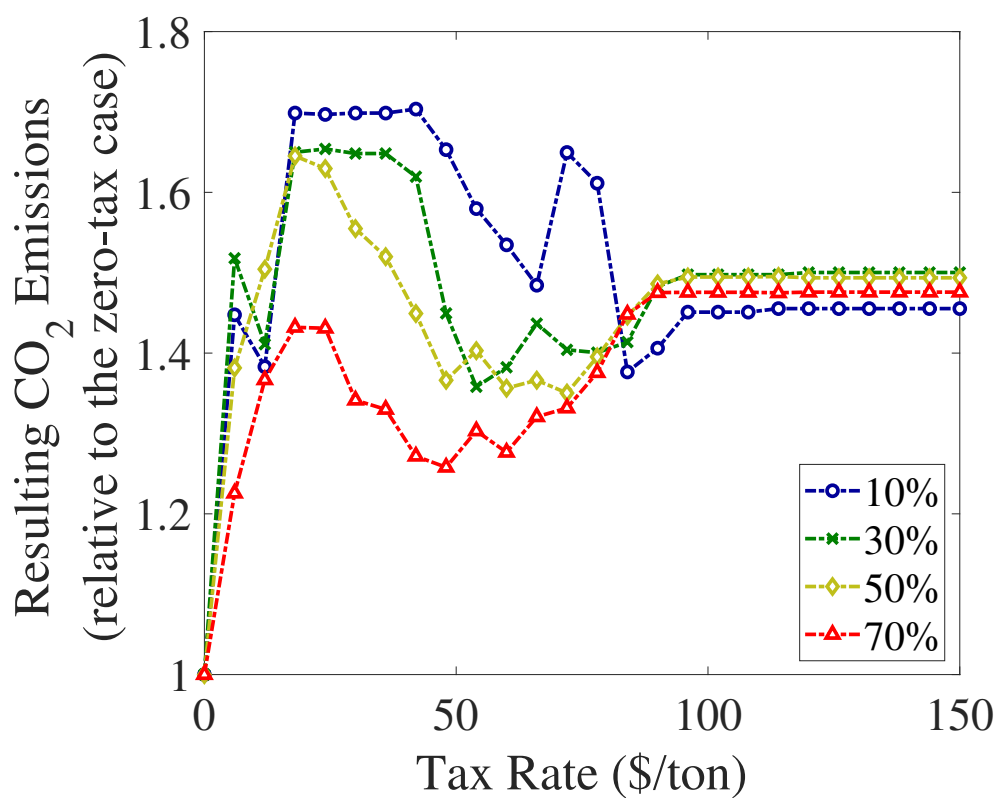


Figure 4.8: CO₂ emissions due to charging EVs, relative to the zero-tax case, for different tax rates.

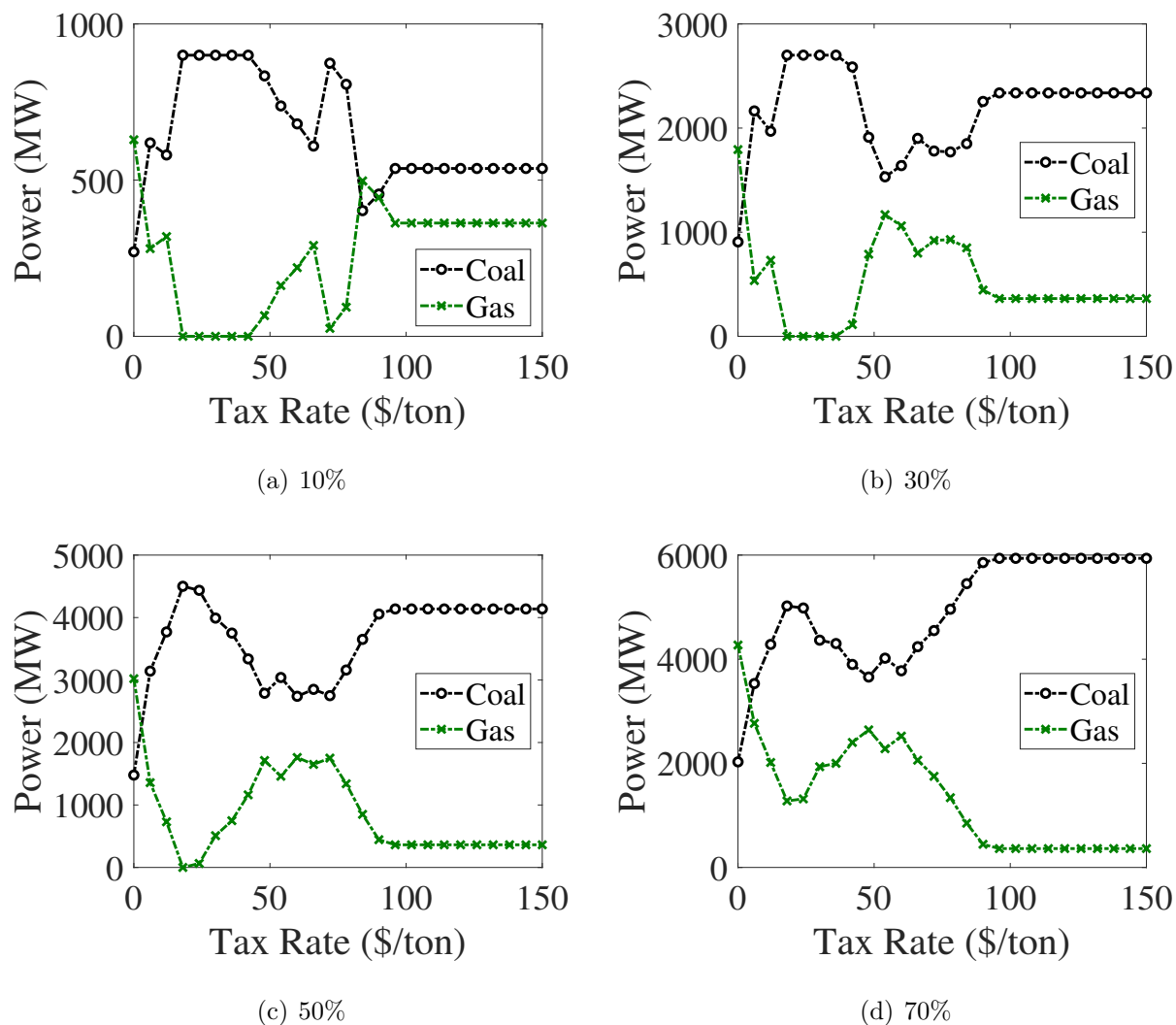


Figure 4.9: The increase in power output of gas and coal units under different tax rates for different penetration levels. Note that nuclear, hydro, and oil units exhibit zero change.

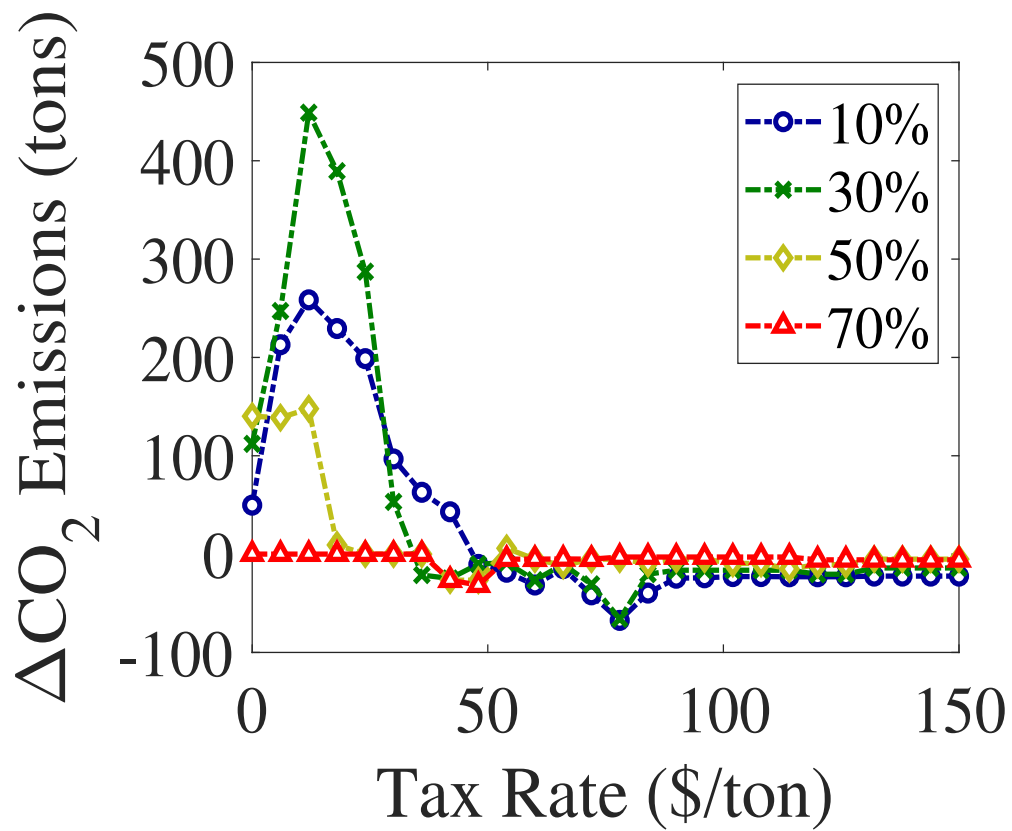
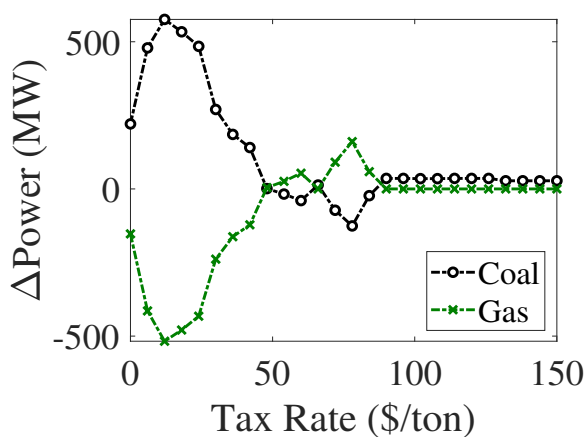
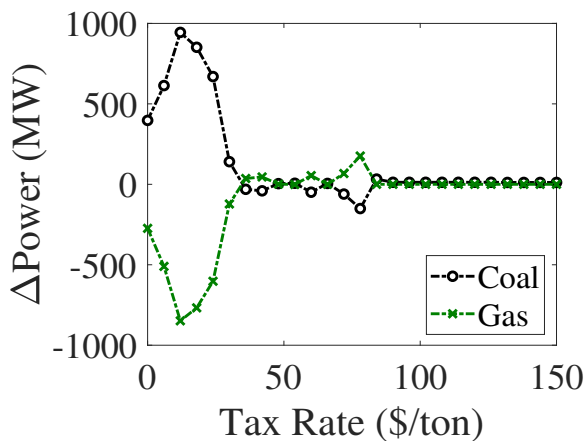


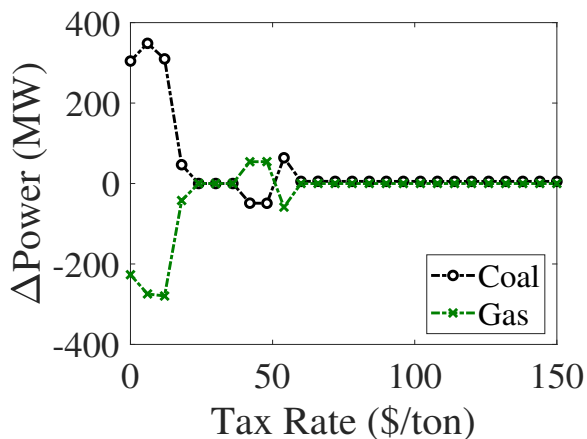
Figure 4.10: The change in CO₂ emissions due to arbitrage for different tax rates.



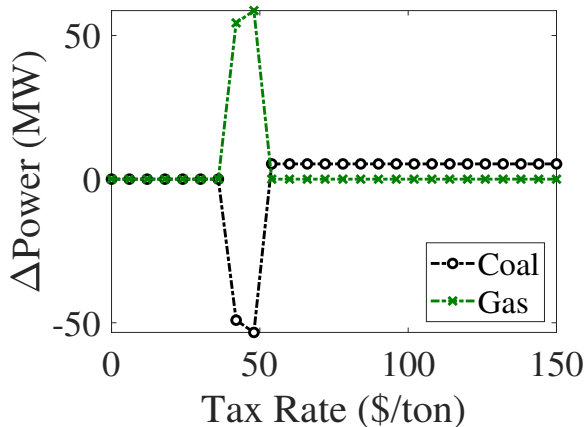
(a) 10%



(b) 30%



(c) 50%



(d) 70%

Figure 4.11: The difference in power output, relative to the unidirectional case, of gas and coal units under different tax rates for different penetration levels. Note that nuclear, hydro, and oil units exhibit zero change.

4.9 Summary

In this chapter, we present a bilevel optimization that models the optimal participation of EV aggregators in carbon-taxed electric energy markets. This bilevel optimization is then transformed to a single-level MILP equivalent using the KKT optimality conditions, the strong duality theorem, and linearization techniques available in the literature. Applying the developed model to a 24-bus test system leads to the following major conclusions:

- For low penetration levels of EVs, imposing a carbon tax has an adverse affect on the capability of EVs to benefit from arbitrage since it lowers the amount of energy sold in the day-ahead market which leads to decreased savings. Conversely, the opposite is observed for high levels of EV penetration.
- Electrifying the transportation sector will increase the level of CO₂ emissions associated with the power sector due to the increased load from EVs. Levying a carbon tax will further exasperate the problem by increasing the amount of CO₂ emissions added due to the additional EV load, which defies the purpose of introducing carbon taxes in power systems.

Chapter 5

CONCLUSION AND FUTURE WORK

5.1 *Conclusions*

This dissertation utilizes complementary models to look at the effects of carbon taxes in electric power systems from three different perspectives. The first being the regulating authority or policy maker whose main goal is to mitigate the level of emissions that result as a by-product from the production of electric energy. In Chapter 2, we propose a multilevel, computationally tractable model to achieve any feasible reduction in power systems through the optimal design of a carbon tax and subsidy policy. We show that by doing so, the tax rate needed to achieve a specific reduction target in CO₂ emissions is much lower by comparison to traditional methods. Consequently, the increase in energy prices is much more manageable which helps to ease the worries of consumers who fear rising costs as a result of the imposed carbon tax.

Secondly, we investigate the impact of carbon taxes on the market power of producers in electricity markets. Since electricity markets are considered susceptible to strategic behavior which has adverse effects on the outcomes of electricity markets, it is imperative that we ensure that carbon taxes do not exacerbate the problem. In Chapter 3, we show that carbon taxes can lead to an increase in market power of low-emitting producers which would then lead to higher energy prices and deviation from the expected level of CO₂ emissions.

Finally, in Chapter 4, we address the issue of decarbonizing the transportation sector and the ensuing consequences that result from such a task. We develop a bilevel optimization with the goal of modeling the optimal participation of EV aggregators in the day-ahead market for electric energy while incorporating the costs associated with carbon taxes. We show that our model predicts a decrease in the revenue stream obtained by arbitraging when imposing a

carbon tax. Furthermore, the level of CO₂ emissions due to the additional EV load increases with the imposition of a carbon tax due to the fact that many high-polluting units become marginal units, and therefore, are dispatched to satisfy the EV demand. Therefore, for a successful roll-out of EVs must be accompanied by a concurrent investment in cleaner energy sources or at least retrofitting high-polluting units with carbon capture and sequestration technology [165].

5.2 *Suggestions for Future Work*

In this section, suggestions for improvements to further enhance the models developed in this dissertations are discussed, and potential future research directions are proposed.

- In all of the frameworks proposed in this thesis, we use a linear model to represent the electric power system in our mathematical formulations. In doing so, we neglect real power systems/markets constraints that would impact the solutions of our models. Mainly, the exclusion of unit commitment (UC) decision variables (i.e. when to start-up or shutdown a generating unit) overestimates the flexibility of generating units since some of the inter-temporal constraints (minimum up- and down-times) and additional costs¹ are both neglected. Although mathematical formulations that accurately represent the UC model exist in the literature [166], the inclusion of such decision variables would introduce binary variables in the lower-level problem for all of the multi-level models that were developed. This effectively makes the lower-level problem a MILP instead of an LP, and thus, we cannot recast the problem as a single-level equivalent by replacing the lower-level with its KKT optimality conditions in the case of bilevel problems. Furthermore, we assumed a dc lossless power flow to represent the transmissions network, which not only neglected the reactive power flow and its impacts on the system, but also used a linear approximation to solve for the real power flow. In actuality, both real and reactive power are non-linear sinusoidal functions.

¹Such as fixed costs and start-up costs.

- The effects of demand side participation should be incorporated in the day-ahead market clearing process. In this thesis, we assumed that the demand for electric energy is inelastic, which is a reasonable assumption for all the reasons that have been stated previously. However, in reality, the demand does play an active role in electricity markets by submitting bids which are then collected and included in the objective function when maximizing the social welfare. The addition of demand bids would undoubtedly affect the results of our models. For example, in Chapter 2, one of the major benefits of implementing the proposed ODS method is that it leads to lower energy prices, which would consequently increase energy consumption, and by extension, CO₂ emissions as opposed to the case where we have higher prices. Therefore, the net benefit is still unclear and further examination is of utmost importance. In Chapter 3, the inclusion of demand bids would cause strategic producers to alter their strategy since inflating energy prices would suppress the demand, and hence, result in a decrease in their revenue. We would still expect prices to rise, but not as much since the demand is more flexible by comparison.
- We use deterministic models in this thesis, therefore, sources of uncertainty must be addressed. For example, the net load is assumed to be forecasted perfectly, which is highly optimistic since load cannot be predicted with 100% accuracy. One solution is to use stochastic optimization models [167] where we include scenarios of different net load profiles that are weighted based on their probability of occurrence.
- In Chapters 3 and 4, we assumed a perfect information setting where the strategic producer and EV aggregator know the offers/bids of other market participants ex-ante. Although relying on historical data produces good estimates as mentioned in the literature, the actual results would still be different and it is interesting to see how the strategic firm/aggregator would react under an uncontrolled setting.
- Since generating units that depend on natural gas as their primary source of energy

release lower carbon emissions as a by-product of the production in electric energy, we expect an increase in demand for natural gas whenever any kind of carbon pricing is enforced. As the rules of supply and demand dictate, an increase in demand would lead to higher prices. This is concerning since as seen in Chapter 2, when the price of natural gas increases, the tax rate rises due to the increase in the cost of subsidies. Therefore, an accurate mathematical representation of the gas system [168–172] must be included in our model to co-optimize both the electric power system and the gas system. By doing so, we account for gas price fluctuations due to market conditions (e.g. shortages in supply or increases in demand) and due to other system conditions (e.g. gas flow limits in the pipelines).

- In Chapter 3, we assumed that the strategic firm only owned generating units of one fuel type only. However, it would be interesting to see the effects of owning multiple assets with different fuel types, and the resulting effects that carbon taxes have on the participation of the strategic firm and system-wide carbon emissions.
- In Chapters 3 and 4, we considered a single leader (the strategic firm in Chapter 3 and the EV aggregator in Chapter 4) in our mathematical model. In reality, there might be other firms/aggregators that are also planning to participate in a strategic manner. In order to account for the strategic behavior of other market participants, the model must be reformulated to be an Equilibrium Problem with Equilibrium Constraints (EPEC). The added complexity of EPECs would indeed give a more realistic market setting, but at the expense of an increase in computational costs since EPECs are notoriously difficult to solve, and currently, only heuristic techniques exist to adequately solve them.
- One of the results observed in Chapter 2 concerns how normal operational changes in power systems could lead to different tax rates. In reality, it is highly unlikely that a carbon tax would change regularly everyday. Furthermore, a carbon tax is usually set

based on multiple considerations (e.g. public acceptance), and not solely to achieve a specific reduction target in carbon emissions as was done in Chapter 2. Therefore, an alternative, more realistic approach to the one proposed in Chapter 2 is to find the minimum carbon emissions via revenue recycling that can be obtained for a specific carbon tax rate. This can be formulated as a multi-objective optimization model [173–178] where the objective is to minimize the total system-wide carbon emissions plus the total cost of monetary subsidies. Such an approach would guarantee that we would exploit all of the benefits that are associated with subsidizing no- and low-emitting producers without having to change the carbon tax.

- The model developed in Chapter 4 considers only the optimal participation in the day-ahead energy market, and therefore, neglects the capability of EV aggregators to participate in the reserves market as well as the possible revenue stream that can be accrued by offering ancillary services in that market. The charging and discharging profiles scheduled for the day-ahead market will change when co-optimizing for both the energy and reserves markets, and so will the emissions performance of the different strategies carried out by the aggregator.

BIBLIOGRAPHY

- [1] What are greenhouse gases? [Online]. Available: <https://www.ncdc.noaa.gov/monitoring-references/faq/greenhouse-gases.php>.
- [2] “Global Climate Change Impacts in the United States”. Report, U.S. Global Change Research Program, 2009. [Online]. Available: <https://downloads.globalchange.gov/usimpacts/pdfs/climate-impacts-report.pdf>.
- [3] 7.a Kyoto Protocol to the United Nations Framework Convention on Climate Change. [Online]. Available: https://treaties.un.org/doc/Treaties/1998/09/19980921%2004-41%20PM/Ch_XXVII_07_ap.pdf.
- [4] Fact Sheet: The Kyoto Protocol. [Online]. Available: https://unfccc.int/files/press/backgrounders/application/pdf/fact_sheet_the_kyoto_protocol.pdf.
- [5] 7.c Doha Amendment to the Kyoto Protocol. [Online]. Available: <https://treaties.un.org/doc/Treaties/2012/12/20121217%2011-40%20AM/CN.718.2012.pdf>.
- [6] 7.d Paris Agreement. [Online]. Available: https://treaties.un.org/doc/Treaties/2016/02/20160215%2006-03%20PM/Ch_XXVII-7-d.pdf.
- [7] “Climate Change 2014 Synthesis Report Summary for Policymakers”. Report, Intergovernmental Panel on Climate Change, 2014. [Online]. Available: http://ipcc.ch/pdf/assessment-report/ar5/syr/AR5_SYR_FINAL_SPM.pdf.
- [8] Daniel A. Lashof and Dilip R. Ahuja. Relative contributions of greenhouse gas emissions to global warming. *Nature*, 344(6266):529–531, 1990.
- [9] “Climate Change 2013: The Physical Science Basis”. Report, Intergovernmental Panel on Climate Change, 2013. [Online]. Available: https://www.ipcc.ch/pdf/assessment-report/ar5/wg1/WG1AR5_TS_FINAL.pdf.
- [10] “Inventory of U.S. Greenhouse Gas Emissions and Sinks: 1990-2016”. Report, U.S. Environmental Protection Agency, 2018. [Online]. Available: https://www.epa.gov/sites/production/files/2018-01/documents/2018_complete_report.pdf.

- [11] P. Portney and R. N. Stavins. *Public Policies for Environmental Protection*. New York: Routledge, 2nd edition, 2000.
- [12] Gilbert E. Metcalf. Market-based policy options to control u.s. greenhouse gas emissions. *Journal of Economic Perspectives*, 23(2):5–27, June 2009.
- [13] Center for Climate and Energy Solutions. Cap and trade v taxes. [Online]. Available: <https://www.c2es.org/site/assets/uploads/2009/03/climate-policy-memo-1-cap-and-trade-vs-taxes.pdf>.
- [14] EU Emissions Trading System (EU ETS). [Online]. Available: https://ec.europa.eu/clima/policies/ets_en.
- [15] A. C Pigou. *The economics of welfare*. Macmillan, 1932.
- [16] British Columbia's Carbon Tax. [Online]. Available: <https://www2.gov.bc.ca/gov/content/environment/climate-change/planning-and-action/carbon-tax>.
- [17] Martin L. Weitzman. Prices vs. quantities. *The Review of Economic Studies*, 41(4):477–491, 1974.
- [18] Lawrence H. Goulder and Andrew R. Schein. Carbon taxes versus cap and trade: A critical review. *Climate Change Economics*, 04(03):1350010, 2013.
- [19] Daniel Kirschen and Goran Strbac. *Fundamentals of Power System Economics*. John Wiley & Sons, 2004.
- [20] H. Park and R. Baldick. Stochastic generation capacity expansion planning reducing greenhouse gas emissions. *IEEE Transactions on Power Systems*, 30(2):1026–1034, March 2015.
- [21] Carlos Benavides, Luis Gonzales, Manuel Diaz, Rodrigo Fuentes, Gonzalo Garca, Rodrigo Palma-Behnke, and Catalina Ravizza. The impact of a carbon tax on the chilean electricity generation sector. *Energies*, 8(4):2674–2700, 2015.
- [22] Sonia Vera and Enzo Sauma. Does a carbon tax make sense in countries with still a high potential for energy efficiency? comparison between the reducing-emissions effects of carbon tax and energy efficiency measures in the chilean case. *Energy*, 88:478 – 488, 2015.
- [23] Chuanyi Lu, Qing Tong, and Xuemei Liu. The impacts of carbon tax and complementary policies on chinese economy. *Energy Policy*, 38(11):7278 – 7285, 2010. Energy Efficiency Policies and Strategies with regular papers.

- [24] P. Eser, N. Chokani, and R. S. Abhari. Impact of carbon taxes on the interconnected central european power system of 2030. In *2016 13th International Conference on the European Energy Market (EEM)*, pages 1–6, June 2016.
- [25] Qian Wang, Klaus Hubacek, Kuishuang Feng, Yi-Ming Wei, and Qiao-Mei Liang. Distributional effects of carbon taxation. *Applied Energy*, 184:1123 – 1131, 2016.
- [26] Yazid Dissou and Muhammad Shahid Siddiqui. Can carbon taxes be progressive? *Energy Economics*, 42:88 – 100, 2014.
- [27] Brian Murray and Nicholas Rivers. British columbia's revenue-neutral carbon tax: A review of the latest grand experiment in environmental policy. *Energy Policy*, 86:674 – 683, 2015.
- [28] Alfredo M. Pereira, Rui M. Pereira, and Pedro G. Rodrigues. A new carbon tax in portugal: A missed opportunity to achieve the triple dividend? *Energy Policy*, 93:110 – 118, 2016.
- [29] Shenglu Zhou, Minjun Shi, Na Li, and Yongna Yuan. Impacts of carbon tax policy on co2 mitigation and economic growth in china. *Advances in Climate Change Research*, 2(3):124 – 133, 2011.
- [30] Yu Liu and Yingying Lu. The economic impact of different carbon tax revenue recycling schemes in china: A model-based scenario analysis. *Applied Energy*, 141:96 – 105, 2015.
- [31] David Klenert and Linus Mattauch. How to make a carbon tax reform progressive: The role of subsistence consumption. *Economics Letters*, 138:100 – 103, 2016.
- [32] Gregmar I. Galinato and Jonathan K. Yoder. An integrated tax-subsidy policy for carbon emission reduction. *Resource and Energy Economics*, 32(3):310 – 326, 2010.
- [33] Reyer Gerlagh and Bob van der Zwaan. Options and instruments for a deep cut in co2 emissions: Carbon dioxide capture or renewables, taxes or subsidies? *The Energy Journal*, 27(3):25–48, 2006.
- [34] M. Kainuma, Y. Matsuoka, T. Morita, and G. Hibino. Development of an end-use model for analyzing policy options to reduce greenhouse gas emissions. *IEEE Transactions on Systems, Man, and Cybernetics, Part C (Applications and Reviews)*, 29(3):317–324, Aug 1999.
- [35] Ying Zhou, Lizhi Wang, and James D. McCalley. Designing effective and efficient incentive policies for renewable energy in generation expansion planning. *Applied Energy*, 88(6):2201 – 2209, 2011.

- [36] Wei Wei, Yile Liang, Feng Liu, Shengwei Mei, and Fang Tian. Taxing strategies for carbon emissions: A bilevel optimization approach. *Energies*, 7(4):2228–2245, 2014.
- [37] A. G. Bakirtzis, N. P. Ziogos, A. C. Tellidou, and G. A. Bakirtzis. Electricity producer offering strategies in day-ahead energy market with step-wise offers. *IEEE Transactions on Power Systems*, 22(4):1804–1818, Nov 2007.
- [38] J. Wang, M. Shahidehpour, Z. Li, and A. Botterud. Strategic generation capacity expansion planning with incomplete information. *IEEE Transactions on Power Systems*, 24(2):1002–1010, May 2009.
- [39] L. P. Garces, A. J. Conejo, R. Garcia-Bertrand, and R. Romero. A bilevel approach to transmission expansion planning within a market environment. *IEEE Transactions on Power Systems*, 24(3):1513–1522, Aug 2009.
- [40] R. Fernandez-Blanco, J. M. Arroyo, and N. Alguacil. Network-constrained day-ahead auction for consumer payment minimization. *IEEE Transactions on Power Systems*, 29(2):526–536, March 2014.
- [41] R. Fernandez-Blanco, J. M. Arroyo, N. Alguacil, and X. Guan. Incorporating price-responsive demand in energy scheduling based on consumer payment minimization. *IEEE Transactions on Smart Grid*, 7(2):817–826, March 2016.
- [42] J. M. Arroyo and F. D. Galiana. On the solution of the bilevel programming formulation of the terrorist threat problem. *IEEE Transactions on Power Systems*, 20(2):789–797, May 2005.
- [43] A. Delgadillo, J. M. Arroyo, and N. Alguacil. Analysis of electric grid interdiction with line switching. *IEEE Transactions on Power Systems*, 25(2):633–641, May 2010.
- [44] L. Zhao and B. Zeng. Vulnerability analysis of power grids with line switching. *IEEE Transactions on Power Systems*, 28(3):2727–2736, Aug 2013.
- [45] B. Xu, Y. Wang, Y. Dvorkin, R. Fernandez-Blanco, C. A. Silva-Monroy, J. P. Watson, and D. S. Kirschen. Scalable planning for energy storage in energy and reserve markets. *IEEE Transactions on Power Systems*, 32(6):4515–4527, Nov 2017.
- [46] Y. Wang, Y. Dvorkin, R. Fernandez-Blanco, B. Xu, T. Qiu, and D. S. Kirschen. Look-ahead bidding strategy for energy storage. *IEEE Transactions on Sustainable Energy*, 8(3):1106–1117, July 2017.

- [47] H. Pandzic and I. Kuzle. Energy storage operation in the day-ahead electricity market. In *2015 12th International Conference on the European Energy Market (EEM)*, pages 1–6, May 2015.
- [48] L. Xie and M. D. Ilic. Emission-concerned economic dispatch: Possible formulations and implementations. In *IEEE PES T D 2010*, pages 1–6, April 2010.
- [49] M. Shao and W. T. Jewell. Co2 emission-incorporated ac optimal power flow and its primary impacts on power system dispatch and operations. In *IEEE PES General Meeting*, pages 1–8, July 2010.
- [50] Antonio Gomez-Exposito, Antonio J. Conejo, and Claudio Canizares. *Electric Energy Systems: Analysis and Operation*. CRC Press, 2008.
- [51] Ricardo Fernandez-Blanco, J. M. Arroyo, and N Alguacil. A unified bilevel programming framework for price-based market clearing under marginal pricing. *IEEE Transactions on Power Systems*, 27(1):517–525, Feb 2012.
- [52] J. M. Arroyo. Bilevel programming applied to power system vulnerability analysis under multiple contingencies. *IET Generation, Transmission Distribution*, 4(2):178–190, February 2010.
- [53] David G. Luenberger and Yinyu Ye. *Linear and Nonlinear Programming*. Springer US, 3 edition, 2008.
- [54] J. Fortuny-Amat and B. McCarl. A representation and economic interpretation of a two-level programming problem. *J. Oper. Res. Soc.*, 32(9):783–792, Sep 1981.
- [55] Steven A. Gabriel and Florian U. Leuthold. Solving discretely-constrained mpec problems with applications in electric power markets. *Energy Economics*, 32(1):3 – 14, 2010.
- [56] Juan M. Morales, Antonio J. Conejo, Henrik Madsen, Pierre Pinson, and Marco Zugno. *Integrating Renewables in Electricity Markets*. Springer US, 2014.
- [57] Daniel Julius Olsen, Yury Dvorkin, Ricardo Fernandez-Blanco, and Miguel Ortega-Vazquez. Optimal carbon taxes for emissions targets in the electricity sector. *IEEE Transactions on Power Systems*, PP:1–1, 2018.
- [58] J.M. Ortega and W.C. Rheinboldt. *Iterative Solution of Nonlinear Equations in Several Variables*. Academic Press, 1970.

- [59] The IBM ILOG CPLEX Website. [Online]. Available: <http://www-01.ibm.com/software/commerce/optimization/cplex-optimizer>.
- [60] GAMS Development Corporation, Washington, DC, USA. *GAMS - A User's Guide, GAMS Release 24.2.1*, 2013.
- [61] University of Washington Power Systems Test Case Archive. [Online]. Available: https://www2.ee.washington.edu/research/pstca/pf14/pg_tca14bus.htm.
- [62] Reliability Test System Task Force. The iee reliability test system-1996. a report prepared by the reliability test system task force of the application of probability methods subcommittee. *IEEE Transactions on Power Systems*, 14(3):1010–1020, Aug 1999.
- [63] R. Billinton and W. Li. *Reliability Assessment of Electric Power Systems Using Monte Carlo Methods*. Springer US, New York, 1 edition, 1994.
- [64] Reliability Test System of the Grid Modernization Laboratory Consortium. [Online]. Available: <https://github.com/GridMod/RTS-GMLC>.
- [65] Henry Hub Natural Gas Spot Price. [Online]. Available: <https://www.eia.gov/dnav/ng/hist/rngwhhdD.htm>.
- [66] Benjamin M. Kefford, Benjamin Ballinger, Diego R. Schmeda-Lopez, Chris Greig, and Simon Smart. The early retirement challenge for fossil fuel power plants in deep decarbonisation scenarios. *Energy Policy*, 119:294 – 306, 2018.
- [67] Mohsen Rahmani, Paulina Jaramillo, and Gabriela Hug. Implications of environmental regulation and coal plant retirements in systems with large scale penetration of wind power. *Energy Policy*, 95:196 – 210, 2016.
- [68] H. He and Z. Xu. Transmission congestion and its social effects. In *IEEE Power Engineering Society General Meeting, 2005*, pages 350–354 Vol. 1, June 2005.
- [69] Severin Borenstein. Understanding competitive pricing and market power in wholesale electricity markets. *The Electricity Journal*, 13(6):49 – 57, 2000.
- [70] Darryl R. (Darryl Ross) Biggar. *The economics of electricity markets*. Wiley, Chichester, West Sussex, United Kingdom, 2014.
- [71] Barry Posner. The Fundamentals of Electricity Markets, EBF 200: Introduction to Energy and Earth Sciences Economics, PennState College of Earth and Mineral Sciences. [Online]. Available: <https://www.e-education.psu.edu/ebf200/node/151>.

- [72] Federal Energy Regulatory Commission. [Online]. Available: <https://www.ferc.gov/>.
- [73] California ISO - Market monitoring. [Online]. Available: <http://www.caiso.com/market/Pages/MarketMonitoring/Default.aspx>.
- [74] A. Y. Sheffrin, , and B. F. Hobbs. Watching watts to prevent abuse of power. *IEEE Power and Energy Magazine*, 2(4):58–65, July 2004.
- [75] A. Kumar David and F. Wen. Market power in electricity supply. *IEEE Transactions on Energy Conversion*, 16(4):352–360, Dec 2001.
- [76] Miguel Perez de Arce and Enzo Sauma. Comparison of incentive policies for renewable energy in an oligopolistic market with price-responsive demand. *The Energy Journal*, 37(3), 2016.
- [77] H. Von Stackelberg. *The Theory of Market Economy*. Oxford University Press, New York, 1952.
- [78] Felix Müsgens. Quantifying market power in the german wholesale electricity market using a dynamic multi-regional dispatch model. *The Journal of Industrial Economics*, 54(4):471498, Dec 2006.
- [79] C. Ruiz and A. J. Conejo. Pool strategy of a producer with endogenous formation of locational marginal prices. *IEEE Transactions on Power Systems*, 24(4):1855–1866, Nov 2009.
- [80] L. Baringo and A. J. Conejo. Strategic offering for a wind power producer. *IEEE Transactions on Power Systems*, 28(4):4645–4654, Nov. 2013.
- [81] M. Zugno, J. M. Morales, P. Pinson, and H. Madsen. Pool strategy of a price-maker wind power producer. *IEEE Transactions on Power Systems*, 28(3):3440–3450, Aug. 2013.
- [82] T. Dai and W. Qiao. Optimal bidding strategy of a strategic wind power producer in the short-term market. *IEEE Transactions on Sustainable Energy*, 6(3):707–719, July 2015.
- [83] G. Bautista, M. F. Anjos, and A. Vannelli. Formulation of oligopolistic competition in ac power networks: An nlp approach. *IEEE Transactions on Power Systems*, 22(1):105–115, Feb 2007.

- [84] P. Chitkara, J. Zhong, and K. Bhattacharya. Oligopolistic competition of gencos in reactive power ancillary service provisions. *IEEE Transactions on Power Systems*, 24(3):1256–1265, Aug 2009.
- [85] S. J. Kazempour, A. J. Conejo, and C. Ruiz. Strategic bidding for a large consumer. *IEEE Transactions on Power Systems*, 30(2):848–856, March 2015.
- [86] A. Daraeepour, S. J. Kazempour, D. Patino-Echeverri, A. J. Conejo, and C. Ruiz. Strategic demand-side response to wind power integration. *IEEE Transactions on Power Systems*, 31(5):3495–3505, Sept. 2016.
- [87] J. E. Contereras-Ocana, Y. Wang, M. A. Ortega-Vazquez, and B. Zhang. Energy storage: Market power and social welfare. In *IEEE Power & Energy Society General Meeting*, July 2017.
- [88] Jonathan Kolstad and Frank Wolak. Using environmental emissions permit prices to raise electricity prices: Evidence from the california electricity market. *UC Berkeley: Center for the Study of Energy Markets*, 2003.
- [89] Severin Borenstein. The trouble with electricity markets: Understanding california’s restructuring disaster. *Journal of Economic Perspectives*, 16(1):191–211, March 2002.
- [90] Yihsu Chen and Benjamin F. Hobbs. An oligopolistic power market model with tradable NO_x permits. *IEEE Transactions on Power Systems*, 20(1):119–129, Feb 2005.
- [91] Yihsu Chen, Benjamin F. Hobbs, Sven Leyffer, and Todd S. Munson. Leader-follower equilibria for electric power and NO_x allowances markets. *Computational Management Science*, 3(4):307–330, Sep 2006.
- [92] Tanachai Limpitton, Yihsu Chen, and Shmuel S. Oren. The impact of carbon cap and trade regulation on congested electricity market equilibrium. *Journal of Regulatory Economics*, 40(3):237–260, Dec 2011.
- [93] A. Papavasiliou, Y. Chen, and S. S. Oren. Environmental regulation in transmission-constrained electricity markets. In *IEEE Power Engineering Society General Meeting*, July 2009.
- [94] Anthony Downward. Carbon charges in electricity markets with strategic behavior and transmission. *The Energy Journal*, 31(4):159–166, 2010.

- [95] Yihsu Chen, Makoto Tanaka, and Afzal S. Siddiqui. Tradable performance-based co2 emissions standards: Walking on thin ice? In *Energy: Expectations and Uncertainty: 39th International Conference Proceedings of the International Association for Energy Economics*, June 2016.
- [96] Pedro Linares, Francisco Javier Santos, Mariano Ventosa, and Luis Lapiedra. Incorporating oligopoly, co2 emissions trading and green certificates into a power generation expansion model. *Automatica*, 44(6):1608 – 1620, 2008. Stochastic Modelling, Control, and Robust Optimization at the Crossroads of Engineering, Environmental Economics, and Finance.
- [97] M. Jenabi, S. M. T. Fatemi Ghomi, and Y. Smeers. Bi-level game approaches for coordination of generation and transmission expansion planning within a market environment. *IEEE Transactions on Power Systems*, 28(3):2639–2650, Aug 2013.
- [98] Marco Zugno, Juan Miguel Morales, Pierre Pinson, and Henrik Madsen. A bilevel model for electricity retailers’ participation in a demand response market environment. *Energy Economics*, 36:182 – 197, 2013.
- [99] W. Tushar, W. Saad, H. V. Poor, and D. B. Smith. Economics of electric vehicle charging: A game theoretic approach. *IEEE Transactions on Smart Grid*, 3(4):1767–1778, Dec 2012.
- [100] Hélène Le Cadre. On the efficiency of local electricity markets under decentralized and centralized designs: a multi-leader stackelberg game analysis. *Central European Journal of Operations Research*, Jan 2018.
- [101] Sven Leyffer and Todd Munson. Solving multi-leader-follower games. *Mathematics and Computer Science Division, Argonne National Laboratory, Report No. ANL/MCS-P1243-0405 (2005).*, 2005.
- [102] Ankur A. Kulkarni and Uday V. Shanbhag. A shared-constraint approach to multi-leader multi-follower games. *Set-Valued and Variational Analysis*, 22(4):691–720, Dec 2014.
- [103] S. Maharjan, Q. Zhu, Y. Zhang, S. Gjessing, and T. Basar. Dependable demand response management in the smart grid: A stackelberg game approach. *IEEE Transactions on Smart Grid*, 4(1):120–132, March 2013.
- [104] A. Belgana, B. P. Rimal, and M. Maier. Open energy market strategies in microgrids: A stackelberg game approach based on a hybrid multiobjective evolutionary algorithm. *IEEE Transactions on Smart Grid*, 6(3):1243–1252, May 2015.

- [105] A. Mondal and S. Misra. Game-theoretic energy trading network topology control for electric vehicles in mobile smart grid. *IET Networks*, 4(4):220–228, 2015.
- [106] J. C. Dalton. Assessing the competitiveness of restructured generation service markets. *The Electricity Journal*, 10(3):30–39, 1997.
- [107] David L. Greene, Howard H. Baker, Jr., and Steven E. Plotkin. Reducing greenhouse gas emissions from u.s. transportation. 2011. [Online]. Available: <https://rosap.ntl.bts.gov/view/dot/23588>.
- [108] CL Myung and Simsoo Park. Exhaust nanoparticle emissions from internal combustion engines: A review. *International Journal of Automotive Technology*, 13(1):9, 2012.
- [109] AA Abdel-Rahman. On the emissions from internal-combustion engines: a review. *International Journal of Energy Research*, 22(6):483–513, 1998.
- [110] “Global EV Outlook: Two million and counting”. Report, International Energy Agency, 2017. [Online]. Available: <https://webstore.iea.org/global-ev-outlook-2018>.
- [111] “Global EV Outlook: Towards cross-modal electrification”. Report, International Energy Agency, 2018. [Online]. Available: <https://webstore.iea.org/global-ev-outlook-2018>.
- [112] C. Tudor, E. Sprung, L. Nguyen, and R. Tatro. Plug-in amp; hybrid electric vehicle charging impacts: A survey of california’s utility companies. In *2012 IEEE 13th International Conference on Information Reuse Integration (IRI)*, pages 513–518, Aug 2012.
- [113] P. Jain and T. Jain. Impacts of g2v and v2g power on electricity demand profile. In *2014 IEEE International Electric Vehicle Conference (IEVC)*, pages 1–8, Dec 2014.
- [114] J. Quiros-Tortos, L. F. Ochoa, and T. Butler. How electric vehicles and the grid work together: Lessons learned from one of the largest electric vehicle trials in the world. *IEEE Power and Energy Magazine*, 16(6):64–76, Nov 2018.
- [115] S. Rahman and G. B. Shrestha. An investigation into the impact of electric vehicle load on the electric utility distribution system. *IEEE Transactions on Power Delivery*, 8(2):591–597, April 1993.

- [116] F. Koyanagi, T. Inuzuka, Y. Uriu, and R. Yokoyama. Monte carlo simulation on the demand impact by quick chargers for electric vehicles. In *1999 IEEE Power Engineering Society Summer Meeting. Conference Proceedings (Cat. No.99CH36364)*, volume 2, pages 1031–1036 vol.2, July 1999.
- [117] L. Pieltain Fernandez, T. Gomez San Roman, R. Cossent, C. Mateo Domingo, and P. Frias. Assessment of the impact of plug-in electric vehicles on distribution networks. *IEEE Transactions on Power Systems*, 26(1):206–213, Feb 2011.
- [118] J. A. P. Lopes, F. J. Soares, and P. M. R. Almeida. Integration of electric vehicles in the electric power system. *Proceedings of the IEEE*, 99(1):168–183, Jan 2011.
- [119] Z. Ma, D. Callaway, and I. Hiskens. Decentralized charging control for large populations of plug-in electric vehicles: Application of the nash certainty equivalence principle. In *2010 IEEE International Conference on Control Applications*, pages 191–195, Sep. 2010.
- [120] Jasna Tomić and Willett Kempton. Using fleets of electric-drive vehicles for grid support. *Journal of Power Sources*, 168(2):459 – 468, 2007.
- [121] Stephanie Morse and Karen Glitman. Electric vehicles as grid resources in iso-ne and vermont. May 2014. [Online]. Available: <https://www.veic.org/documents/default-source/resources/reports/evt-rd-electric-vehicles-grid-resource-final-report.pdf>.
- [122] F. Tuffner and M. Kintner-Meyer. Using electric vehicles to meet balancing requirements associated with wind power. July 2011. [Online]. Available: https://www.pnnl.gov/main/publications/external/technical_reports/PNNL-20501.pdf.
- [123] Ivan Pavi, Tomislav Capuder, and Igor Kuzle. Value of flexible electric vehicles in providing spinning reserve services. *Applied Energy*, 157:60 – 74, 2015.
- [124] D. Rua, D. Issicaba, F. J. Soares, P. M. R. Almeida, R. J. Rei, and J. A. P. Lopes. Advanced metering infrastructure functionalities for electric mobility. In *2010 IEEE PES Innovative Smart Grid Technologies Conference Europe (ISGT Europe)*, pages 1–7, Oct 2010.
- [125] T. Markel, M. Kuss, and P. Denholm. Communication and control of electric drive vehicles supporting renewables. In *2009 IEEE Vehicle Power and Propulsion Conference*, pages 27–34, Sep. 2009.

- [126] “PJM Manual 11: Energy & Ancillary Services Market Operations”. Report, Pennsylvania-Jersey-Maryland Interconnection (PJM), 2019. [Online]. Available: <https://www.pjm.com/~media/documents/manuals/m11.ashx>.
- [127] “Load Participation in the ERCOT Nodal Market”. Report, Electric Reliability Council of Texas (ERCOT), 2015. [Online]. Available: http://www.ercot.com/content/services/programs/load/Load%20Participation%20in%20the%20ERCOT%20Nodal%20Market_3.02.doc.
- [128] “Demand Response User Guide”. Report, California Independent System Operator (CAISO), 2018. [Online]. Available: <http://www.caiso.com/Documents/DemandResponseUserGuide.pdf>.
- [129] M. G. Vayá and G. Andersson. Optimal bidding strategy of a plug-in electric vehicle aggregator in day-ahead electricity markets. In *2013 10th International Conference on the European Energy Market (EEM)*, pages 1–6, May 2013.
- [130] M. Gonzalez Vayá and G. Andersson. Optimal bidding strategy of a plug-in electric vehicle aggregator in day-ahead electricity markets under uncertainty. *IEEE Transactions on Power Systems*, 30(5):2375–2385, Sep. 2015.
- [131] E. Sortomme and M. A. El-Sharkawi. Optimal charging strategies for unidirectional vehicle-to-grid. *IEEE Transactions on Smart Grid*, 2(1):131–138, March 2011.
- [132] E. Sortomme and M. A. El-Sharkawi. Optimal combined bidding of vehicle-to-grid ancillary services. *IEEE Transactions on Smart Grid*, 3(1):70–79, March 2012.
- [133] E. Sortomme and M. A. El-Sharkawi. Optimal scheduling of vehicle-to-grid energy and ancillary services. *IEEE Transactions on Smart Grid*, 3(1):351–359, March 2012.
- [134] R. J. Bessa, M. A. Matos, F. J. Soares, and J. A. P. Lopes. Optimized bidding of a ev aggregation agent in the electricity market. *IEEE Transactions on Smart Grid*, 3(1):443–452, March 2012.
- [135] M. A. Ortega-Vazquez, F. Bouffard, and V. Silva. Electric vehicle aggregator/system operator coordination for charging scheduling and services procurement. *IEEE Transactions on Power Systems*, 28(2):1806–1815, May 2013.
- [136] S. I. Vagropoulos and A. G. Bakirtzis. Optimal bidding strategy for electric vehicle aggregators in electricity markets. *IEEE Transactions on Power Systems*, 28(4):4031–4041, Nov 2013.

- [137] M. Ansari, A. T. Al-Awami, E. Sortomme, and M. A. Abido. Coordinated bidding of ancillary services for vehicle-to-grid using fuzzy optimization. *IEEE Transactions on Smart Grid*, 6(1):261–270, Jan 2015.
- [138] M. R. Sarker, Y. Dvorkin, and M. A. Ortega-Vazquez. Optimal participation of an electric vehicle aggregator in day-ahead energy and reserve markets. *IEEE Transactions on Power Systems*, 31(5):3506–3515, Sep. 2016.
- [139] H. Wu, M. Shahidehpour, A. Alabdulwahab, and A. Abusorrah. A game theoretic approach to risk-based optimal bidding strategies for electric vehicle aggregators in electricity markets with variable wind energy resources. *IEEE Transactions on Sustainable Energy*, 7(1):374–385, Jan 2016.
- [140] Trine Krogh Kristoffersen, Karsten Capion, and Peter Meibom. Optimal charging of electric drive vehicles in a market environment. *Applied Energy*, 88(5):1940 – 1948, 2011.
- [141] A. T. Al-Awami and E. Sortomme. Coordinating vehicle-to-grid services with energy trading. *IEEE Transactions on Smart Grid*, 3(1):453–462, March 2012.
- [142] A. Tavakoli, M. Negnevitsky, D. T. Nguyen, and K. M. Muttaqi. Energy exchange between electric vehicle load and wind generating utilities. *IEEE Transactions on Power Systems*, 31(2):1248–1258, March 2016.
- [143] A. Tavakoli, M. Negnevitsky, and K. M. Muttaqi. Pool strategy of a producer coordinated with vehicle-to-grid services to maximize profitability. In *2015 Australasian Universities Power Engineering Conference (AUPEC)*, pages 1–6, Sep. 2015.
- [144] M. R. Sarker, M. A. Ortega-Vazquez, and D. S. Kirschen. Optimal coordination and scheduling of demand response via monetary incentives. *IEEE Transactions on Smart Grid*, 6(3):1341–1352, May 2015.
- [145] B. Mattlet and J. Maun. Optimal bilevel scheduling of electric vehicles in distribution system using dynamic pricing. In *2016 IEEE Power and Energy Society General Meeting (PESGM)*, pages 1–4, July 2016.
- [146] Surendraprabu Rangaraju, Laurent De Vroey, Maarten Messagie, Jan Mertens, and Joeri Van Mierlo. Impacts of electricity mix, charging profile, and driving behavior on the emissions performance of battery electric vehicles: A belgian case study. *Applied Energy*, 148:496 – 505, 2015.

- [147] Lluc Canals Casals, Egoitz Martinez-Laserna, Beatriz Amante Garca, and Nerea Nieto. Sustainability analysis of the electric vehicle use in europe for co2 emissions reduction. *Journal of Cleaner Production*, 127:425 – 437, 2016.
- [148] Allison Weis, Jeremy J. Michalek, Paulina Jaramillo, and Roger Lueken. Emissions and cost implications of controlled electric vehicle charging in the u.s. pjm interconnection. *Environmental Science & Technology*, 49(9):5813–5819, 2015. PMID: 25830471.
- [149] Christopher G. Hoehne and Mikhail V. Chester. Optimizing plug-in electric vehicle and vehicle-to-grid charge scheduling to minimize carbon emissions. *Energy*, 115:646 – 657, 2016.
- [150] Ramteen Sioshansi and Paul Denholm. Emissions impacts and benefits of plug-in hybrid electric vehicles and vehicle-to-grid services. *Environmental Science & Technology*, 43(4):1199–1204, 2009. PMID: 19320180.
- [151] Scott B. Peterson, J. F. Whitacre, and Jay Apt. Net air emissions from electric vehicles: The effect of carbon price and charging strategies. *Environmental Science & Technology*, 45(5):1792–1797, 2011. PMID: 21309508.
- [152] Gerard M. Freeman, Thomas E. Drennen, and Andrew D. White. Can parked cars and carbon taxes create a profit? the economics of vehicle-to-grid energy storage for peak reduction. *Energy Policy*, 106:183 – 190, 2017.
- [153] Matthias Galus, Marina Gonzalez Vaya, Thilo Krause, and Göran Andersson. The role of electric vehicles in smart grids. *Wiley Interdisciplinary Reviews: Energy and Environment*, 2, July 2013.
- [154] M. G. Vayá and G. Andersson. Centralized and decentralized approaches to smart charging of plug-in vehicles. In *2012 IEEE Power and Energy Society General Meeting*, pages 1–8, July 2012.
- [155] M. G. Vayá and G. Andersson. Plug-in electric vehicle charging approaches: Centralized versus decentralized and strategic versus cooperative. In *2015 IEEE Eindhoven PowerTech*, pages 1–6, June 2015.
- [156] I. Momber, S. Wogrin, and T. Gmez San Romn. Retail pricing: A bilevel program for pev aggregator decisions using indirect load control. *IEEE Transactions on Power Systems*, 31(1):464–473, Jan 2016.
- [157] M. A. Ortega-Vazquez. Optimal scheduling of electric vehicle charging and vehicle-to-grid services at household level including battery degradation and price uncertainty. *IET Generation, Transmission Distribution*, 8(6):1007–1016, June 2014.

- [158] Daniel H Doughty. Vehicle battery safety roadmap guidance. Technical report, National Renewable Energy Lab.(NREL), Golden, CO (United States), 2012.
- [159] J. E. Contreras-Ocaa, M. R. Sarker, and M. A. Ortega-Vazquez. Decentralized coordination of a building manager and an electric vehicle aggregator. *IEEE Transactions on Smart Grid*, 9(4):2625–2637, July 2018.
- [160] K. Sun, M. R. Sarker, and M. A. Ortega-Vazquez. Statistical characterization of electric vehicle charging in different locations of the grid. In *2015 IEEE Power Energy Society General Meeting*, pages 1–5, July 2015.
- [161] “National Household Travel Survey (NHTS)”. Report, U.S. Department of Transportation, 2009. [Online]. Available: <https://nhts.ornl.gov/>.
- [162] M. R. Sarker, H. Pandi, and M. A. Ortega-Vazquez. Optimal operation and services scheduling for an electric vehicle battery swapping station. *IEEE Transactions on Power Systems*, 30(2):901–910, March 2015.
- [163] M. Yilmaz and P. T. Krein. Review of battery charger topologies, charging power levels, and infrastructure for plug-in electric and hybrid vehicles. *IEEE Transactions on Power Electronics*, 28(5):2151–2169, May 2013.
- [164] M. R. Sarker, H. Pandi, K. Sun, and M. A. Ortega-Vazquez. Optimal operation of aggregated electric vehicle charging stations coupled with energy storage. *IET Generation, Transmission Distribution*, 12(5):1127–1136, 2018.
- [165] José D Figueroa, Timothy Fout, Sean Plasynski, Howard McIlvried, and Rameshwar D Srivastava. Advances in co2 capture technologythe us department of energy’s carbon sequestration program. *International journal of greenhouse gas control*, 2(1):9–20, 2008.
- [166] N. P. Padhy. Unit commitment-a bibliographical survey. *IEEE Transactions on Power Systems*, 19(2):1196–1205, May 2004.
- [167] Antonio J. Conejo, Miguel Carrión, and Juan M. Morales. *Decision Making Under Uncertainty in Electricity Markets*. Springer US, 2010.
- [168] C. He, L. Wu, T. Liu, and Z. Bie. Robust co-optimization planning of interdependent electricity and natural gas systems with a joint n-1 and probabilistic reliability criterion. *IEEE Transactions on Power Systems*, 33(2):2140–2154, March 2018.

- [169] X. Zhang, M. Shahidehpour, A. S. Alabdulwahab, and A. Abusorrah. Security-constrained co-optimization planning of electricity and natural gas transportation infrastructures. *IEEE Transactions on Power Systems*, 30(6):2984–2993, Nov 2015.
- [170] C. He, L. Wu, T. Liu, and M. Shahidehpour. Robust co-optimization scheduling of electricity and natural gas systems via adm. *IEEE Transactions on Sustainable Energy*, 8(2):658–670, April 2017.
- [171] J. Qiu, Z. Y. Dong, J. H. Zhao, K. Meng, Y. Zheng, and D. J. Hill. Low carbon oriented expansion planning of integrated gas and power systems. *IEEE Transactions on Power Systems*, 30(2):1035–1046, March 2015.
- [172] Y. Zhang, Y. Hu, J. Ma, and Z. Bie. A mixed-integer linear programming approach to security-constrained co-optimization expansion planning of natural gas and electricity transmission systems. *IEEE Transactions on Power Systems*, 33(6):6368–6378, Nov 2018.
- [173] S. Ruzika and M. M. Wiecek. Approximation methods in multiobjective programming. *Journal of Optimization Theory and Applications*, 126(3):473–501, Sep 2005.
- [174] G. T. Heydt. Multiobjective optimization: An educational opportunity in power engineering. *IEEE Transactions on Power Systems*, 24(3):1631–1632, Aug 2009.
- [175] J. Hazra and A. K. Sinha. Congestion management using multiobjective particle swarm optimization. *IEEE Transactions on Power Systems*, 22(4):1726–1734, Nov 2007.
- [176] P. Hilber, V. Miranda, M. A. Matos, and L. Bertling. Multiobjective optimization applied to maintenance policy for electrical networks. *IEEE Transactions on Power Systems*, 22(4):1675–1682, Nov 2007.
- [177] H. Louie and K. Strunz. Hierarchical multiobjective optimization for independent system operators (isos) in electricity markets. *IEEE Transactions on Power Systems*, 21(4):1583–1591, Nov 2006.
- [178] B. A. de Souza and A. M. F. de Almeida. Multiobjective optimization and fuzzy logic applied to planning of the volt/var problem in distributions systems. *IEEE Transactions on Power Systems*, 25(3):1274–1281, Aug 2010.

Appendix A

NOMENCLATURE

A.0.1 Sets and Indices

- \mathcal{T} Set of time periods, indexed by t .
- \mathcal{G} Set of generating units, indexed by g .
- \mathcal{B}_g Set of generation offer blocks of unit g , indexed by b .
- \mathcal{L} Set of transmission lines, indexed by l .
- \mathcal{N} Set of buses, indexed by n .
- Ω^{SG} Set of strategic generators.
- Ω^{NS} Set of non-strategic generators.

A.0.2 Parameters

- c_g Fuel price for generating unit g (\$/MBtu).
- $h_{g,b}$ Incremental heat rate of block b for generating unit g (MBtu/MWh).
- $m_{l,n}^{line}$ Network incidence matrix whose elements are equal to 1 if bus n is the sending bus of line l , -1 if bus n is the receiving bus of line l , and 0 otherwise.
- $m_{g,n}^{gen}$ Generating units map whose elements are equal to 1 if unit g is located at bus n and zero otherwise.

\bar{F}_l	Transmission capacity of line l (MW).
B_l	Susceptance of transmission line l (Siemens).
$\bar{P}_{g,b}$	Production upper limit of block b for generating unit g (MW).
$D_{t,n}$	Inelastic demand located at bus n in time period t (MW).
$R_g^{up/dn}$	Ramp up/down limit for generating unit g (MW).
E^{max}	Maximum carbon emissions allowed (tCO ₂ e).
\bar{S}	Subsidy rate cap (\$/MWh).
$\bar{\beta}$	Strategic bid cap (\$/MWh).
P^{CO_2}	Carbon tax imposed (\$/tCO ₂ e).
e_g	Generating unit g carbon emissions (tCO ₂ e/MBtu).
η_v^{chg}	Charging efficiency of electric vehicle v .
η_v^{dis}	Discharging efficiency of electric vehicle v .
C_v^{bat}	Battery cost per unit energy (\$/kWh)
m_v	Slope of the linear approximation of the battery life as a function of the number of cycles.
\bar{B}	Market bid cap (\$/MWh).
\bar{O}	Market offer cap (\$/MWh).
\bar{P}_v	Maximum charging/discharging power of electric vehicle v (MW).

- $\alpha_{t,v}$ Availability of electric vehicle v at time t . $\alpha_{t,v}$ equals 1 if available and 0 otherwise.
- $S_{t,v}$ Motion status of electric vehicle v at time t . $S_{t,v}$ equals 1 if the vehicle is in motion and 0 otherwise.
- E_v Total energy required for motion for electric vehicle v (kWh).
- n_T Number of time periods.
- Δt Time interval.

A.0.3 Variables

- $p_{t,v}^{chg}$ Charging power of electric vehicle v in time period t (MW).
- $p_{t,v}^{dis}$ Discharging power of electric vehicle v in time period t (MW).
- $soc_{t,v}$ Battery state-of-charge of electric vehicle v in time period t (kWh).
- $C_{t,v}$ Strategic bid of electric vehicle v in time period t .
- $O_{t,v}$ Strategic offer of electric vehicle v in time period t .
- $pf_{t,l}$ Power flow in time period t in line l (MW).
- $p_{t,g,b}$ Power produced by block b by generating unit g in time period t (MW).
- $p_{t,g}$ Power produced by generating unit g in time period t (MW).
- $\theta_{t,n}$ Voltage angle of bus n in time period t (Rad).
- $S_{t,g,b}$ Subsidy for block b of unit g in time period t (\$/MWh).
- $\beta_{t,g,b}$ Strategic bid for block b of unit g in time period t (\$/MWh).

A.0.4 Dual Variables

- $\lambda_{t,n}$ Dual variable associated with the power balance equation of bus n in time t .
- $\gamma_{t,l}$ Dual variable associated with the definition of $pf_{t,l}$ for line l in time t .
- $\mu_{t,n}^{min/max}$ Dual variable associated with the constraint imposing the lower/upper limit of $pf_{t,l}$ for line l in time t .
- $\xi_{t,g,b}^{min/max}$ Dual variable associated with the constraint imposing the lower/upper limit of $p_{t,g,b}$ for block b of generating unit g in time t .
- $\chi_{t,g}$ Dual variable associated with the definition of $p_{t,g}$ as the sum of block generation levels for generating unit g in time t .
- $\zeta_{t,g}^{dn/up}$ Dual variable associated with the constraint modeling the ramp-down/ramp-up rate of generating unit g in time t .
- $\rho_{t,n}^{min/max}$ Dual variable associated with the constraint imposing the lower/upper limit of $\theta_{t,n}$ for bus n in time t .
- σ_t Dual variable associated with the assignment of the slack bus in time t .

Appendix B

14-BUS TEST SYSTEM DATA

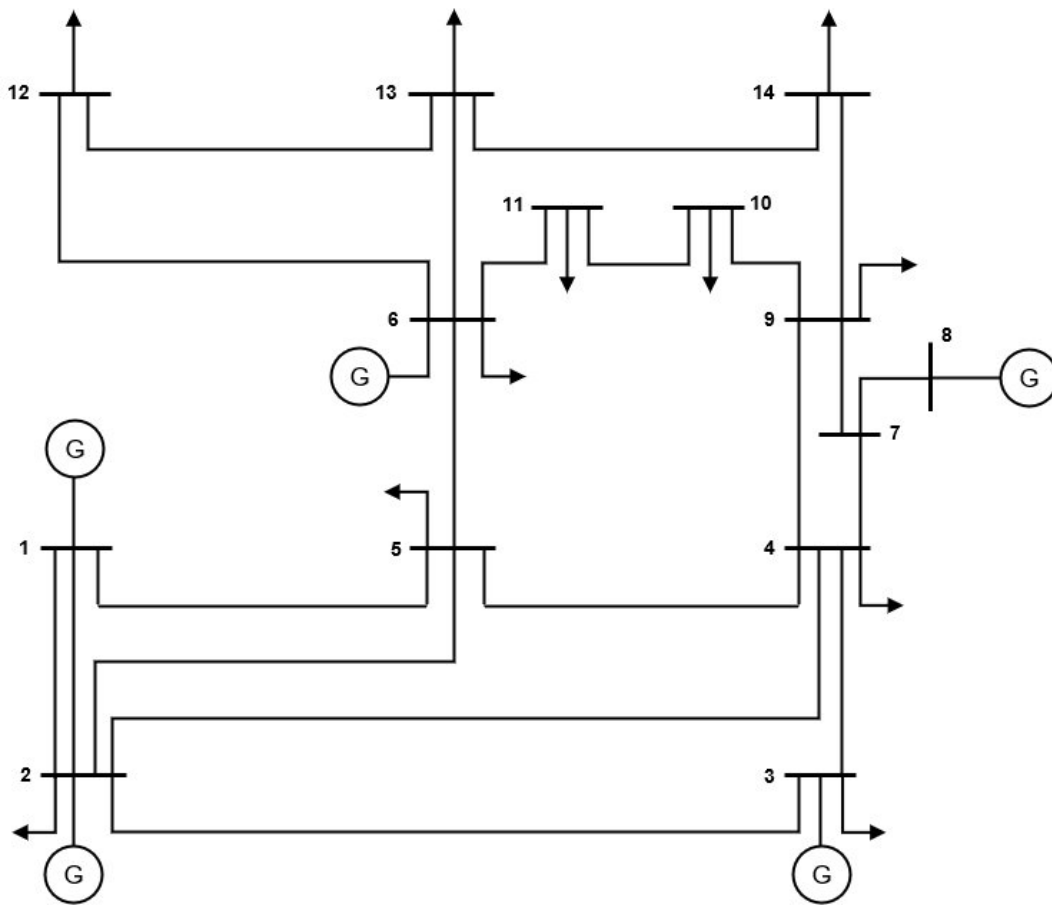


Figure B.1: 14-Bus System Topology

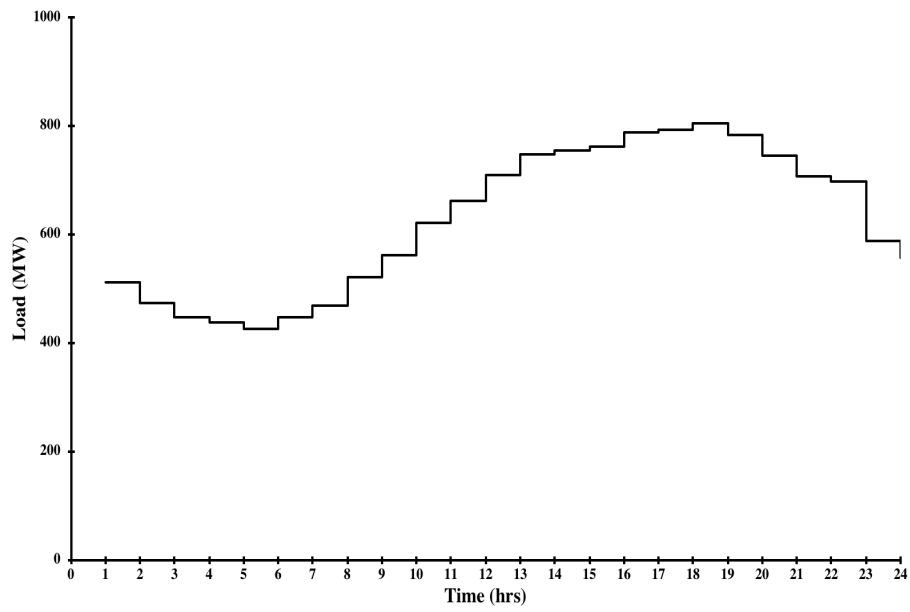


Figure B.2: Total System Load

Table B.1: Load Distribution Among Buses

Bus	Load Distribution (%)
2	8.38
3	36.37
4	18.46
5	2.93
6	4.32
9	11.39
10	3.47
11	1.35
12	2.36
13	5.21
14	5.75

Table B.2: Transmission Line Data

Line	From Bus	To Bus	Susceptance (Siemens)	Flow Limit (MW)
1	1	2	1690.05	9900
2	1	5	448.35	9900
3	2	3	505.13	9900
4	2	4	567.15	9900
5	2	5	575.11	9900
6	3	4	584.69	9900
7	4	5	2374.73	9900
8	4	7	478.19	9900
9	4	9	179.80	9900
10	5	6	396.79	9900
11	6	11	502.77	9900
12	6	12	390.92	9900
13	6	13	767.64	9900
14	7	8	567.70	9900
15	7	9	909.01	9900
16	9	10	1183.43	9900
17	9	14	369.85	9900
18	10	11	520.64	9900
19	12	13	500.3	9900
20	13	14	287.34	9900

Table B.3: Generating Units Data

Unit Type	Bus No.	Capacity (MW)	Block Output (MW)	IHR (MBtu/MWh)	Ramp Down (MW)	Ramp Up (MW)	Fuel Price (\$/MBtu)	CO ₂ Emissions (tCO ₂ e/MBtu)	
U76 Coal	8	76	15.2	9.548					
			22.8	9.966	76	76	1.6	0.105	
			22.8	11.576					
			15.2	13.311					
U100 #6 Oil	6	100	25	8.089					
			25	8.708	100	100	2.3	0.085	
			30	9.42					
			20	9.877					
U155 Coal	3	155	54.25	8.265					
			38.75	8.541	155	155	1.6	0.105	
			31	8.9					
			31	9.381					
U197 #6 Oil	2	197	68.95	8.348					
			49.25	8.833	180	180	2.3	0.085	
			39.4	9.225					
			39.4	9.62					
U400 Nuclear	1	400	100	8.848					
			100	8.965	400	400	0.6	0	
			120	9.21					
			80	9.438					

Appendix C

LINEAR EQUIVALENT OF THE UPPER-LEVEL OBJECTIVE FUNCTION

C.1 Competitive Model

The strong duality theorem for the competitive model will yield the following identity:

$$\begin{aligned}
\sum_{t \in \mathcal{T}} \sum_{g \in \mathcal{G}} \sum_{b \in \mathcal{B}_g} (c_g + e_g \cdot P^{CO_2}) h_{g,b} \cdot p_{t,g,b} = & \\
& \sum_{t \in \mathcal{T}} \sum_{n \in \mathcal{N}} D_{t,n} \cdot \lambda_{t,n} \\
& + \sum_{t \in \mathcal{T}} \sum_{v \in \mathcal{V}} (p_{t,v}^{chg} - \eta_v^{dis} \cdot p_{t,v}^{dis}) \cdot \lambda_{t,n(v)} \\
& - \sum_{t \in \mathcal{T}} \sum_{l \in \mathcal{L}} \bar{F}_l \cdot (\mu_{t,g}^{min} + \mu_{t,g}^{max}) \\
& - \sum_{t \in \mathcal{T}} \sum_{g \in \mathcal{G}} \sum_{b \in \mathcal{B}_g} \bar{P}_{g,b} \cdot \xi_{t,g,b}^{max} \\
& - \sum_{t=1}^{n_T-1} \sum_{g \in \mathcal{G}} R_g^{up} \cdot \zeta_{t,g}^{up} + \sum_{t=1}^{n_T-1} \sum_{g \in \mathcal{G}} R_g^{dn} \cdot \zeta_{t,g}^{dn} \\
& - \sum_{t \in \mathcal{T}} \sum_{n \in \mathcal{N}} \pi \cdot (\rho_{t,g}^{min} + \rho_{t,g}^{max}) \tag{C.1}
\end{aligned}$$

We can then rearrange the terms in (C.1) to get the desired linear form of the UL objective function:

$$\begin{aligned}
\sum_{t \in \mathcal{T}} \sum_{v \in \mathcal{V}} \left(p_{t,v}^{chg} - \eta_v^{dis} \cdot p_{t,v}^{dis} \right) \cdot \lambda_{t,n(v)} &= \sum_{t \in \mathcal{T}} \sum_{g \in \mathcal{G}} \sum_{b \in \mathcal{B}_g} (c_g + e_g \cdot P^{CO_2}) h_{g,b} \cdot p_{t,g,b} \\
&+ \sum_{t \in \mathcal{T}} \sum_{l \in \mathcal{L}} \bar{F}_l \cdot (\mu_{t,g}^{min} + \mu_{t,g}^{max}) + \sum_{t \in \mathcal{T}} \sum_{g \in \mathcal{G}} \sum_{b \in \mathcal{B}_g} \bar{P}_{g,b} \cdot \xi_{t,g,b}^{max} \\
&+ \sum_{t=1}^{n_T-1} \sum_{g \in \mathcal{G}} R_g^{up} \cdot \zeta_{t,g}^{up} + \sum_{t=1}^{n_T-1} \sum_{g \in \mathcal{G}} R_g^{dn} \cdot \zeta_{t,g}^{dn} \\
&+ \sum_{t \in \mathcal{T}} \sum_{n \in \mathcal{N}} \pi \cdot (\rho_{t,g}^{min} + \rho_{t,g}^{max}) - \sum_{t \in \mathcal{T}} \sum_{n \in \mathcal{N}} D_{t,n} \cdot \lambda_{t,n} \quad (C.2)
\end{aligned}$$

C.2 Strategic Model

The following steps are followed to linearize the UL objective function of the strategic model:

1. Using the strong duality theorem, we obtain the following identity:

$$\begin{aligned}
\sum_{t \in \mathcal{T}} \sum_{g \in \mathcal{G}} \sum_{b \in \mathcal{B}_g} (c_g + e_g \cdot P^{CO_2}) h_{g,b} \cdot p_{t,g,b} \\
+ \sum_{t \in \mathcal{T}} \sum_{v \in \mathcal{V}} O_{t,v} \cdot \eta_v^{dis} \cdot p_{t,v}^{dis} \\
- \sum_{t \in \mathcal{T}} \sum_{v \in \mathcal{V}} B_{t,v} \cdot p_{t,v}^{chg} = \\
\sum_{t \in \mathcal{T}} \sum_{n \in \mathcal{N}} D_{t,n} \cdot \lambda_{t,n} - \sum_{t \in \mathcal{T}} \sum_{v \in \mathcal{V}} \bar{\varphi}_{t,v}^{chg} \cdot \alpha_{t,v} \cdot \bar{P}_v \\
- \sum_{t \in \mathcal{T}} \sum_{v \in \mathcal{V}} \bar{\varphi}_{t,v}^{dis} \cdot \alpha_{t,v} \cdot \bar{P}_v - \sum_{t \in \mathcal{T}} \sum_{g \in \mathcal{G}} \sum_{b \in \mathcal{B}_g} \bar{P}_{g,b} \cdot \xi_{t,g,b}^{max} \\
- \sum_{t \in \mathcal{T}} \sum_{l \in \mathcal{L}} \bar{F}_l \cdot (\mu_{t,g}^{min} + \mu_{t,g}^{max}) \\
- \sum_{t=1}^{n_T-1} \sum_{g \in \mathcal{G}} R_g^{up} \cdot \zeta_{t,g}^{up} + \sum_{t=1}^{n_T-1} \sum_{g \in \mathcal{G}} R_g^{dn} \cdot \zeta_{t,g}^{dn} \\
- \sum_{t \in \mathcal{T}} \sum_{n \in \mathcal{N}} \pi \cdot (\rho_{t,g}^{min} + \rho_{t,g}^{max}) \quad (C.3)
\end{aligned}$$

2. From (4.6d), we can replace $B_{t,v}$ with the following:

$$B_{t,v} = \lambda_{t,n(v)} + \overline{\varphi}_{t,v}^{chg} - \underline{\varphi}_{t,v}^{chg},$$

3. From (4.6e), we can replace $\eta_v^{dis} \cdot O_{t,v}$ with the following:

$$\eta_v^{dis} \cdot O_{t,v} = \eta_v^{dis} \cdot \lambda_{t,n(v)} - \overline{\varphi}_{t,v}^{dis} + \underline{\varphi}_{t,v}^{dis};$$

4. From (4.6f)—(4.6i), we know that:

$$\overline{\varphi}_{t,v}^{chg} \cdot p_{t,v}^{chg} = \overline{\varphi}_{t,v}^{chg} \cdot \alpha_{t,v} \cdot \overline{P}_v$$

$$\underline{\varphi}_{t,v}^{chg} \cdot p_{t,v}^{chg} = 0$$

$$\overline{\varphi}_{t,v}^{dis} \cdot p_{t,v}^{dis} = \overline{\varphi}_{t,v}^{dis} \cdot \alpha_{t,v} \cdot \overline{P}_v$$

$$\underline{\varphi}_{t,v}^{dis} \cdot p_{t,v}^{dis} = 0$$

5. Finally, we substitute the results from (2) and (3) back in (C.3) to get the following linear equivalent:

$$\begin{aligned} \sum_{t \in \mathcal{T}} \sum_{v \in \mathcal{V}} \left(p_{t,v}^{chg} - \eta_v^{dis} \cdot p_{t,v}^{dis} \right) \cdot \lambda_{t,n(v)} &= \sum_{t \in \mathcal{T}} \sum_{g \in \mathcal{G}} \sum_{b \in \mathcal{B}_g} (c_g + e_g \cdot P^{CO_2}) h_{g,b} \cdot p_{t,g,b} \\ &+ \sum_{t \in \mathcal{T}} \sum_{l \in \mathcal{L}} \overline{F}_l \cdot (\mu_{t,g}^{min} + \mu_{t,g}^{max}) + \sum_{t \in \mathcal{T}} \sum_{g \in \mathcal{G}} \sum_{b \in \mathcal{B}_g} \overline{P}_{g,b} \cdot \xi_{t,g,b}^{max} \\ &+ \sum_{t=1}^{n_T-1} \sum_{g \in \mathcal{G}} R_g^{up} \cdot \zeta_{t,g}^{up} + \sum_{t=1}^{n_T-1} \sum_{g \in \mathcal{G}} R_g^{dn} \cdot \zeta_{t,g}^{dn} \\ &+ \sum_{t \in \mathcal{T}} \sum_{n \in \mathcal{N}} \pi \cdot (\rho_{t,g}^{min} + \rho_{t,g}^{max}) - \sum_{t \in \mathcal{T}} \sum_{n \in \mathcal{N}} D_{t,n} \cdot \lambda_{t,n} \end{aligned} \tag{C.4}$$